Università degli Studi di Ferrara

Doctorate of Philosophy in
Biomedical Sciences and Biotechnology

CYCLE XXXI

Coordinator: Prof. Pinton Paolo

Cellular and animal ALS models: studies on TDP-43 aggregate clearance

SSD: BIO/10

PhD student
Spinelli Greta

Tutor
Prof. Pagani Franco

Year 2015-2018

Table of contents

List of figures

List of abbreviations

AD Alzheimer's disease

ALS Amyotrophic Lateral Sclerosis

CFTR9 Cystic Fibrosis Trans-membrane Regulator

CNS Central Nervous System

CP Core particle

CTF C-terminal fragments

DMEM Dulbecco's Modified Eagle Medium

fALS Familial Amyotrophic Lateral Sclerosis

FDA Food and Drug Administration

FUS/TLS Sarcoma/translocated in liposarcoma

GOF Gain of function

GWAS Genome-wide association studies

HD Huntington's disease

HIV Human Immunodeficiency Virus

hnRNP Heterogeneous nuclear ribonucleoprotein

LC3 Light chain 3

LOF Loss of function

NES Nuclear export signal

NLS Nuclear localization signal

NMJ Neuromuscular Junction

NTF N-terminal fragments

mTOR Mammalian Target of Rapamycin

OPTN Optineurin

PD Parkinson's disease

POLDIP3 Polymerase delta interacting protein

PrP Protease-resistant prion protein

RAN Repeat-associated non-ATG-dependent

RP Regulatory particle

RRM RNA recognition motifs

sALS Sporadic Amyotrophic Lateral Sclerosis

SDS-PAGE Sodium Dodecyl Sulphate Polyacrylamide Gel Electrophoresis

SOD1 Superoxide dismutase-1

SQSTM1 Sequestosome 1

TBPH Drosophila melanogaster TDP-43 orthologue

TCA Tricyclic antidepressant

TDP-43 TAR-Binding Protein 43

TDPBR TDP-43 binding region

UAS Upstream activating sequence

UBQLN2 Ubiquilin 2

UPS Ubiquitin-proteasome system

UTR Untranslated Region

VCP Valosin-containing protein

Introduction

1. Neurodegenerative diseases

Neurodegenerative diseases are age-related progressive disorders characterized by the loss of neurons in specific regions of the human nervous system. Different disease phenotypes occur with neuron loss depending on the neuronal population affected (Soto 2003). Although these diseases have different clinical signs and symptoms, some similarities exist between them. This subset, defined as “proteinopathies”, is characterized by the accumulation of specific proteins (Giacomelli, Daniele et al. 2017). A common pathological hallmark is indeed the presence of inclusions derived from the accumulation and deposition of misfolded proteins in neurons; aggregates can be nuclear, cytoplasmic or extracellular. The classification of neurodegenerative disorders relies on the different distribution of the aggregates within the brain, and the different composition of the aggregates (**table 1**). Protein aggregation can result from a mutation in the sequence of the disease-related protein, a genetic alteration that causes an elevation in the amounts of a protein, or can occur in the absence of genetic alterations, perhaps triggered by environmental stress or aging (Ross and Poirier 2005).

Inclusion bodies are frequent pathological features of neurodegenerative disorders; however, the role of aggregation in the disease process is not fully understood. Many indirect lines of evidence link aggregation to toxicity while other studies suggest that inclusion body formation might represent a cellular protective response against misfolded proteins (Ross and Poirier 2005).

Based on their nature of inheritance, neurodegenerative diseases can be classified into two types: idiopathic or sporadic when there is no definable pattern of inheritance, and familial. Genetic risk factors as well as environmental factors are associated with the development of sporadic forms.

Alzheimer's disease (AD), Parkinson's disease (PD), Huntington's disease (HD), Amyotrophic Lateral Sclerosis (ALS) and Frontotemporal Dementia (FTD) are the best known neurodegenerative diseases; tauopathies (e.g. Pick’s diseases, frontotemporal dementia with parkinsonism) and other polyQ diseases (e.g. Spinocerebellar ataxia) and synucleopathies such as Dementia with Lewy Bodies are also included in the category of neurodegeneration.

In each neurodegenerative disease, different neuronal populations are affected. Common factors that are potential mediators of the disease process include: increased oxidative burden (reactive oxygen species), impaired energy metabolism, lysosomal dysfunction, protein aggregation/inclusion-body formation, inflammation, excitoxicity, necrosis and/or apoptosis (Jellinger 2010).

Disease	Affected brain regions	Aggregating proteins	Type of protein deposits
Alzheimer's Disease (AD)	Cerebral cortex, hippocampus	Amyloid β (Aβ), tau	Extracellular plaques, Intracellular tangles
Amyotrophic lateral sclerosis (ALS)	Spinal cord, motor cortex, brain stem	TDP-43, SOD1, FUS	Intracellular cytoplasmic inclusions
Huntington's Disease (HD)	Striatum, cerebral cortex	Huntingtin	Intracellular nuclear inclusions
Parkinson's Disease (PD)	Substantia nigra	α - synuclein	Intracellular cytoplasmic inclusions (Lewy bodies)
Spinocerebellar ataxias (SCAs)	Cerebellum	Ataxin-1, ataxin-2, ataxin-3, ataxin-7..	Intracellular nuclear or cytoplasmic inclusions

Table 1. Main neurodegenerative diseases characterized by deposition of aggregated proteins.

1.1. Amyotrophic lateral sclerosis

1.1.1. General overview

Amyotrophic Lateral Sclerosis (ALS), also known as Lou Gehrig's disease is a muscle wasting disease that is characterized by the degeneration of upper motor neurons in the motor cortex and lower motor neurons in the brain stem and anterior horn of the spinal cord (Robberecht and Philips 2013). This disease was first described in 1869 by the neurologist Jean-Martin Charcot, and its name reflects the degeneration and consequent hardening of the anterior and lateral corticospinal motor

neurons (“Lateral Sclerosis”) with secondary denervation of muscles, which progressively lose the ability to contract leading to muscle wasting (“Amyotrophy”) (**figure 1**) (Rowland and Shneider 2001).

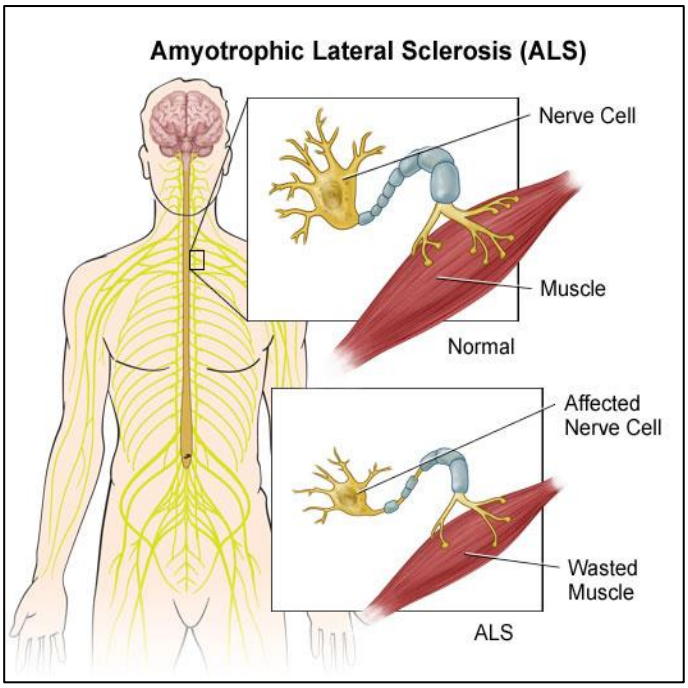

Figure 1. Denervation of muscles due to motor neuron degeneration leads to muscle wasting. Adapted from ALS Foundation

Degeneration of these neurons leads to typical symptoms of ALS such as progressive muscle weakness, muscular atrophy, spasticity and fasciculations (Robberecht and Philips 2013). Any voluntary muscle can be affected, however muscles responsible for eye movement and sphincter control usually remain unaffected (van Es, Hardiman et al. 2017). ALS is a very heterogeneous disease. Initial symptoms are different depending on the involvement of different sets of motor neurons; in about two-thirds of ALS cases, lower motor neurons are the first to be affected (spinal-onset), causing patients to develop weakness and atrophy of the limbs. On the other hand, when the brainstem is involved (bulbar-onset), tongue atrophy followed by difficulty in swallowing

(dysphagia) and speaking (dysarthria) are the first symptoms to appear (**figure 2**). However, symptoms progressively spread to other body regions and eventually to respiratory muscles (Taylor, Brown et al. 2016, Hardiman, Al-Chalabi et al. 2017). Most people die because of respiratory failure typically after 3-5 years from the onset of the disease (Ajroud-Driss and Siddique 2015).

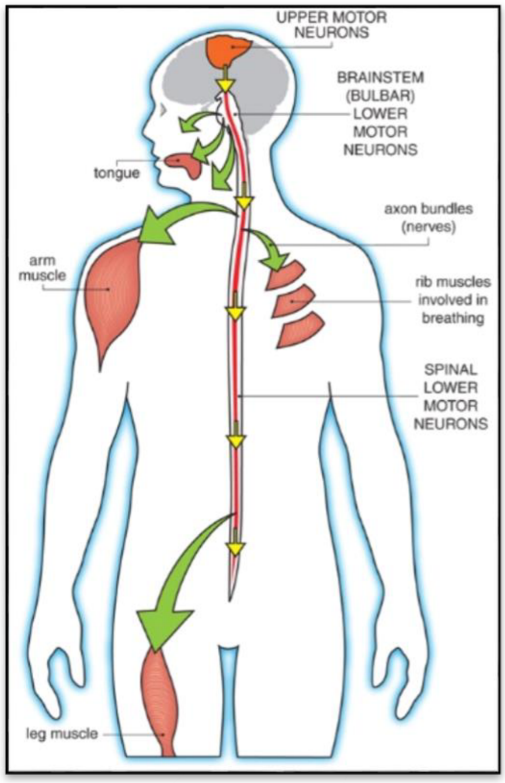

Figure 2. ALS mechanism. Upper motor neurons send signals to lower motor neurons, which in turn send signals to muscles. In ALS patients both upper and lower motor neuron are lost. Adapted from MD's ALS Division Publication.

Prefrontal and temporal lobes can also be affected in some forms of ALS; degeneration of neurons in these areas of the brain results in frontal executive dysfunction in many patients. In fact, currently at least 50% of patients with ALS show cognitive or behavioural dysfunction (ALS-Ci/Bi), and in around 15% the cognitive impairment is severe enough to meet the criteria of FTD (ALS-FTD) (Ringholz, Appel et al. 2005, Swinnen and Robberecht 2014).

The age onset is usually between 55 and 65 years of age and the life expectancy is 2-5 years after the diagnosis (Chiò, Logroscino et al. 2013). ALS is diagnosed in approximately 2/100,000 people each year in most of the countries, while the prevalence is about 5/100,000 individuals, which reflects the rapid lethality of the disease (Logroscino, Traynor et al. 2010, Al-Chalabi and Hardiman 2013). In most population-based studies, ALS is found to be more common in men than in women (Logroscino, Traynor et al. 2010, Huisman, de Jong et al. 2011).

1.1.2. Diagnosis

Diagnosing ALS is based on the El Escorial and Airlie House criteria (Brooks, Miller et al. 2000). According to these criteria, ALS diagnosis requires progressive weakness spreading within a region or to other regions, such as bulbar regions (affecting speech and swallowing), cervical regions (affecting the upper limbs), thoracic regions (affecting the chest wall and abdominal muscles) or lumbar regions (affecting the lower limbs). Moreover, the involvement of both lower motor neurons (through the presence of specific symptoms or evidence of denervation on electromyography) and upper motor neurons (through the presence of specific symptoms and brisk deep tendon reflexes) has to be visible (Hardiman, Al-Chalabi et al. 2017). However, the absence of specific biomarkers, the growing understanding of the extra-motor features of ALS and the presence of phenotypic overlap with other neurodegenerative diseases can make ALS diagnosis extremely challenging (Al-Chalabi, Hardiman et al. 2016).

1.1.3. Pathophysiology

The causes underlying cell death in ALS are still not fully understood. Several cellular and molecular mechanisms are thought to be involved in motor neurons degeneration, such as mitochondrial dysfunction (Muyderman and Chen 2014), hyperactivation of microglia (Lee, Hyeon et al. 2016), impaired axonal transport (De Vos and Hafezparast 2017), defective protein degradation (Webster, Smith et al. 2017) and aberrant RNA metabolism (Hardiman, Al-Chalabi et al. 2017). Glutamate-

induced excitotoxicity has also been found to be involved in ALS pathogenesis (Van Damme, Dewil et al. 2005), but the mechanism by which glutamate mediates motor neuron degeneration remains unclear (Kiernan, Vucic et al. 2011) (**figure 3**). Even though multiple processes seem to be involved in the pathogenesis of the disease, the main pathological hallmark is the abnormal accumulation of protein aggregates, called inclusions, in the affected areas of the nervous system (Van Langenhove, van der Zee et al. 2012, Blokhuis, Groen et al. 2013). Ubiquitin positive inclusions were first observed in the degenerating motor neurons of ALS patients in 1988 (Leigh, Anderton et al. 1988). In 2006, TDP-43 was discovered as the main component of inclusions in 97% of ALS cases (Arai, Hasegawa et al. 2006, Neumann, Sampathu et al. 2006).

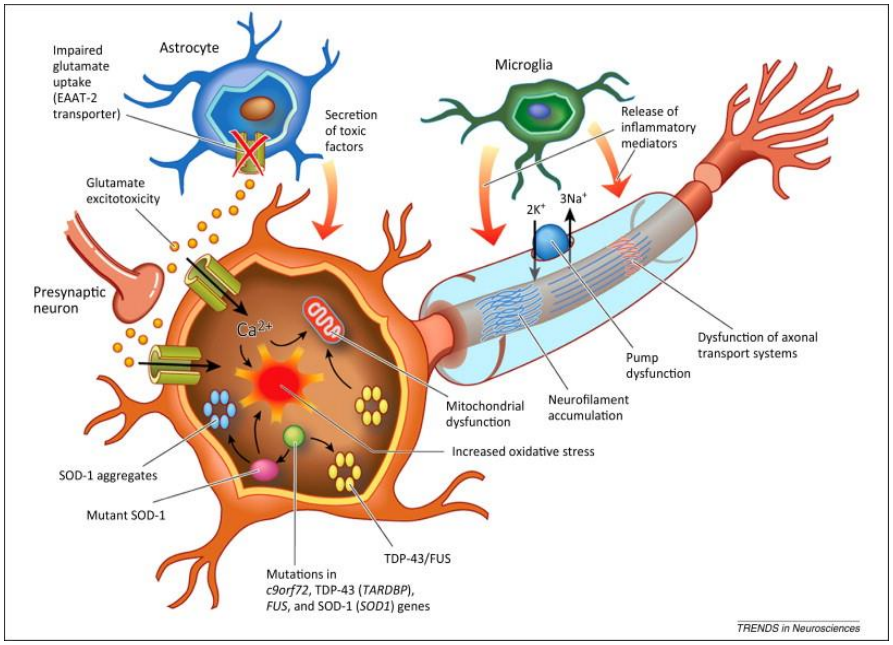

Figure 3. Cellular and molecular mechanisms mediating neurodegeneration in ALS.
Adapted from Kiernan *et al*., 2014.

1.1.4. Familial and sporadic ALS

In 5-10% of patients with ALS a family history exists. In these cases, an inherited genetic mutation, usually dominant, is responsible for the disease (familial ALS or fALS). In all the others (90-95%), the disease is thought to be caused by environmental and genetic risk factors, such as smoking, exposure to pesticides and organic toxins. This form is commonly known as sporadic ALS (Al-Chalabi

and Hardiman 2013). Genome-wide association studies that have the objective of identifying genetic variants associated with an increased or decreased risk for developing sporadic ALS have led to the conclusion that also sporadic ALS can occur in presence of a genetic mutation although not inherited (**figure 4**) (Renton, Chiò et al. 2014).

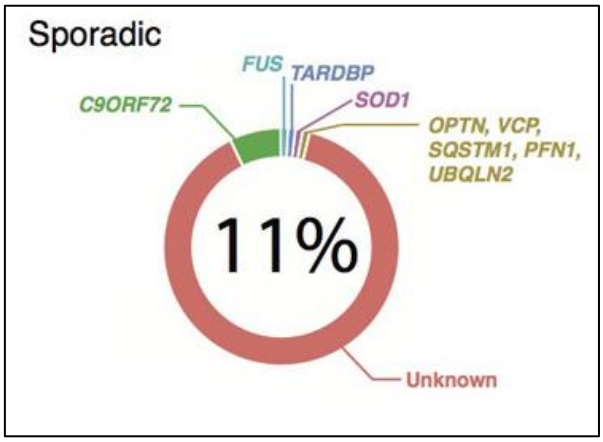

Figure 4. Proportion of ALS explained by each gene known to carry mutations in sALS.
Adapted from Renton *et al*., 2014.

Mutations in 9 genes account for the etiology of about two-thirds (68%) of fALS cases (**figure 5**). The remaining one-third is still unknown. Among the identified genes, Cu/Zn superoxide dismutase 1 (SOD1)(Rosen 1993), TAR-Binding protein 43 (TARDBP)(Kabashi, Valdmanis et al. 2008, Sreedharan, Blair et al. 2008), fused in sarcoma/translocated in liposarcoma (FUS/TSL)(Kwiatkowski, Bosco et al. 2009, Vance, Rogelj et al. 2009) and C9ORF72 (DeJesus-Hernandez, Mackenzie et al. 2011, Renton, Majounie et al. 2011) account for over 50% of fALS cases. Mutations in Optineurin (OPTN), Valosin-containing protein (VCP), Ubiquilin 2 (UBQLN2), Sequestosome 1 (SQSTM1) and Profilin 1 (PFN1) are known to cause the other 18% of the cases.

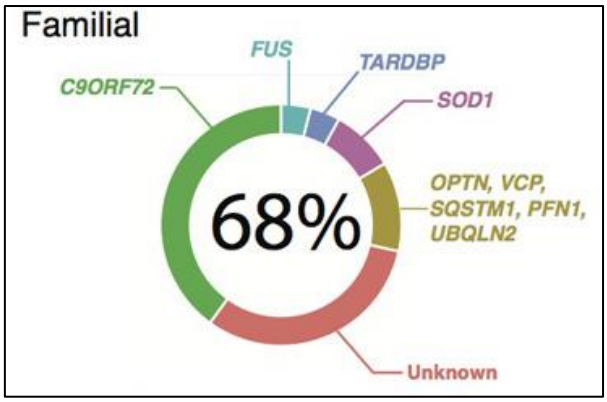

Figure 5. Proportion of ALS explained by each gene known to carry mutations in fALS.
Adapted from Renton *et al.,* 2014.

1.1.5. ALS-related genes

1.1.5.1. SOD1

The first ALS gene to be identified was SOD1 (Rosen 1993), which accounts for about 20% of familial ALS and 2-3% of sporadic cases (Renton, Chiò et al. 2014). SOD1 encodes for the Cu/Zn superoxide dismutase, a cytoplasmic enzyme responsible for the conversion of superoxide, a natural by-product of respiration, to oxygen or hydrogen peroxide. It is expressed ubiquitously and highly conserved through species. So far, more than 140 mutations, spanning the five exons of SOD1 have been described (Taylor, Brown et al. 2016). The A4V mutation is the most common mutation in North America (responsible for about 50% of cases), followed by the I113T mutations (Cudkowicz, McKenna-Yasek et al. 1997). One of the proposed pathogenic mechanisms underlying SOD1 pathology is that the enzymatic activity of the protein might be impaired, thus causing the increase of reactive oxygen species inside the cell (Boillée, Vande Velde et al. 2006). However, mutants expressing dismutase active (Wong, Pardo et al. 1995) as well as inactive (Bruijn, Becher et al. 1997) forms of the enzyme develop comparable disease pathologies similar to those observed in patients. Furthermore, SOD1 deletion in mice does not cause motor neuron disease (Reaume, Elliott et al. 1996) arguing against the loss-of-function hypothesis. Our current understanding of the pathogenic role of mutant SOD1 comes primarily from the study of transgenic rodents overexpressing mutant SOD1 and in particular from the G93A mouse model (Gurney 1994) as it recapitulates many features

of the human SOD1 type disease. Although the exact toxic mechanism of SOD1 mutations is not completely elucidated, the mutant protein gains many toxic functions that can cause endoplasmic reticulum (ER) stress and include: overloading the unfolded protein response, mitochondrial dysfunction and disruption of axonal transport (Boillée, Vande Velde et al. 2006, Ajroud-Driss and Siddique 2015). Moreover, several studies showed that mutant SOD1 is prone to misfolding, leading to accumulation and formation of ubiquitinated cytoplasmic aggregates (Johnston, Dalton et al. 2000, Wang, Xu et al. 2002, Ip, Mulligan et al. 2011, Tokuda, Nomura et al. 2018). In turn, aggregates may lead to cell death by sequestering other cytoplasmic proteins essential for cell survival. Mutant SOD1 forms aggregates through an oxidation-mediated mechanism and recruit wild-type SOD1 by crosslinking of intermolecular disulifide bonds (Deng, Shi et al. 2006, Furukawa, Fu et al. 2006). Inclusions containing these aggregates are observed in lower motor neurons of both sporadic and familial ALS due to SOD1 mutations and in the SOD1 mouse models (Dal Canto and Gurney 1995, Bruijn, Houseweart et al. 1998, Kato, Takikawa et al. 2000). Not only mutant SOD1 but also wild type SOD1 has been shown to undergo misfolding and aggregation (Ezzi, Urushitani et al. 2007, Medinas, Rozas et al. 2018). Using conformation-specific antibodies, misfolded wild-type SOD1 has been reported in the spinal cord of sporadic ALS patients and in non-SOD1 familial ALS but not in controls, implicating wild-type SOD1 aggregation in the pathogenesis of sporadic ALS (Bosco, Morfini et al. 2010, Rotunno and Bosco 2013).

1.1.5.2. TARDBP

A major step forward in ALS was the identification in 2006 of TAR DNA-binding protein (TDP-43) as the major component of ubiquitin-positive neuronal inclusions observed in patients' brain and subsequently also in those of other neurodegenerative diseases such as frontotemporal lobar degeneration (FTLD) (Neumann, Sampathu et al. 2006). This finding was followed by the discovery of mutations in the TARDBP gene in some cases of ALS (Kabashi, Valdmanis et al. 2008, Sreedharan, Blair et al. 2008). TARDBP is located on chromosome 1p36.22 and contains five coding and one non-coding exon. It encodes for TDP-43, a highly conserved DNA/RNA binding protein expressed ubiquitously (Buratti and Baralle 2001); TDP-43 is predominantly localized in the nucleus where it is involved in many aspects of RNA metabolism (Buratti and Baralle 2010, Ratti and Buratti 2016). TDP-

43 contains two RNA recognition motifs (RRM), a nuclear localization signal (NLS) in the N-terminus and a nuclear export signal (NES) within the second RRM that allows the protein to shuttle between the nucleus and the cytoplasm (Ayala, Zago et al. 2008). To date, about 50 TARDBP missense mutations have been identified in both familial and sporadic ALS accounting for 1-2% of total cases (Renton, Chiò et al. 2014, Buratti 2015). Most of TARDBP mutations identified were found in exon 6 (**figure 6**) (Mackenzie and Rademakers 2008, Gendron, Rademakers et al. 2013, Buratti 2015), which encodes for the C-terminus of the protein, known to be involved in protein-protein interactions (Mackenzie and Rademakers 2008, D'Ambrogio, Buratti et al. 2009). These mutations were suggested to increase TDP-43 phosphorylation due to a change of the original amino acid to threonine or serine residues. A change in phosphorylation could interfere with protein interactions or nuclear transport leading to accumulation of the protein in the cytoplasm (Pesiridis, Lee et al. 2009, Newell, Paron et al. 2018). Two exceptions are the Asp169Gly mutation, located on exon 4, and the Tyr374X that leads to a truncated and inactive form of the protein; however, these two mutations have been identified in just one patient with sporadic ALS (Mackenzie, Rademakers et al. 2010). A deeper overview of TDP-43 will be given in chapter 2.

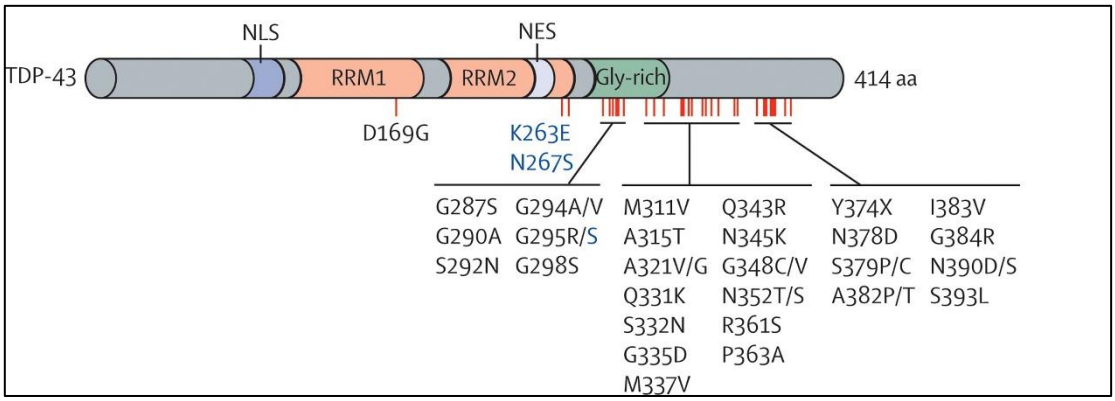

Figure 6. Schematic overview of protein domains of TDP-43 and identified gene mutations associated with ALS. Adapted from Mackenzie *et al*., 2010.

1.1.5.3. FUS

Shortly after the discovery of TARDBP as an ALS-related gene, mutations in fused in sarcoma/translocated in liposarcoma (FUS/TLS) were identified (Kwiatkowski, Bosco et al. 2009, Vance, Rogelj et al. 2009). Thirty mutations have been reported so far which account for 4% of fALS and 1% of sALS and they are associated with young onset disease (Lagier-Tourenne, Polymenidou et al. 2010, Renton, Chiò et al. 2014). Most are missense mutations, affecting highly conserved regions in exon 15 that encodes the C-terminus. The inheritance pattern is usually dominant with the exception of one family with autosomal recessive disease (Kwiatkowski, Bosco et al. 2009). Most patients with FUS mutations show a typical ALS clinical phenotype, with no associated cognitive dysfunction (Lagier-Tourenne, Polymenidou et al. 2010). The FUS gene, located on chromosome 16, encodes for a 15-exon RNA binding protein formed by 526 amino acids, which is involved in many cellular processes such as splicing, transcription and miRNA processing (Aman, Panagopoulos et al. 1996, Ratti and Buratti 2016). FUS/TSL contains different functional domains including an N-terminal domain enriched in glutamine, glycine, serine and tyrosine residues (QGSY region), a glycine-rich region, a RNA-recognition motif (RRM) and a highly conserved C-terminal nuclear localization signal (NLS) where the majority of the mutations reported occur (**figure 7**) (Iko, Kodama et al. 2004). FUS is ubiquitously expressed and is present in both the nucleus and cytoplasm; however, in neurons there is proportionally more in the nucleus and expression in glia is exclusively nuclear (Andersson, Ståhlberg et al. 2008). Post-mortem analysis of brain and spinal cord from patients with FUS/TLS mutations found abnormal FUS/TLS cytoplasmic inclusions in neurons and glial cells (Neumann, Rademakers et al. 2009). The presence of FUS inclusions in the cytoplasm of ALS-FUS patients suggested that mislocalization of FUS to the cytoplasm may have a role in the pathogenesis of the disease. FUS is an aggregation prone protein, but this may not be influenced by ALS-linked mutations.

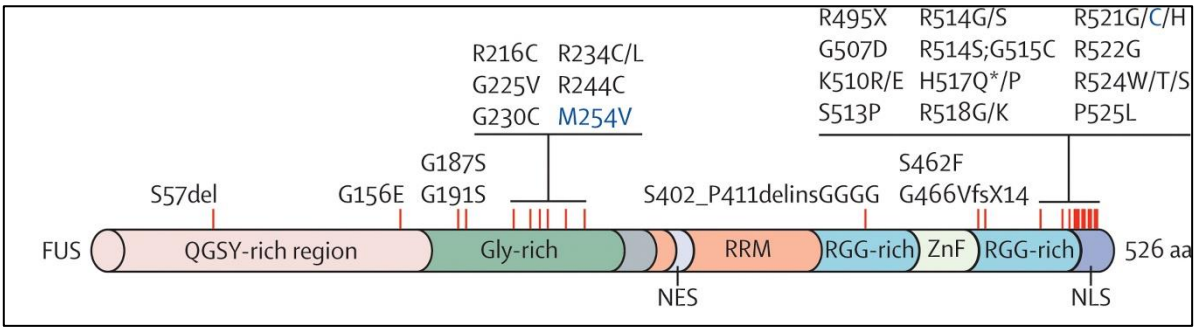

Figure 7. Schematic overview of protein domains of FUS and identified gene mutations associated with ALS. Adapted from Mackenzie *et al*., 2010.

1.1.5.4. C9ORF72

Recently, linkage analysis of single kindreds presenting both ALS and FTLD phenotypes and genome wide association studies (GWAS) identified a locus on chromosome 9p21 as a potential cause of ALS (Vance, Al-Chalabi et al. 2006, Laaksovirta, Peuralinna et al. 2010, Shatunov, Mok et al. 2010). A huge GGGGCC hexanucleotide repeat expansion within the first intron of chromosome 9 open reading frame 72 (C9ORF72), which was shown to co segregate with the disease in several families, was found to be causative (DeJesus-Hernandez, Mackenzie et al. 2011, Renton, Majounie et al. 2011). The size of the expansion has been estimated to range between 700 and 1600 units in ALS and FTLD patients, while in healthy individuals the repeat length is usually between 2 and 23 hexanucleotide units (DeJesus-Hernandez, Mackenzie et al. 2011). This mutation now accounts for 20-80% of familial and 5-15% of sporadic ALS (Renton, Chiò et al. 2014). There are three potential mechanisms associated with the GGGGCC repeat expansion: haploinsufficiency, RNA gain of function and RAN translation (Ling, Polymenidou et al. 2013). The first mechanism to be proposed is a reduction in the expression levels of C9ORF72. Loss of function as a potential underlying mechanism leading to neurodegeneration was indeed reported by different studies (Ciura, Lattante et al. 2013, Xi, Rainero et al. 2014). Moreover, RNA foci containing the hexanucleotide repeat expansion have been found to accumulate in the brain and spinal cord of people with ALS (DeJesus-Hernandez, Mackenzie et al. 2011); RNA foci are able to sequester RNA-binding proteins thus affecting RNA metabolism (Mori, Lammich et al. 2013), suggesting another possible disease

mechanism. Another pathogenic pathway underlying C9ORF72-related neurodegeneration is repeat associated non-ATG translation (RAN). RAN translation is an unconventional mechanism of translation that occurs in the absence of an upstream AUG codon and was first described by Zu et al. in 2011 (Zu, Gibbens et al. 2011). In C9 ALS, RAN translation occurs from sense and antisense transcripts and it results in the production of different dipeptide repeats proteins (DPRs) that can accumulate inside the cell (Mori, Arzberger et al. 2013, Mori, Weng et al. 2013, Zu, Liu et al. 2013).

2. TDP-43

2.1. TDP-43 in physiological conditions

TDP-43 is a DNA/RNA binding protein expressed ubiquitously. It is formed by 414 amino acids and contains an N-terminal domain (NTD), two well-folded and stable RNA recognition motifs (RRM1 and RRM2), spanning residues 106-177 and 192-259, respectively, followed by a long intrinsically disordered C-terminal region. TDP-43 and, in particular, its N-terminal and RRM domains are well conserved in animals. Recent findings show that the NTD is stably folded and that its structure is crucial for TDP-43 to be able to carry out its physiological functions (Mompeán, Romano et al. 2016, Mompeán, Romano et al. 2017). The deletion of a short segment of the NTD corresponding to the first β-strand, which causes the domain's denaturation, has severe physiological effects in mice (Sasaguri, Chew et al. 2016). The stably folded NTD also promotes dimerization, which is relevant to the protein's activities (Mompeán, Romano et al. 2017). In contrast to the N-terminal and RRM domains, the C-terminal region of the protein is intrinsically disordered and consists of four segments. Two of which (residues 267–320 and 367–414) are rich with Gly and trigger the formation of liquid phases (known as “microdroplets” such as stress granules). A third segment is hydrophobic and tends to adopt helical conformations (Jiang, Che et al. 2013, Lim, Wei et al. 2016) and also drives the formation of a distinct, non-aqueous liquid phase (Conicella, Zerze et al. 2016). The fourh segment of TDP-43 is the Q/N-rich region, as it contains high proportion of Gln and Asn residues (Budini, Buratti et al. 2012, Mompeán, Hervás et al. 2015).

The nuclear localization signal (NLS) and the leucine-rich nuclear export signal (NES) allow TDP-43 to shuttle between the nucleus and the cytoplasm, although under physiological conditions the majority seems to be nuclear (Ayala, Zago et al. 2008). The first RRM is necessary and sufficient for nucleic acid binding activity with high specificity for UG-rich sequences (Buratti and Baralle 2001). In particular, Phenylalanine 147 and 149, which are located in the RNP-1 sequence of RRM-1, form a structure that allows DNA and RNA binding (Buratti and Baralle 2001, D'Ambrogio, Buratti et al. 2009). The role of RRM2 is still unclear, however it does not appear to be involved in RNA interaction since its RNA binding affinity was found to be much lower than that of RRM-1 (Kuo, Doudeva et al. 2009). Furthermore, the C-terminal domain as well is involved in regulating the alternative splicing of CFTR exon 9 through the recruitment of other hnRNPs (D'Ambrogio, Buratti et al. 2009).

TDP-43 was originally described as a factor binding to the long terminal repeat (LTR) of the Human Immunodeficiency Virus type 1 (HIV-1) and thereby suppressing its transcription and gene expression (Ou, Wu et al. 1995). Since then however this role has come into question. In 2001, TDP-43 was indeed identified as a heterogeneous nuclear ribonucleoprotein (hnRNP), involved in the splicing regulation of human cystic fibrosis transmembrane regulator (CFTR) by binding to the UG repeats near the 3' splice site of CFTR exon 9 (Buratti and Baralle 2001). Subsequently, TDP-43 has been shown to regulate gene expression and alternative splicing of several other targets, and to be involved in microRNA and mRNA biogenesis as well as RNA turnover and stability (Buratti and Baralle 2010, Ratti and Buratti 2016).

2.1.1. Regulation of POLDIP3 exon 3 alternative splicing

Particular relevant to this thesis is TDP-43 known role as regulator of polymerase delta interacting protein (POLDIP3) alternative splicing. POLDIP3 is a substrate for S6K1, which is downstream of mTOR, and has been reported to enhance mTOR/S6K1 dependent translation of mRNA, which is involved in cell proliferation and growth (Ma, Yoon et al. 2008). It can exist in two isoforms according to the inclusion or exclusion of exon 3 in the mature mRNA: variant-1, which includes exon 3, and variant-2 that lacks exon 3. It was reported by two different groups that, when TDP-43 is silenced in cells, POLDIP3 variant-1 decreases while variant-2 increases, meaning that alternative splicing is dependent on TDP-43 activity (**figure 8**) (Fiesel, Weber et al. 2012, Shiga, Ishihara et al. 2012).

Furthermore, POLDIP3 variant-2 was found to increase in the affected tissues of ALS patients, including motor cortex and spinal cord, suggesting that a loss of function of TDP-43 may be involved in the pathogenesis of ALS (Shiga, Ishihara et al. 2012, Yang, Wang et al. 2014).

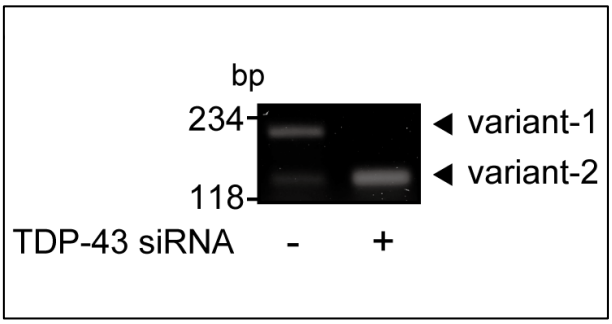

Figure 8. POLDIP3 alternative splicing is regulated by TDP-43.

Representative gel of RT-PCR products from control cells, and cells treated with TDP-43 siRNA, using POLDIP3 specific primers spanning exon 3. Adapted from Shiga et al., 2012.

The RNA binding ability of TDP-43 is necessary for the inclusion of exon 3. In fact, mutations in Phe147 and Phe149 in RRM1, which abolish TDP-43 nucleic acid binding activity, prevent exon 3 inclusion (Budini, Romano et al. 2015). TDP-43 binds to the intronic sequences, preferentially $(UG)_n$ sequence, and the position of the TDP-43 binding site is associated with exclusion or inclusion of an exon. However, the precise mechanism for regulation of splicing is still not clear (Tollervey, Curk et al. 2011, Shiga, Ishihara et al. 2012).

Variant-1 and variant-2 are both located in the nucleus. However, the function of variant-2 has not been well elucidated (Richardson, Bröenstrup et al. 2004). Most recently, it has been reported that POLDIP3 variant-2 enhanced the mTOR/S6K1-dependent translation of mRNA, and the depletion of TDP-43 increased cell size in HEK293E cells (Fiesel, Weber et al. 2012).

2.2. TDP-43 in ALS

Although predominantly nuclear, in pathological conditions TDP-43 is mislocalized to the cytoplasm in the form of inclusion bodies leading to a loss of normal TDP-43 immunoreactivity in the nucleus of inclusion-bearing cells (**figure 9**); this is a striking feature of ALS and the other TDP-43 proteinopathies (Neumann, Sampathu et al. 2006, Geser, Martinez-Lage et al. 2009, Igaz, Kwong et al. 2009, Neumann 2009). TDP-43 proteinopathy has indeed been found in the majority of sporadic and familial ALS cases (97%), with the exception of patients harbouring SOD1 mutations, which have ubiquitin-positive neuronal inclusions that are negative for TDP-43 (Mackenzie, Bigio et al. 2007).

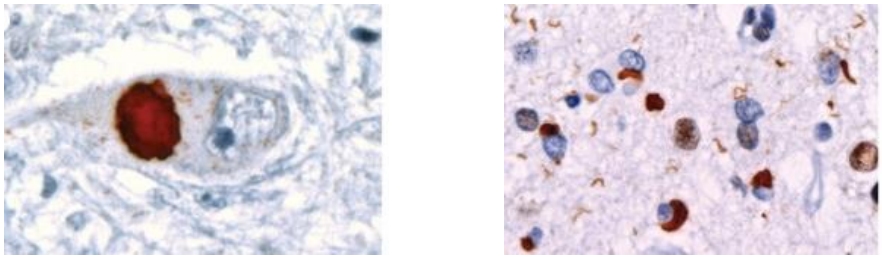

Figure 9. Representation of TDP-43 cytoplasmic inclusions in motor neurons in ALS.

The presence of abnormal proteinaceous aggregates in affected neurons and glia is a pathological hallmark of most age-related neurodegenerative diseases (Ross and Poirier 2005). However, the presence of inclusions does not necessarily lead to the reduction of a protein in its normal location; clearance of huntingtin protein is not observed in cells that show huntingtin inclusions associated with Huntington's disease (DiFiglia, Sapp et al. 1997).

What triggers aggregation in disease is one of the most unresolved questions in ALS and other neurodegenerative diseases characterized by the presence of protein inclusions. Dysfunction of proteostasis (e.g. misregulation of protein folding) that occurs with aging and mutations that increase the aggregation propensity of proteins (e.g. the A90V ALS-linked mutation of TDP-43 results in increased cytoplasmic localization (Winton, Van Deerlin et al. 2008)) are thought to be involved.

As for sporadic diseases, environmental/stress and genetic-risk factors might contribute to the pathogenic process (Lee, Lee et al. 2011, Polymenidou and Cleveland 2011).

Whether inclusions are toxic themselves or they are protective is also in many cases still unclear. In the case of TDP-43, several experimental models have demonstrated that TDP-43 aggregates are not necessary to induce neurodegeneration, however they might still contribute to cell death. Other pathogenic changes such as nuclear clearance and post-translational modifications of TDP-43 such as ubiquitylation, truncation and phosphorylation could also be important to trigger disease.

Currently, two main hypotheses have been proposed for TDP-43-mediated neurodegeneration in ALS: the loss-of-function hypothesis suggests that nuclear depletion of TDP-43 following its aggregation in the cytoplasm might cause a dysfunction in RNA processing thus affecting the whole cell metabolism. In this case, the aggregates act as sinks, entrapping TDP-43 in the cytoplasm and causing loss of function (Winton, Igaz et al. 2008, Budini, Buratti et al. 2012). On the other hand, the second hypothesis, known as gain-of-function, suggests that inclusions might be toxic by themselves (Johnson, Snead et al. 2009, Zhang, Xu et al. 2009). It is still not clear which hypothesis is correct; however, both mechanisms could equally contribute to disease onset and progression. Different experimental models have been created in order to address this issue; most of them have been developed by over expression of different C-terminal regions of TDP-43 (Igaz, Kwong et al. 2009) or by restricting its localization to the cytoplasm (Winton, Igaz et al. 2008). A deeper overview on TDP-43 ALS models will be given in the next chapter.

2.2.1. TDP-43 autoregulation

Considering the gain and loss of function models, many studies have concentrated their efforts on better understanding the way TDP-43 protein levels are regulated. We now know that regulation of protein levels occurs through a negative feedback loop that has been reported for different RNA processing factors including hnRNP members (Rossbach, Hung et al. 2009).

Overexpression of exogenous TDP-43 leads to a decrease in endogenous TDP-43 mRNA and protein in mice and cultured cells (Winton, Igaz et al. 2008, Igaz, Kwong et al. 2011). Indeed, as for other RNA regulatory proteins, TDP-43 acts as a regulator of its own expression through a negative

feedback loop (Ayala, De Conti et al. 2011). This happens at the transcript level through a mechanism that involves binding to a specific region of its 3' UTR that is called the TDP-43 binding region (TDPBR). This region has been found to contain low affinity binding sites for TDP-43 that are not made by continuous UG repeats that has been identified as the highest affinity-binding sequence for TDP-43. This suggests that several TDP-43 molecules would be required to bind to that region in order to have an effect (Ayala, De Conti et al. 2011). When TDP-43 nuclear levels increase, binding to the 3' UTR promotes mRNA instability, which in turn will result in lower levels of protein being produced (Ayala, De Conti et al. 2011, Avendaño-Vázquez, Dhir et al. 2012). The opposite effect should be achieved in the case of a drop of TDP-43 levels under the physiological threshold. The interaction between TDP-43 and its own 3' UTR has been confirmed by crosslinking and immunoprecipitation as well (Tollervey, Curk et al. 2011). Increased instability of mRNA is not the only active mechanism in mediating autoregulation. The exosome system, has also been observed to reduce the levels of TDP-43 mRNA under overexpression conditions (Buratti and Baralle 2011). Moreover, it has been shown that the C-terminal domain, and in particular the region between aa 321 and 366, is also involved in the autoregulation process and is likely to involve hnRNP recruitment. This suggested that TDP-43 mutations might interfere with its homeostatic control resulting in the aberrant accumulation of the protein (Ayala, De Conti et al. 2011).

2.2.2. Autoregulation and disease

It has been shown that both an increase and a decrease in the levels of TDP-43 lead to cytotoxicity (Ling, Polymenidou et al. 2013). Homozygous TDP-43 null mice do not survive beyond embryonic day 6, while heterozygote mice are viable with autoregulation keeping TDP-43 levels nearly normal (Kraemer, Schuck et al. 2010); ubiquitous post-natal knock down of TDP-43 caused lethality (Chiang, Ling et al. 2010), while selective removal of TDP-43 from motor neurons produced age-dependent progressive degeneration with ALS-like pathology (Iguchi, Katsuno et al. 2013). On the other side, increased TDP-43 levels are highly deleterious as well (Wils, Kleinberger et al. 2010, Igaz, Kwong et al. 2011). Increasing TDP-43 levels in mice and rats by expression of RNAs missing the autoregulatory sequences (Wegorzewska, Bell et al. 2009) or by disrupting autoregulation (Igaz, Kwong et al. 2011)

led to neurodegeneration. Thus, TDP-43 levels has to be tightly regulated in order to guarantee cell function and survival.

However, it is still not clear whether nuclear or cytoplasmic TDP-43 regulates the amount of TDP-43. In ALS, nuclear TDP-43 decreases, while cytoplasmic TDP-43 increases as inclusions. The newly synthetized protein is indeed sequestered into the cytoplasmic aggregates constantly depleting it from the nucleus. If cytoplasmic TDP-43 contributes to the autoregulation mechanism, mislocalization and subsequent accumulation of the protein in the cytoplasm will trigger a negative-feedback loop that decreases TDP-43 synthesis leading to a drop in nuclear levels (Lee, Lee et al. 2011). On the other hand, if nuclear TDP-43 is involved in autoregulation, then loss of TDP-43 from the nucleus due to sequestration into the insoluble aggregates might stimulate an upregulation of the synthesis of TDP-43 in order to maintain its physiological levels. Increased production of TDP-43 could lead to an increase in aggregate formation, creating a vicious cycle that might accelerate disease progression (Buratti and Baralle 2011). Different studies found the amount of cytoplasmic TARDBP mRNA increased in affected neurons from ALS patients, indicating that nuclear TDP-43 is involved in the autoregulation mechanism (Koyama, Sugai et al. 2016).

2.2.3. Post translational modifications of TDP-43

As already mentioned, TDP-43 is the major component of ubiquitin-positive inclusions in the affected regions of the central nervous system of approximately 97% of patients suffering from ALS. It was shown that these aggregates were formed by full-length as well as C-terminal fragments of TDP-43 that were abnormally phosphorylated and ubiquitinated (Arai, Hasegawa et al. 2006, Neumann, Sampathu et al. 2006). In physiological conditions, these post translational modifications do not occur, making the presence of these modified TDP-43 species in ALS disease-specific. However, it is not clear whether they are a cause of aggregate formation and/or neurotoxicity or they are a normal reaction to the presence of inclusions. Studies on human tissue show that not all TDP-43 inclusions are ubiquitin positive; in particular, the so-called pre-inclusions, that are granular and less dense cytoplasmic inclusion, are often not ubiquitin positive (Giordana, Piccinini et al. 2010), suggesting that ubiquitination might not be involved in aggregate formation but might be a later event in the disease process. However, the presence of ubiquitinated aggregates might also be

an indirect evidence of a failure in the degradation of defective proteins, which normally occurs through the proteasome or autophagy (Winton, Igaz et al. 2008). A more detailed discussion on autophagy and proteasome dysfunction in ALS will be given in a separate chapter.

On the other side, phosphorylation seems to be an early event in the onset and progression of ALS (Hasegawa, Arai et al. 2008, Neumann, Kwong et al. 2009). However, the precise role of TDP-43 phosphorylation in the disease mechanisms is still unclear. A recent paper by Nonaka and collaborators shows that hyperphosphorylation of TDP-43 causes its mislocalization and accumulation in the cytoplasm. According to them, multiple phopsphorylation at Ser393/395 and/or Ser403/404 is likely to trigger aggregation by causing conformational changes in the structure of the protein. The phosphorylated amino acid residues are located in the C-terminal domain, which is thought to be important in the self-aggregation process (Nonaka, Suzuki et al. 2016). Alternatively, as TDP-43 was shown to be associated with insolubility, it is also possible that phosphorylation may inhibit UPS-mediated degradation thus contributing to aggregation (Zhang, Gendron et al. 2010). Whether phosphorylation enhances TDP-43 accumulation, or it is a defence mechanism to reduce aggregation remains unknown (Li, Yeh et al. 2011).

The presence of detergent-insoluble TDP-43 C-terminal fragments (CTFs) is a pathological hallmark of ALS pathology in the brain (Neumann, Sampathu et al. 2006, Hasegawa, Arai et al. 2008). CTFs derive from the proteolytic cleavage of full-length TDP-43 that results in the accumulation of 35 and 20/25 kDa fragments. CTFs identified in brain are more prone to form aggregates than the full-length protein, in cultured cells (Igaz, Kwong et al. 2009, Nonaka, Arai et al. 2009); the C-terminal domain has indeed been shown to be important for aggregation in vitro (Johnson, Snead et al. 2009). Further, CTFs are able to bind endogenous TDP-43 inducing aggregation, as reported in different papers (Nonaka, Kametani et al. 2009, Zhang, Xu et al. 2009). Therefore, generation of CTFs may have a crucial role in the disease pathogenesis. However, Nonaka and collaborators reported that full-length TDP-43 aggregation occurred before the deposition of CTFs, suggesting that cleavage of TDP-43 is not a trigger for cytoplasmic accumulation. On the contrary, CTFs might be a consequence of the degradation of phosphorylated full-length TDP-43 (Nonaka, Masuda-Suzukake et al. 2013).

Multiple mechanisms for the generation of CTFs have been proposed; alternative splicing has been shown to generate 35 kDa CTFs (Xiao, Sanelli et al. 2015). However, proteolytic cleavage seems to be more likely. Caspase 3 is indeed able to cut full-length TDP-43 into 25 and 35 kDa C-terminal fragments (Dormann, Capell et al. 2009); furthermore, TDP-43 has several calpain cleavage sites for

the generation of 33-36 kDa fragments (Yamashita, Hideyama et al. 2012). Further studies are required to better understand the mechanisms underlying CTFs generation and their role in the development of TDP-43 pathology in ALS and other TDP-43 proteinopathies.

2.2.4. TDP-43 prion-like properties

Prions are infectious agents formed by a misfolded form of a normal protein. Prions replicate by recruiting the wild-type protein into prion-containing aggregates and inducing a pathological misfolded conformation (Prusiner 1982). In the past years, several neurodegenerative diseases have shown "prion-like" phenomena. The term "prion-like" is normally used to describe molecular events that resemble the infectious cycle of prion proteins, which include seeded aggregation and spreading of misfolded conformations of proteins involved in neurodegenerative diseases (Polymenidou and Cleveland 2011).

TDP-43 forms aggregates *in vitro* (Johnson, McCaffery et al. 2008, Johnson, Snead et al. 2009, Furukawa, Kaneko et al. 2011) and ALS-linked mutations were shown to enhance this behaviour (Johnson, Snead et al. 2009, Guo, Chen et al. 2011). The C-terminal domain of TDP-43, where the majority of the mutations are found (Lagier-Tourenne, Polymenidou et al. 2010), is thought to play an important role in ALS pathogenesis, especially since it was discovered to be the main proteolytic fragment of cytoplasmic inclusions in sporadic patients (Arai, Hasegawa et al. 2006, Neumann, Sampathu et al. 2006, Igaz, Kwong et al. 2008). The same region was found to contain a glutamine/asparagine-rich domain (Q/N) that share similarities with yeast prions (Fuentealba, Udan et al. 2010), proteins that can switch their conformation between an unfolded one and an aggregated one that imposes its conformation to its unfolded counterpart, showing self-perpetuating aggregation (Chien, Weissman et al. 2004, Cushman, Johnson et al. 2010). Results coming from a structural characterization of this Q/N prion-like region, has recently shown that this domain is normally in a disordered conformation that can form β-sheet strands spontaneously over time (Mompeán, Buratti et al. 2014), suggesting a possible TDP-43 aggregation pathway during disease. Moreover, overexpression of tandem repetitions of the Q/N region of TDP-43 (residues 339-369) linked to enhanced green fluorescent protein (EGFP) in cells, produced aggregates that were able to sequester full-length TDP-43 and recapitulated some properties of the inclusions found

in patients such as ubiquitination and phosphorylation (Budini, Buratti et al. 2012). Collectively, these data suggest that aggregation of TDP-43 is probably driven by its prion-like C-terminal region and that ALS-linked mutations are likely to promote this process. A study conducted by Nonaka *et al*. showed that TDP-43 aggregates in brains of ALS patients have prion-like properties, including the ability to trigger intracellular TDP-43 aggregation and cell-to-cell transmissibility. According to them, prion-like aggregates are released from cells and then taken up by neighbouring cells, where they act as seeds for endogenous TDP-43 aggregation. Phosphorylated TDP-43 aggregates are probably propagated between cells via exosomes in a way that is similar to that of prions (Nonaka, Masuda-Suzukake et al. 2013). Different studies suggest that prion-like propagation of protein aggregates may be involved in the pathogenesis and progression of neurodegenerative diseases (Braak, Del Tredici et al. 2003, Goedert, Clavaguera et al. 2010, Nonaka, Watanabe et al. 2010).

3. Intracellular proteolytic pathways

Proteins are dynamic molecules that undergo synthesis, proper folding and assembly and ultimately degradation. A network of pathways called the proteostatic network is responsible for maintaining the balance between these events and involves molecular chaperones and the proteolytic machinery (Crippa, Carra et al. 2010, Carra, Crippa et al. 2012). Proteolysis is important in the elimination of misfolded proteins and aggregates (Balch, Morimoto et al. 2008). Formation of misfolded protein aggregates is indeed a physiological phenomenon, and the quality control mechanisms of the cell either degrade the misfolded proteins to avoid aggregate formation or clears aggregates that have already formed. However, the high presence of protein inclusions in ALS and other neurodegenerative diseases suggests a dysfunction in these mechanisms. In eukaryotic cells there are two main proteolytic pathways: the ubiquitin-proteasome system (UPS) and the lysosome-autophagy pathway (Ramesh and Pandey 2017).

3.1. The ubiquitin-proteasome system

The proteasome is responsible for the degradation of the majority of intracellular misfolded or short-lived proteins in all tissues (Rock, Gramm et al. 1994). Cellular proteins that are targeted for degradation by the proteasome are tagged to ubiquitin, a protein formed by 76 amino acids. Ubiquitin is conjugated to the target protein through a covalent bound that is created between the C-terminal glycine of ubiquitin and a specific lysine residue on the target protein (Lecker, Goldberg et al. 2006). A similar linkage is formed between ubiquitin and another ubiquitin molecule to form poly-ubiquitin chains. The lysine residue on which polybiquitination occurs is important; formation of polyubiquitin chains by linkage at Lys-48 and Lys-29 act as a signal for proteasome-mediated degradation, whereas ubiquitination at other lysine residues may act as signals for DNA repair or activation of transcription factors *etc*. (Weissman 2001). Three enzymatic components are required to link ubiquitin chains onto proteins that are destined for degradation; an activating enzyme (E1) transfers ubiquitin to a carrier enzyme (E2) which tags ubiquitin to the substrate with the help of an E3 ligase (**figure 10**). In cells, there are more than 1000 E3s, which conjugate Ub to proteins in a highly regulated manner. E3s catalyse the transfer of the activated Ub from an E2 enzyme initially to a lysine in the target protein and subsequently to lysines that are present in Ub, yielding a substrate-anchored chain of Ub molecules (Jentsch 1992).

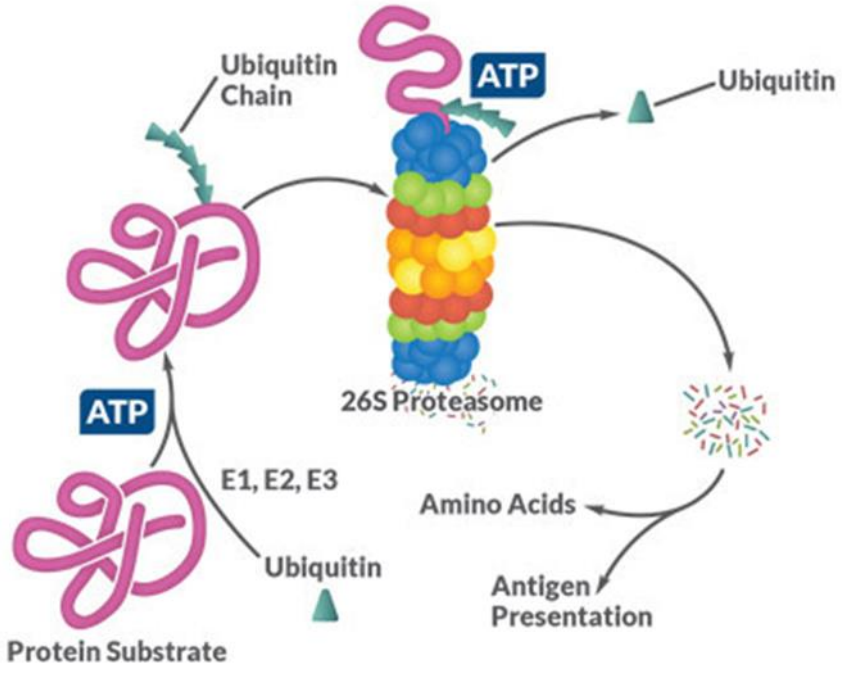

Figure 10. The Ubiquitin-Proteasome Pathway.

Target proteins are ubiquitinated in a three-step ATP-dependent process involving E1, E2, and E3. The protein is then unfolded and degraded into small peptides in the proteasome, where they can be used in antigen presentation or hydrolyzed to individual amino acids. Adapted from (Lecker, Goldberg et al. 2006).

The structure of the proteasome consists of the 20S subunit, harbouring the proteolytic core, linked to the 19S subunit or cap complex. The proteasome degrades unfolded proteins in an ATP-independent manner, but it cannot degrade ubiquitin-protein conjugates. Thus, ubiquitin has to be removed from the tagged proteins before they enter the proteolytic core of the proteasome. The 19S complex, also known as regulatory particle, has the role of directing ubiquitinated proteins into the catalytic core for degradation. The active sites of the 20S subunit are indeed located within the lumen of the catalytic core particle to avoid non-specific degradation of cellular proteins. The 19S contains subunits that bind the polyubiquitin chains plus two deubiquitinating enzymes (also called isopeptidases) that disassemble the Ub chain so that ubiquitin can be reused in the degradation of other proteins. By utilizing its ATPase activity, the 19S acts as a reverse chaperone to unfold target proteins and facilitates opening the pore of 20S. (Glickman and Maytal 2002). The core particle consists of four heptameric rings (two outer α rings and two inner β rings) that are made of seven different but related subunits. The α subunits form a selective barrier between the catalytic chamber and the cytoplasm. On the other hand, β subunits harbour the proteolytic site (Voges, Zwickl et al. 1999). Eukaryotic proteasomes have three major peptidase activities: chymotrypsin-like activity (cleavage after hydrophobic amino acids), trypsin-like activity (cleavage after the basic amino acids) and caspase-like activity (cleavage after acidic amino acids) (Voges, Zwickl et al. 1999). After the substrate enters the 20S's central chamber, the polypeptide is cleaved by its six proteolytic sites forming small peptides that range from three to 25 residues in length (Kisselev, Akopian et al. 1999). The proteasome digests the substrates all the way to small peptides that exit the particle, unlike traditional proteases, which cut a protein once and release the fragments. Peptides that are released by the proteasome are quickly digested into amino acids by the abundant cytosolic endopeptidases and aminopeptidases. The amino acids can be then reutilized to synthesize new proteins or metabolized, yielding energy (Saric, Graef et al. 2004).

3.2. Autophagy

Autophagy is a degradative system normally active at basal levels in the majority of cell types where it is involved in maintaining the integrity of intracellular organelles and proteins. However, it is strongly induced by starvation and is a key component of the adaptive response of cells to nutrient deprivation (Mizushima 2007). Under normal conditions, maintenance of the amino acid pool relies primarily on the ubiquitin-proteasome system. During starvation, necessary amino acids are produced by autophagy instead, which is up-regulated as an adaptive response (Vabulas and Hartl 2005). Indeed, it has been shown that in autophagy-deficient yeast cells and mice, amino acids levels decrease when they are under starvation conditions (Kuma, Hatano et al. 2004, Onodera and Ohsumi 2005).

There are three types of autophagy: macro-autophagy, micro-autophagy, and chaperone-mediated autophagy; all of them are degradative-recycling systems coupled with the lysosome. Macro-autophagy delivers cytoplasmic cargo to the lysosome through double membrane vesicles, referred to as autophagosomes, which fuse with the lysosome to form autolysosomes. On the other side, in micro-autophagy cytosolic components are directly taken up by the lysosome itself. Both of them are able to engulf large structures through selective and non-selective mechanisms. Autophagy begins with an isolation membrane, known as phagophore, which expands to engulf intra-cellular cargo such as protein aggregates, organelles and ribosomes forming an autophagosome. Autophagosomes are formed in the cytoplasm and are moved along microtubules in a dynein-dependent manner towards the microtubule-organizing centre; here they fuse to lysosomes forming autolysosomes where the content is degraded by lysosomal acid proteases. Lysosomal permeases and transporters then export amino acids and other by-products of degradation out to the cytoplasm where they can be recycled (**figure 11**) (Mizushima 2007).

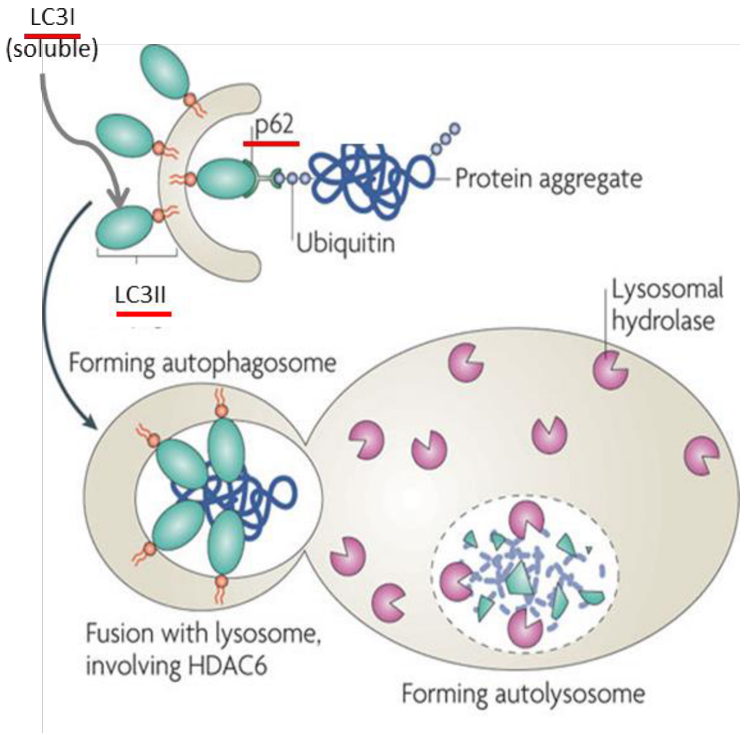

Figure 11. Model of the degradation of protein aggregates through autophagy.
Ubiquitination of the protein aggregates is the signal that triggers the degradation of the protein aggregate. Main players include LC3, p62 and HDAC6. Adapted from Tyedmers *et al.,* 2010.

Although autophagy was considered as a random and non-selective process, there is evidence that the phagophore membrane can interact selectively with protein aggregates and organelles. Microtubule-associated light chain (LC3B-II), which is recruited and integrated into the growing phagophore, has been proposed to function as a receptor that interacts with specific molecules on the target to induce their selective uptake and degradation. In this regard, p62/SQSTM1 is the best characterized molecule. Indeed, p62/SQSTM1 interacts with polyubiquitinated proteins and aggregates through its ubiquitin-binding domain (UBD) and with LC3B-II through its LC3-interacting region (LIR) (Bjørkøy, Lamark et al. 2005, Pankiv, Clausen et al. 2007). P62 has been shown to accumulate in autophagy-deficient cells suggesting that it is usually degraded by autophagy (Wang,

Ding et al. 2006, Nakai, Yamaguchi et al. 2007). LC3B is expressed in most cell types as a full-length cytosolic protein that, upon autophagy induction, is cleaved to generate LC3B-I. The carboxyterminal glycine is then activated in an ATP-dependent manner and conjugated to phosphatidylethanolamine (PE) to generate LC3B-II, which is then integrated into the growing phagophore. The synthesis and processing of LC3 is increased during autophagy, making it a key readout of levels of autophagy in cells (Barth, Glick et al. 2010).

3.3. UPS and autophagy in ALS

Protein aggregates in ALS are ubiquitinated, suggesting that they are marked for degradation by the UPS but eventually deposit due to dysfunction in the UPS system. In this regard, studies on spinal cord tissue from patients showed that ubiquitination occurs before accumulation starts (Giordana, Piccinini et al. 2010). Moreover, proteasome inhibition has been previously found to increase endogenous TDP-43 levels and induce aggregates of full-length TDP-43 (Zhang, Gendron et al. 2010, van Eersel, Ke et al. 2011). Consistently, knockout of different subunits of the proteasome in motor neurons was shown to cause neurodegeneration with loss of spinal motor neurons and locomotor dysfunction in mice (Bedford, Hay et al. 2008, Tashiro, Urushitani et al. 2012). Interestingly, these mice had inclusions positive for TDP-43, indicating that proteasome dysfunction itself was sufficient to trigger aggregation.

The presence of intracellular protein inclusions are a pathological hallmark in the majority of neurodegenerative diseases, and are thought to be dependent on autophagy for their clearance from neurons (Williams, Jahreiss et al. 2006, Rubinsztein, Gestwicki et al. 2007). Different studies reported an increase in the number of autophagosomes in the spinal cord of patients suffering from ALS (Sasaki 2011). This finding suggested that dysfunction in autophagy might contribute to the pathogenesis of this disorder. On the other hand, more recent studies showed that accumulation of autophagosomes represents activation of autophagy as a protective mechanism. However, genetic or functional alterations (e.g. impair in autophagosome-lysosome fusion) and decreased autophagic activity associated with aging may occur leading to aggregate accumulation.

Interestingly, treatment of transgenic TDP-43 mice with autophagy inducers was shown to reduce locomotor deficits and neuron loss (Wang, Guo et al. 2012). This was accompanied by a decrease in

TDP-43 inclusions, indicating that clearance of aggregates by autophagy is able to reduce neurotoxicity. Furthermore, knock out of Atg5 or Atg7 in the central nervous system of mice leads to movement disorders and neurodegeneration characterized by ubiquitin-positive inclusions in different brain areas (Hara, Nakamura et al. 2006, Komatsu, Waguri et al. 2006).

In conclusion, protein degradation pathways have emerged as important modulators of protein aggregation and toxicity in ALS. It is likely that degradation of soluble TDP-43 is mediated primarily by the UPS, and that its accumulation following UPS dysfunction can lead to aggregate formation; on the other hand, autophagy seems to be involved in aggregate clearance. However, in presence of UPS inhibitors, autophagy alone could not degrade aggregates completely indicating that it could not fully compensate for UPS impairment (Scotter, Vance et al. 2014). During aging, the efficiency of both proteolytic pathways declines. Nevertheless, in aged healthy individuals TDP-43 aggregates do not accumulate, suggesting that there might be other causes underlying TDP-43 aggregation. Increasing UPS function could help restoring TDP-43 proteostasis while activation of autophagy might help reducing aggregated TDP-43. Therefore, identifying molecules that selectively enhance each of these processes, and that can be used in combination to reduce TDP-43 accumulation, is a valid therapeutic strategy.

3.4. Tricyclic compounds and their possible role in aggregate clearance

Tricyclic compounds are composed by a three-ring nucleus, which can be substituted on the central ring with a side-chain substituent. They were first used as antihistamines with sedative properties, and later as antipsychotics. They include an important group of tricyclic antidepressants (TCAs), which have been used for over 50 years. TCAs have been identified as inhibitors of mitochondrial permeability transition, which is one of the key factors in the damage to neurons. The increased permeability of the mitochondrial membrane to molecules smaller than 1,500 kDa causes the depolarization of the mitochondria; therefore, the electrochemical gradient, which is necessary for the ATP production, is lost. The common involvement of mitochondria in cell death pathways suggests that heterocyclic compounds might be considered as potential candidates to treat individuals suffering from neurodegenerative diseases that involve neuron loss in the central

nervous system (Stavrovskaya, Narayanan et al. 2004). More recently, other studies reported a neuroprotective role for different tricyclic compounds (Lin, Yeh et al. 2012, Kandil, Abdelkader et al. 2016, Tran, Nguyen et al. 2017). As part of the possible neuroprotective effect, there is evidence that supports that these compounds could reduce protein aggregation (Tsvetkov, Miller et al. 2010, Collier, Srivastava et al. 2017). Regarding this, Tsvetkov and collaborators demonstrated that some tricyclic compounds (nortriptyline, thioridazine and chlorpromazine among others) induce a protective autophagy response in striatal neurons. Moreover, the neuroprotective effect of nortriptyline was further established in a primary striatal culture model of HD. In this study the authors generalized that structurally related tricyclic compounds have similar actions in autophagy induction (Tsvetkov, Miller et al. 2010). Furthermore, in a United States Patent Application Publication the authors confirmed that tricyclic compounds could be used to treat protein aggregation diseases. It was suggested the use of a first active medicament (fluphenazine or thioridazine, among others) to prevent aggregation and a second active medicament (clomipramine or nortriptyline, among others) to disaggregate previously formed inclusions (Wilson & Standley, 2011). From the list of the FDA approved tricyclic compounds, and because of the reasons stated so far, we have selected five compounds for this study as shown in figure 12.

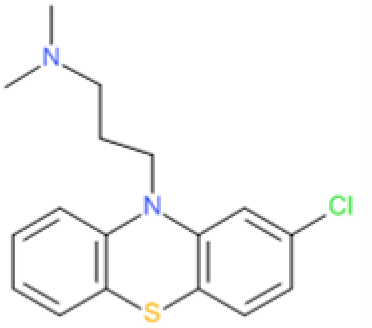

Chlorpromazine

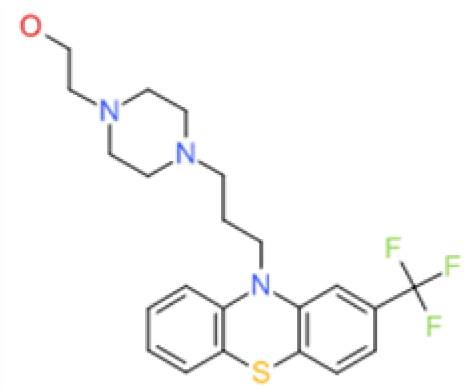

Fluphenazine

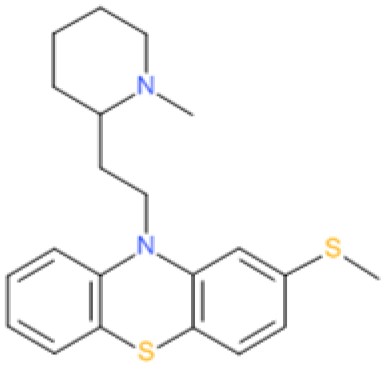

Thioridazine

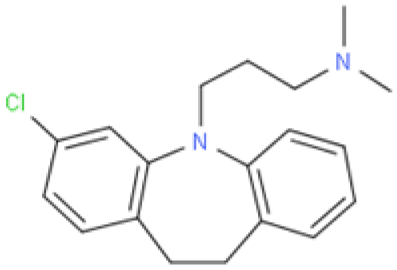

Clomipramine

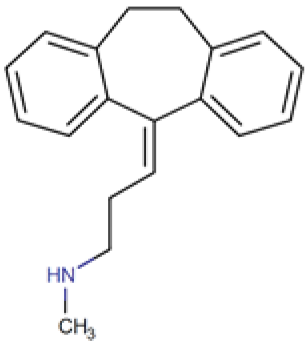

Nortriptyline

Figure 12. Chemical structure of the five FDA-approved tricyclic compounds used in this study.

4. Disease models of TDP-43 proteinopathy

Development of models is the primary stage for understanding the molecular mechanisms behind a disease. In animals these also allow to understand the pathophysiology and for testing future effective therapies.

In order to understand the molecular basis of the pathology, different disease models that overexpress WT human or mouse TDP-43 have been created. Since some consistent mutations in the TARDBP gene have been discovered, transgenic models expressing a mutated form of TDP-43 have also been developed. To evaluate the effect of TDP-43 overexpression, different promoters have been used. Indeed, different promoters trigger different expression patterns of TDP-43, which lead to transgenic animals bearing different phenotypes.

4.1. Cellular ALS TDP-43 models

Several studies have been undertaken in cells trying to mimic TDP-43 aggregation and subsequent nuclear depletion. These models are useful not only to investigate the impact of aggregation on cell survival but also to develop new therapeutic strategies.

As already stated, the majority of the mutations linked to familial ALS are localized in the C-terminal domain of the protein and are likely to increase the aggregation tendency of TDP-43 (Johnson, Snead et al. 2009). Indeed, six of seven ALS-linked TDP-43 mutants, especially the Q331K and M337V mutant, induced the formation of TDP-43 aggregates. Thus, a single amino acid change is sufficient to accelerate TDP-43 misfolding, supporting the notion that some ALS-linked mutations can cause disease by a toxic “gain-of-function mechanism” at the protein level (Johnson *at al.,* 2009).

Several of the more successful models make use of the previously described TDP-43 C-terminal domain that contains a Q/N-rich region that is involved in protein-protein interactions (D'Ambrogio, Buratti et al. 2009); this region has also been recently found to be involved in the self-aggregation process (Fuentealba, Udan et al. 2010). Moreover, the expression of C-terminal fragments of TDP-43 was observed to be sufficient to generate cytoplasmic aggregates (Igaz, Kwong et al. 2009).

Based on these findings, our laboratory developed a cellular model of aggregation using a 30 amino acid TDP-43 C-terminal peptide to induce aggregation (Budini, Buratti et al. 2012, Budini, Romano et al. 2012). The introduction of tandem repeats of the Q/N rich amino acid sequence 331-366 (12xQ/N) linked to EGFP is able to trigger the formation of cytoplasmic aggregates that are capable of sequestering endogenous TDP-43 (**figure 13**). However, there was no detectable splicing function deterioration in the presence of these aggregates, suggesting that they were not efficient enough in trapping endogenous TDP-43 to cause loss of function.

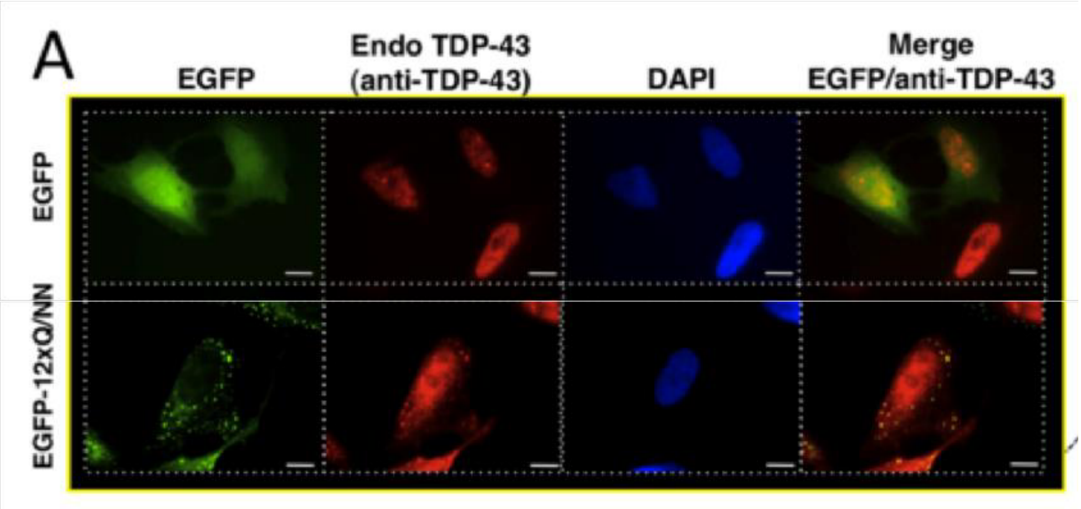

Figure 13. Immunoflorescence of U2OS cells transfected with EGFP or EGFP-12xQ/N constructs. EGFP-12xQ/N forms aggregates, which co-localizes with endogenous TDP-43. Adapted from Budini *et al*., 2012a.

In order to generate a model that could accomplish the nuclear loss of function of TDP-43 seen in ALS, a new variant of the previous model was created. This model was based on the overexpression of the TDP-43 molecule itself linked to tandem repeats of the Q/N region (TDP-12xQ/N). The two phenylalanine in RRM1 and RRM2 were mutated to abolish the RNA binding ability of TDP-43, in order to avoid toxicity due to TDP-43 overexpression. The TDP-12xQ/N model was shown to induce cytoplasmic aggregation (**figure 14**) followed by TDP-43 nuclear depletion and consequent loss of function as assessed by the POLDIP3 splicing pattern (**figure 15**) (Budini, Romano et al. 2015).

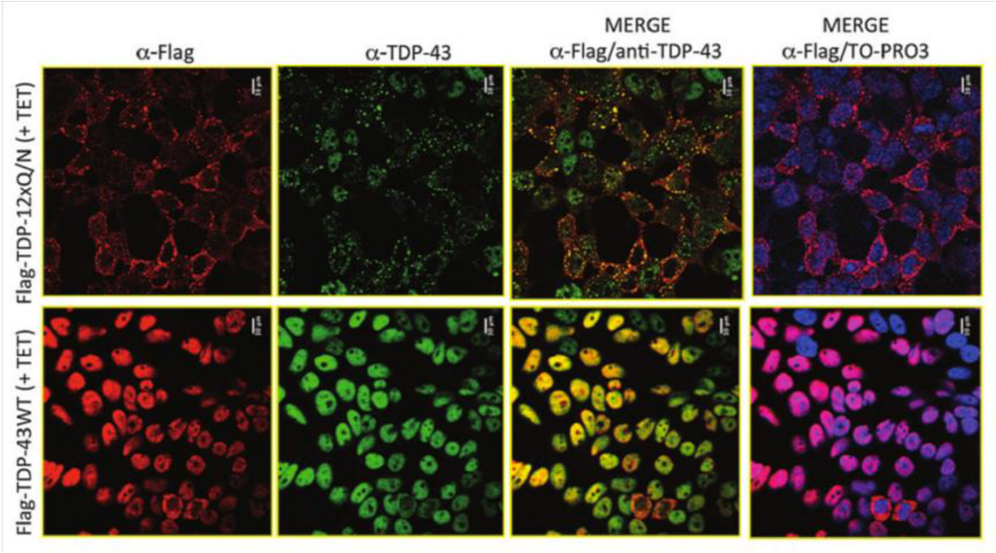

Figure 14. Immunoflorescence of TDP-12xQ/N HEK293 stable cells.

Adapted from Budini *et al*., 2014.

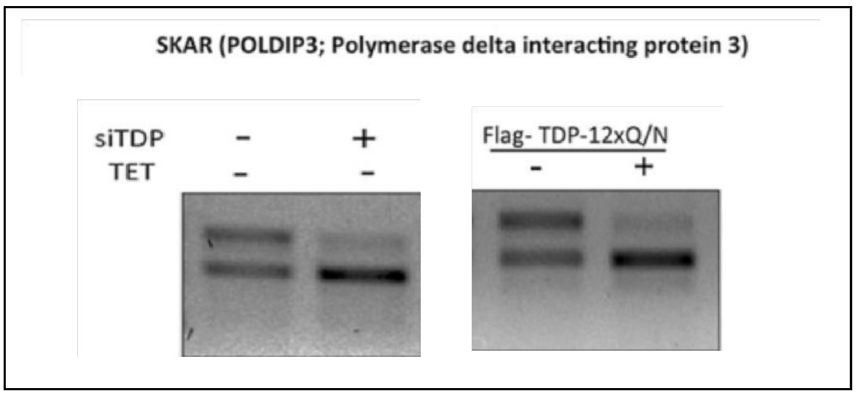

Figure 15. POLDIP3 alternative splicing is affected in cells expressing TDP-12xQ/N.

Representative gel of RT-PCR products from control cells, cells treated with TDP-43 siRNA, and cells expressing TDP-12xQ/N construct (upon tetracycline induction), using POLDIP3 specific primers spanning exon 3. Adapted from Budini *et al.,* 2014.

4.2. Mammalian models

The prion promoter is commonly used to drive the expression of a protein at high levels in the CNS. In ALS, the expression of TDP-43 is around 1.5 fold higher than that of healthy individuals (Cairns, Neumann et al. 2007, Gitcho, Bigio et al. 2009); thus, in an attempt to mimic this scenario, mice overexpressing mutant TDP-43 driven by the mouse prion promoter have been created and were observed to develop motor dysfunction (Wegorzewska, Bell et al. 2009, Stallings, Puttaparthi et al. 2010, Xu, Zhang et al. 2011). However, Xu *et al*. reported that even WT TDP-43 expressed at higher levels is sufficient to trigger TDP-43 proteinopathy (Xu, Gendron et al. 2010). Other transgenic mice lines have been created for the human mutant A315T TDP-43 that has been associated with ALS. These mice had a shorter lifespan with cytosolic aggregates that were ubiquitinated and phosphorylated (Stallings, Puttaparthi et al. 2010). Moreover, prion-promoted TDP-43 Q331K expressing mice produced age-dependent motor neuron disease with a 50% motor neuron loss in the spinal cord. However, motor neuron degeneration occurred without nuclear depletion or cytoplasmic aggregation of TDP-43. The disease then plateaued and the animals died but not of ALS-like symptoms (Arnold, Ling et al. 2013). Furthermore, WT or mutant TDP-43 overexpression under the control of the prion promoter often results in transgenic mammals with early lethality.

Overexpression of WT or mutant TDP-43 regulated by a human endogenous promoter may be better as it allows the generation of transgenic mice with age-related neurodegeneration and motor dysfunctions mimicking those observed in ALS patients. Both wild type and two mutant (G348C and A315T) TDP-43 lines were generated that similarly overexpress TDP-43 approximately 3-fold as compared to the mouse endogenous TDP-43. These mice developed cytosolic TDP-43 aggregates and age-related motor deficits similar to those observed in ALS. However, they did not die of motor neuron disease (Swarup, Phaneuf et al. 2011).

As loss of nuclear function of TDP-43 is clearly involved in ALS pathogenesis, due to the fact that nuclear depletion together with cytoplasmic accumulation of TDP-43 are observed in the vast majority of patients (Neumann, Sampathu et al. 2006), mice have been created using human TDP-43 lacking the nuclear localization signal (NLS). These animals showed a severe phenotype with motor impairments. However, cytoplasmic aggregates as well as C-terminal fragments were not found (Igaz, Kwong et al. 2011, Alfieri, Pino et al. 2014). Mouse models with TDP-43 knock out in motor neurons have also been generated. The homozygote mice where TDP-43 was conditionally

depleted developed a late onset age-dependent motor neuron degeneration with ALS-like pathology (Iguchi, Katsuno et al. 2013). On the other hand, ubiquitous post-natal removal of TDP-43 through conditional gene inactivation produced early lethality but without significant ALS-symptoms (Chiang, Ling et al. 2010). Furthermore, mice with a complete knock out of TDP-43 results in embryonic lethality (Kraemer, Schuck et al. 2010, Wu, Cheng et al. 2010).

In general, none of the TDP-43 mice models created to date seems to develop ALS disease as seen in humans. Mild phenotypes are usually observed in the CNS of animals expressing TDP-43. Indeed, the loss of cortical and spinal motor neurons is very modest if compared to what is seen in ALS patients. Moreover, these models die of causes unrelated to ALS disease pathogenesis. Both wild type and mutant TDP-43 overexpressing models develop motor dysfunctions meaning that high levels of TDP-43 contributes to the phenotype. However, from the animal studies, it seems that both gain and loss of function of TDP-43 might be involved.

Moreover, pathological changes typical of TDP-43 pathology such as cytoplasmic aggregation, C-terminal fragmentation and phosphorylation are seen in some models but not all and are usually found at more moderate levels when compared to what observed in ALS patients. Furthermore, in humans, these changes have more time to develop than in mice and are thought to contribute to neurodegeneration. Therefore, the use of rodent models to study late onset neurodegenerative diseases might be limited.

4.3. Non-mammalian models

Non-mammalian animal models are convenient for understanding the pathological roles of TDP-43 in ALS. *C. Elegans*, zebrafish and *Drosophila Melanogaster* are the organisms of choice due to the simple nervous system. Transgenic *C. Elegans* expressing either mutated or wild type human TDP-43 developed age-dependent motor dysfunction, shorter lifespan and TDP-43 proteinopathy including TDP-43 aggregation, truncation and phosphorylation (Liachko, Guthrie et al. 2010). Transgenic *Drosophila* models for TDP-43 proteinopathy have also been generated. Neurotoxicity due to abnormal levels of TDP-43 caused by overexpression of mutant or wild type human TDP-43 has been observed in *Drosophila* eyes (Lu, Ferris et al. 2009, Miguel, Frébourg et al. 2011). Specific

overexpression of WT or mutant hTDP-43 in motor neurons leads to progressive motor dysfunction with up-regulation of cytoplasmic TDP-43 (Li, Ray et al. 2010, Estes, Boehringer et al. 2011, Diaper, Adachi et al. 2013). Moreover, pan-neuronal overexpression of either WT dTDP-43 or hTDP-43 caused not only up-regulation of cytoplasmic TDP-43, but also hyperphosphorylated TDP-43 (Li, Yeh et al. 2011, Miguel, Frébourg et al. 2011, Diaper, Adachi et al. 2013).

Knock out studies of TDP-43 have highlighted its essential role during development as they result in embryonic lethality in mammalian models. Loss of TDP-43 in non-mammalian models result in high mortality at the embryonic stage with only a few surviving into the adult stage. These non-mammalian models develop severe motor dysfunctions similar to those seen in ALS (Feiguin, Godena et al. 2009, Diaper, Adachi et al. 2013), indicating the importance of TDP-43 in motor neurons.

Following on from these results, a *Drosophila* model made along the similar lines of the cellular model described in section 4.2 has been created to explore the connection between the reduction of TDP-43 levels and the onset of the disease. These flies started to show significant motor deficits during adulthood. Interestingly, a 4-fold drop in TDP-43 protein levels is observed and coincides with the time point where the locomotive defects start to be visible. Thus, according to this study, the motor phenotype is correlated with a loss of function of TDP-43 due to a drop in its protein levels (Cragnaz *et al*., 2015).

5. *Drosophila melanogaster* as a model system

5.1. General overview

Drosophila melanogaster has emerged as a powerful model to study human neurodegenerative diseases during the last decade. Several characteristics make Drosophila the organism of choice. Among them, the short generation time (approximately 10 days) and short life span (around 60 to 80 days). In particular, these features make Drosophila amenable to study age-related disorders. In addition, approximately 75% of human genes known to be associated with disease have a Drosophila ortholog (Reiter et al., 2001). For each disease, specific neuronal regions begin to

degenerate late in life. In order to study this, several methods are available to express genes in a spatially and temporally restricted manner. Moreover, synaptic activity can be measured in Drosophila using electrophysiological and imaging techniques from the neuromuscular junction and adult central nervous system, making this organism particularly amenable to study neurodegenerative diseases, such as ALS. *Drosophila melanogaster* has a segmented body, composed by head, thorax and abdomen. The six legs and the two wings are attached to the thorax. Drosophila has also two antennae and one pair of red eyes on its head. Flies have four pairs of chromosomes, usually represented as lines for the arms and circles for the centromeres. The X and the fourth chromosome have major left arms and tiny right arms. The size of the X, 2L, 2R, 3L and 3R are roughly comparable, whereas chromosome 4 is only about one-fifth as large (**figure 16**).

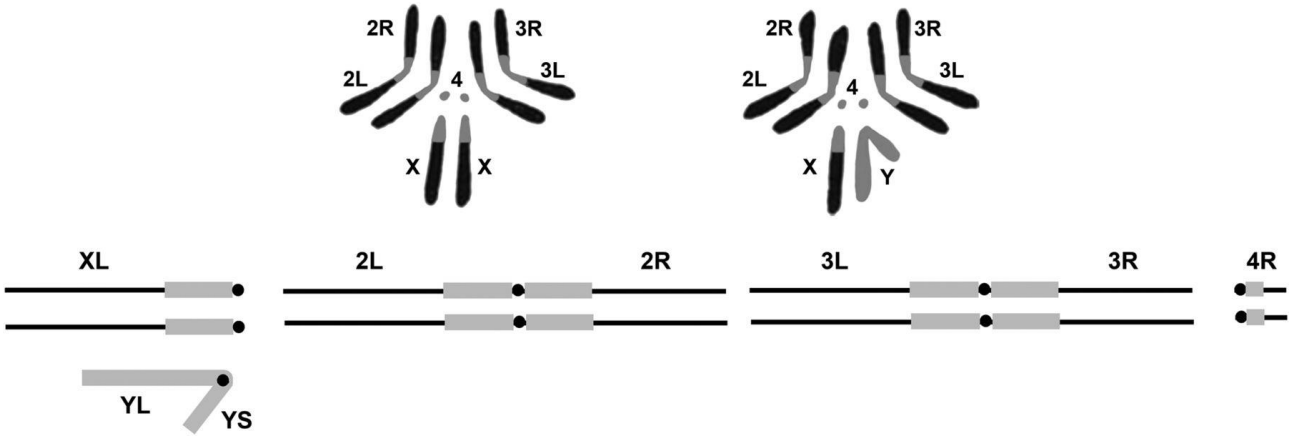

Figure 16. Schematic representation of flies' chromosomes. The upper portion of the figure shows a representation of the karyotype of *D. melanogaster*. Chromosomes from female third instar larval neuroblasts on the left and males on the right. Below is a diagrammatic representation of the genome indicating the names of the arms of the sex chromosomes and autosomes. The euchromatic portions of the genome are shown in black and the heterochromatin in gray. In this figure, arms are represented as lines and centromeres as circles. Adapted from *Genetics* by Thomas C. Kaufman (vol. 206 Issue 2, June 2017)

The sex determination in Drosophila is based on the ratio of X chromosomes to autosomal set. In males, one X with two autosomal sets gives a ratio of 0.5, whereas the ratio is 1 in females. The Y chromosome is not required for most aspects of male development, only for proper sperm motility. One important feature of fly genetics is the total absence of recombination in males. On the other hand, recombination in females is completely normal. Males are smaller and have darker and more rounded abdomens compared to females. Furthermore, the males have black sex combs on their first pair of legs that are important for male mating success (**figure 17**).

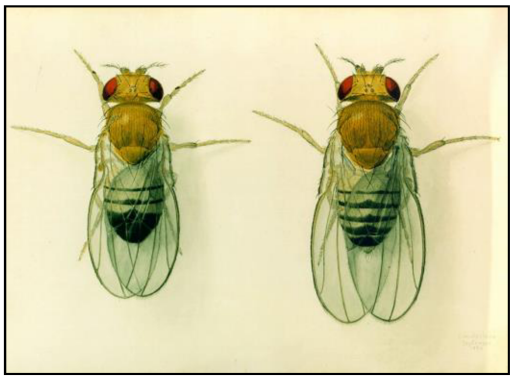

Figure 17. Schematic representation of the adult external dorsal aspect of *Drosophila.* Males (left) and females (right) are phenotypically different. Adapted from St. Pierre et *al*.. 2014

Drosophila melanogaster has a rapid development, but this can vary with the temperature. As other insects, the Drosophila's life cycle consists of four stages: egg, larva, pupa and adult (**Figure 18**). In optimal conditions (25°C with 60% of humidity), it will take approximately 10 days to complete the life cycle. After mating, the females deposit the eggs in the food. Embryogenesis occurs within the egg, and around 24 hours later the first instar larvae hatches. Immediately after hatching the larvae start to feed themselves, moulting 1 day, 2 days and 4 days after hatching, known as the first, second and third instar larval stages. During the growth period that lasts in total 4 to 5 days, the larva increases approximately 200-fold weight. After 2 days, the third instar larva moults one more time to form an immobile pupa. Metamorphosis takes place in the pupal case, lasting 4 to 5 days. After metamorphosis, the newly born fly breaks the pupal case to emerge. Immediately after birth, the fly has the wings still closed and a clear body pigmentation. The wings are completely opened 3 hours after birth, at the same time that the body acquires the normal brownish pigmentation.

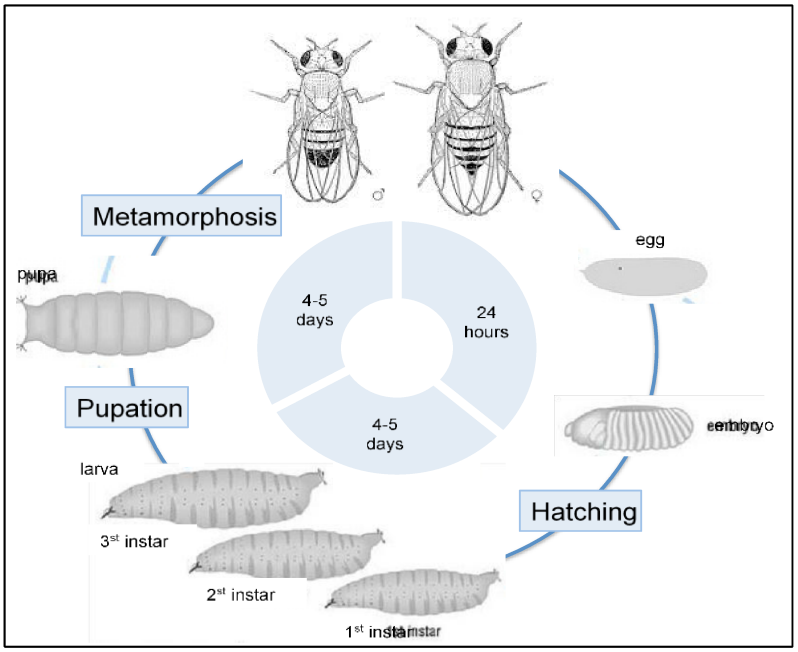

Figure 18. Schematic representation of *Drosophila melanogaster*'s life cycle.

The cycle lasts approximately 10 days and includes four stages: egg, larva, pupa and adult.

5.2. Gal4/UAS system

Currently, almost all Drosophila models of neurodegenerative diseases have been developed using the Gal4/UAS system (Brand & Perrimon, 1993), which allows the expression of a gene of interest in a tissue-specific manner. This system relies on two different components: a transcriptional activator derived from yeast under the control of a tissue specific promoter, and an upstream activating sequence (UAS). The transgene of interest is placed downstream of the UAS that consists of Gal4-binding sites. In the absence of Gal4, the transgene will be transcriptionally repressed. When flies that carry the transgene are crossed with flies that express Gal4 in a specific tissue (also known as "driver" flies), the transgene will be activated in the offspring; however, transgene expression will occur exclusively in those tissues where Gal4 is expressed (**figure 19**). A wide array of "driver" flies has been generated. The Gal4 is placed under a specific cell or tissue specific promoter, and this is of particular interest for the study of neurodegenerative diseases, where specific neuronal regions are compromised in patients' brain.

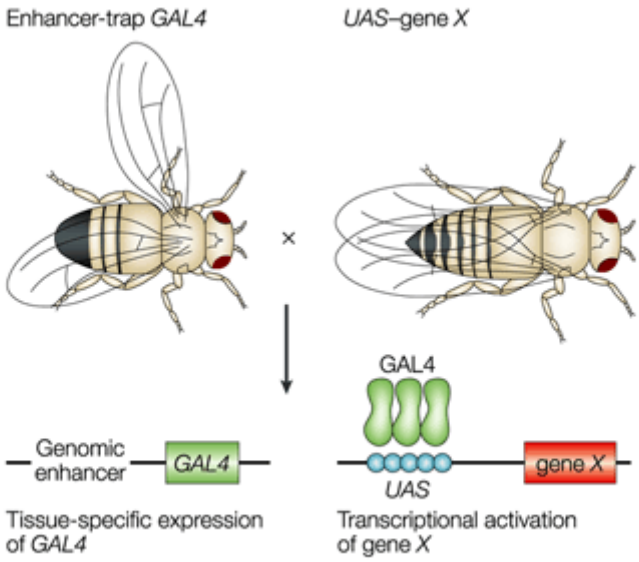

Figure 19. Directed gene expression in *Drosophila melanogaster*. Adapted from (Muqit and Feany 2002).

5.3. Markers and balancers

Marker mutations are the key to deciphering genotypes. A vast array of mutations affecting eye colour, eye shape, wing shape, wing vein morphology, bristle colour, bristle shape, and cuticle pigmentation (these are the main categories) serve to tag the various chromosome arms. They may be used to mark the chromosomes that need to be followed or lost during a cross.

Balancer chromosomes are multiple inverted chromosomes, which cannot undergo exchange with their normal homolog during the homolog recombination process. Balancer chromosomes also carry marker mutations, in order to facilitate the synthesis of defined genotypes by segregation analysis. Many balancers exist for the X, 2 and 3 chromosomes. There is no need of balancer of the fourth because there is no exchange on that chromosome. The most effective balancers are those, which suppress the exchange all along the chromosome.

5.4. TBPH

TDP-43 protein is highly conserved through species. Like many other genes, TDP-43 has a Drosophila homologue, which is called TBPH (Tar DNA Binding Protein Homologue). TBPH contains similar domains to the human protein: the nuclear localization signal (NLS), the nuclear export signal (NES), and the glycine-rich domain are all conserved between these two species. In particular, the human and *Drosophila melanogaster* proteins show striking similarities in their nucleic acid binding domains (75% of identity). However, the C-terminal region is less well conserved. Despite the differences, there is a high degree of functional similarity between the Drosophila and human TDP-43. Moreover, the Drosophila TDP-43 is able to replace the function of the human protein both in vitro and in vivo (Ayala, Pantano et al. 2005, Feiguin, Godena et al. 2009). The Drosophila protein, TBPH, is coded by the homonymous gene, which is located in the second chromosome. Six different isoforms have been identified so far, encoded by 5-6 exons, generated by alternative splicing (**figure 20**).

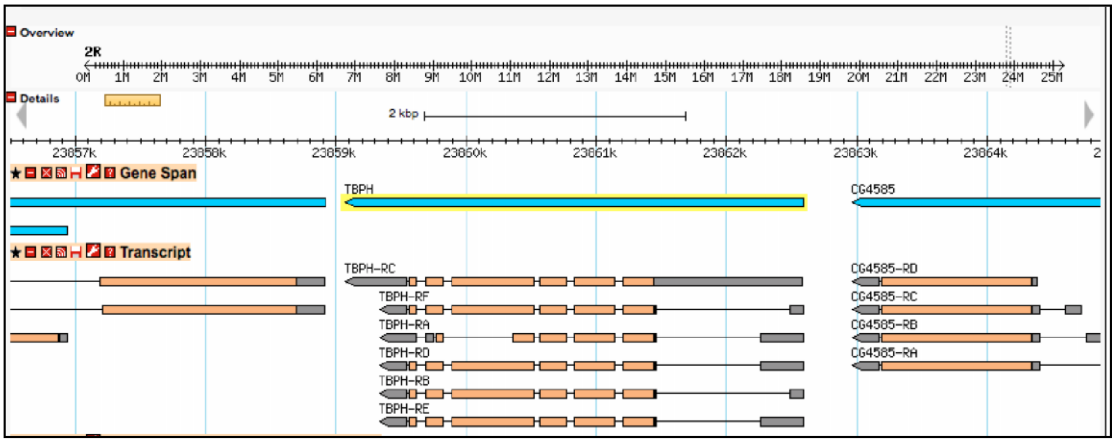

Figure 20. TBPH chromosomal location and representation of its transcripts.

Adapted from FlyBase.

Research aims

The absence of an effective treatment that blocks the progression of Amyotrophic Lateral Sclerosis (ALS) is in part due to the lack of models that faithfully recapitulate ALS phenotypes to use in studies of ALS drug development. The main histologic hallmark of ALS is TDP-43 aggregation in motor neurons. Irrespectively of the exact role of the aggregates, their eventual reduction represents an important therapeutic pathway, either by removal of their potential intrinsic toxicity or by elimination of self-templating conformers that can sequester endogenous TDP-43 into the aggregates resulting in a lack of its soluble and functional form.

The aim of this thesis is to create and characterize a new cellular model of TDP-43 aggregation, developed with the aim of using it in a phenotypic high throughput screen to identify new therapeutic compounds that, by reducing TDP-43 aggregates, could revert the ALS-symptoms. Subsequently, exemplar candidate compounds coming from the screen will be further characterised in regards to their mode of action in the cellular model by knocking out key components of the UPS and autophagy pathway.

A *Drosophila melanogaster* model carrying the same construct used to create the cell line will also be generated and characterised. This model will be used to test the compounds, identified from the high throughput screen using the cellular model, which are able to clear TDP-43 aggregates and restore functional TDP-43 and test whether they are able to rescue or improve the motor phenotype.

Materials and Methods

1. General reagents and protocols

1.1. Bacterial cultures

Escherichia coli K12 strain DH5α was used to perform transformation with all the plasmids of interest. Bacterial colonies were maintained at 4°C on Luria-Bertani (LB) agar plates with the desired antibiotic. When necessary, bacteria were grown overnight in liquid LB medium. In this case the antibiotic was added directly to the medium at a final concentration of 100 µg/ml.

1.2. Preparation of bacterial competent cells

Bacterial competent cells were prepared following standard procedures. Briefly, E. coli K12 strain DH5α was grown overnight in 10 ml liquid LB at 37°C (pre-inoculum). The day after, the pre-inoculum was transferred to a 300 ml fresh liquid LB, and cells were grown at 37°C for about 4-5 hours until OD600 was 0,3-0,4. Cell growth was stopped by putting the cells on ice and then centrifuged at 4°C for 10 minutes at 0,1 x g. The pellet was resuspended in 30 ml of cold TSS solution (10% (w/v) PEG, 5% (v/v) DMSO, 35 mM $MgCl_2$, pH 6.5 in LB medium). Finally, cells were aliquoted and rapidly frozen in liquid nitrogen and stored at -80°C.

1.3. Bacterial transformation

Transformation was performed using 10 µl of ligation reaction, or 20 ng of DNA plasmids. DNA was incubated with 60 µl of competent cells on ice for 20 minutes and then the heat shock was performed by transferring the vial to 42°C for 2 minutes. Another incubation on ice was performed for 5 minutes and finally the bacteria were allow to recover at 37°C for 30 minutes. Cells were then plated on LB agarose plates containing the proper antibiotic and incubated for about 12 hours at 37°C.

1.4. Small-scale preparation of plasmid DNA from bacterial cultures

In order to extract DNA plasmids from bacterial cultures, a single colony was inoculated and grown in 6 ml of Terrific Broth (TB) medium overnight at 37°C. The Wizard plus SV miniprep DNA purification system from Promega (Promega # A1330) was used according to the manufacturer's instructions.

1.5. Digestion of plasmid DNA

DNA digestion was performed using the corresponding digestion buffer specifically created by the same company for each restriction enzyme. In general, the digestion was performed with 100-500 ng of DNA in a final volume of 50 µl containing 5 units of the restriction enzyme of interest. 2-3 hours incubation was performed at the optimal temperature indicated by the manufacturer.

1.6. DNA ligation

To perform DNA ligation the T4 ligase (Roche # 11635379001) was used. This enzyme is able to adjoin double stranded DNA fragments having compatible sticky or blunt ends. The reaction was performed with 20 ng of digested vector and 5-10 fold molar excess of the digested insert in a total volume of 20 µl, containing 1X ligase buffer and 1 unit of T4 DNA ligase. The reaction was incubated for 4-10 hours at room temperature.

1.7. Agarose gel electrophoresis of DNA

Size fractionation of DNA samples was performed through electrophoresis in agarose gel 1-2% (w/v) prepared in TBE 1X (220 mM Tris; 180 mM Borate; 5 mM EDTA; pH 8.3). The samples of interest were loaded in gels containing ethidium bromide (0,5 µg/µl), at 80 mA in TBE 1X running buffer. DNA was visualized by UV trans illuminator machine and the result was photographed using a digital camera.

1.8. DNA sequencing

Sequence analysis was performed by sending 2 µg of plasmid DNA preparation to Macrogen Company.

1.9. Quick change mutagenesis

Two complementary oligonucleotide primers that carry appropriate modifications were designed and used during PCR mutagenesis. The reaction mix was made in a final volume of 50 µl containing 1 µl of PfuDNA polymerase (Promega), 5 µl PfuBuffer 10x, 10 µM of each primers (forward and reverse), dNTPs mix (5mM each) and 50-60 ng of the desired template to be modified. PCR was performed using DNA Polymerase (Biolabs # M0273L) with the following settings: 95 °C for 30 s, 95°C for 30 s, 55°C for 1 min, 68°C for 8 min and 68°C for 7 min repeated 18 times for step 2 to step 5. Following the PCR, the product was digested with 1 µl of *DpnI* enzyme for 2-4 h at 37ºC.
After *DpnI* digestion 10 µl of the nicked plasmid DNA containing the mutation of interest were transformed into DH5α E. coli cells and the clones were then analysed through sequencing.

1.10. SDS-PAGE

Sodium dodecyl sulphate polyacrylamide gel electrophoresis (SDS-PAGE) is a widely used method to separate proteins according to their sizes. Protein samples were diluted in Laemmli buffer (0.1 M Tris-HCl pH 6.8, 30% (v/v) glycerol, 8% (w/v) SDS, 9.8% (v/v) β-mercaptoethanol and 0.1% (w/v) bromophenol blue), and boiled at 95°C for 5 minutes. Gels were prepared as detailed in Table 2.

Components	Resolving gel	Stacking gel
Acrylamide-BIS	8% or 10% (v/v)	5% (v/v)
Tris-HCl pH 8.8	0.37 M	-
Tris-HCl pH 6.8	-	0.125 M
SDS	0.1% (w/v)	0.1% (w/v)
Ammonium persulphate	0.1% (w/v)	0.1% (w/v)
TEMED	0.02% (w/v)	0.02% (w/v)

Table 2. SDS gel preparation

The amperage applied for the running was 25mA in 1X running buffer prepared from a 10X stock solution (table 3).

Reagent	Quantity
Tris (Invitrogen #15504-020)	30,3 gr
Glycine (Sigma #33226)	144 gr
SDS (BDH #301754L)	5 gr

Table 3. 10X running buffer preparation

2. A cellular model of TDP-43 aggregation

2.1. Creation of EGFP-TDPF4L12xQ/N plasmid

The EGFP-TDP43 F4L 12xQ/N plasmid to generate the corresponding stable cell line was prepared taking the advantage of a previously described construct FLAG-TDP43 F4L/pCDNA5/FRT/TO (Budini,

Romano et al. 2015) to which enzyme restriction sites *XhoI* and *BamHI* were introduced in position 1209 of TDP-43 as described in Budini et al 2015. Then FLAG tag was deleted and simultaneously EcoRV enzyme restriction site was inserted by Quick Change mutagenesis strategy (Stratagene) using the following oligonucleotides: F4L/pcDNA5 FLAGdel-EcoRVins Fw 5'-ATCCAGCCTCCGGACTCTAGCGTTTAAATTtAAatcgttaagatatcctttctgaatatattcgggtaaccgaagatgaga-3' and F4L/pcDNA5 FLAGdel-EcoRVins Rv 5'-tctcatcttcggttacccgaatatattcagaaaggatatcttaacgatTTaAATTTAAACGCTAGAGTCCGGAGGCTGGAT-3'. EGFP tag was amplified from pEGFP-C2 plasmid using oligonucleotides carrying EcoRV target sequence (EcoRV EGFP Fw 5'-ccggatatcATGGTGAGCAAGGGCGA-3' and EcoRV EGFP Rv 5'-ccggatatcgATCTGAGTCCGGCCGGACTT-3'), cut using EcoRV restriction enzyme and ligated into the already digested and dephosphorylated plasmid generating the EGFP-TDP43-F4L/pcDNA5/FRT/TO plasmid. As final step, the plasmid was digested using *XhoI* and *BamHI* restriction enzymes and 12 repetitions of the Q/N rich region of TDP-43 were inserted as previously described (Budini, Romano et al. 2015). All the cloning steps were followed by sequencing procedure to check that all the inserted fragments were correct.

2.2. Creation of EGFP-TDPF4L12xQ/N cell line

The HEK293 EGFP-TDPF4L12xQ/N cell line used in this study was developed in our lab using the Flp-In System (Invitrogen # K6010-01) and the T-Rex-293 cells (Invitrogen # R710-07). The cell line was cultured in Dulbecco's Mem with Glutamax I (Dulbecco's modified Eagle's medium with glutamine, sodium pyruvate, pyridoxine and glucose) supplemented with 10% (v/v) heat inactivated fetal bovine serum (FBS) and 1X antibiotic-antimycotic (Sigma # A5955). Plasmid transfections were carried out using Effectene Transfection reagent (Qiagen # 301425) according to the manufacturer's instructions. To generate the stable clones, 0.5 µg of plasmid EGFP-TDPF4L12xQ/N was co-transfected with 0.5 µg pOG44 vector that expresses the Flp-recombinase. After 24 hours from co-transfection, the stable integration was gradually selected using 100 µg/ml of Hygromycin B (Invitrogen # 10687-010). 10 µg/ml Blasticidin S (Sigma # 15205) was used to select the T-Rex-293 plasmid containing the tetracycline repressor (pcDNA6/TR). The expression of the gene of interest is controlled by the CMV promoter into which two copies of the Tet operator 2 (TetO2) sequence have been inserted in tandem. Insertion of these TetO2 sequences into the CMV promoter confers

regulation by tetracycline to the promoter. For the induction of the transgenic protein, 1 µg/ml of anhydrous-tetracycline (Sigma # 87128) was added to the culture media.

For cell seeding, dishes containing confluent monolayer of cells were washed with PBS 1X, treated with 3 ml of PBS/EDTA/trypsin solution (PBS containing 0.04% (w/v) EDTA and 0.1% (w/v) trypsin) at 37°C for 30 seconds in order to detach the cells. Then, trypsin was deactivated by adding complete DMEM, and the cells were collected and pelleted by centrifugation for 5 minutes at 0,1 x g at room temperature. The cellular pellet was suspended in 10 ml of DMEM and cells were counted with the Neubauer chamber and plated.

2.3. Immunohistochemisty

Cells were plated into a 6-well plate, containing, in each well, a cover glass that was previously sterilized. After induction with tetracycline, cells were washed with 3 ml of PBS 1X (NaCl 137 mM, KCl 2.7 mM, Na_2HPO_4 10 mM, KH_2PO_4 1.8 mM pH 7.4) and fixed with 3.7% (v/v) paraformaldehyde for 40 minutes at room temperature. After fixing, three 5-minutes washes were performed with PBS 1X. Subsequently, the plate was placed on ice and 2 ml of PBS with 0.3% (v/v) Triton X-100 were added for 5 minutes. This step was done in order to permeabilize the cells, and after it, a washing step (three 5-minutes washes with PBS 1X) was performed to remove the permeabilization solution. The cells were then blocked for 20 minutes at room temperature with 2% (w/v) of BSA prepared in PBS 1X. Then, the slides were incubated in a humidified chamber with the primary antibodies: rabbit anti-TDP-43 (1:200, Proteintech # 10782-2-AP). After 1-hour incubation at room temperature, three 5-minutes washes with PBS 1X were performed and the secondary antibody Alexa 594 anti-rabbit (1:500, Invitrogen # 997874) was added and incubated for 1 hour at room temperature in a humidified chamber. Finally, the slides were rinsed with PBS 1X for 5 minutes. For the mounting, the slide was placed up side down on a cover slip with a small drop of mounting medium containing DAPI (Vector Laboratories # H1200), and sealed with nail polish. The samples were imaged under a confocal laser-scanning microscope (LSM 510 META; Carl Zeiss, Inc). Images were acquired by using 63X oil immersion objective. Image processing was done with ImageJ software.

2.4. Clearance assay

100,000 cells/well were seeded in a 6-well plate, and induced for 24 hours with tetracycline 1 µg/ml. After induction, cells were washed twice with PBS 1X in order to get rid of the tetracycline. Fresh DMEM without antibiotic-antimycotic was added to the wells, and cells were incubated for 24 hours with five different FDA approved drugs at different concentrations: Thioridazine 4 µM (Sigma # T9025), Nortriptyline 10 µM (Sigma # N7261), Clomipramine 10 µM (Sigma # C7291), Fluphenazine 5 µM (Sigma # F4765) and Chlorpomazine 10 µM (Sigma #C8138). Subsequently, the medium was replaced with fresh medium and cells were further cultured for 24 hours in presence of the selected drugs. Control cells were also induced for 24 hours and then kept in culture for 48 hours without any additive. After the incubation time was finished, cells were collected and pelleted at 0,1 x g for 5 minutes at room temperature. Finally, protein and RNA were extracted.

2.5. Inhibitors experiment

After 24 hours of EGFP-TDPF4L-12XQ/N induction, tetracycline was washed out with PBS 1X twice. Subsequently, DMEM without antibiotic/antimycotic was added to the wells. One hour prior to the addition of either Nortriptyline 10 µM or Thioridazine 4 µM, the proteasome or autophagy inhibitors were added to the culture medium. For the autophagy blockage NH_4Cl 30 mM (Merck # 101145) and chloroquine 10 µM (Sigma # C6628) were used and as a proteasome inhibitor Bortezomib 7nM (Selleckem # S1013) was used. These concentrations were used based on standard procedures. As for the clearance assay, cells were incubated for 24 hours with the inhibitors plus the drugs. Subsequently, the medium together with inhibitors and selected compounds were replaced and cells were further cultured for 24 hours. As for control cells, after tetracycline was washed out, they were incubated with the inhibitors alone for 48 hours (24h+24h). After 48 hours of incubation, cells were collected and proteins and RNA were extracted. SDS-PAGE followed by immunoblotting and POLDIP3 splicing analyses were performed.

2.6. Protein extraction

For cellular protein analysis, cells with and without drug treatment were harvested and cellular lysis was performed using home-made Lysis buffer (15 mM Hepes pH=7.5, 250 mM NaCl, 0.5% (v/v) NP-40, 10% (v/v) Glycerol and protease inhibitors (Roche Diagnostic # 11836170001)). Cell lysates were then sonicated for 10 minutes at the highest potency. The total amount of protein per each sample was quantified by Bradford assay using Biorad reagent (Biorad # 500-0006).

2.7. Immunoblotting

Proteins (20-30 µg/sample) were separated by 10 or 12,5% SDS-PAGE, transferred to nitrocellulose membranes (Whatman # NBA083C) and probed with primary antibodies: rabbit anti-GFP (1:1,000, Santa Cruz # sc-8334), rabbit anti-TDP-43 (1:1,000, Proteintech # 10782-2-AP), rabbit anti-LC3B (1:1,000, Sigma # L7543), guinea pig anti-p62 (1:2,000, Progen # GP62-C), rabbit anti-ubiquitin (1:1,000, Cell Signaling technology # 3933), mouse anti-Flag (1:1,000, Sigma # F1804) and mouse anti-tubulin (1:4,000, Calbiochem # CP06). The membranes were incubated with the secondary antibodies: HRP-labeled anti-mouse (1:2,000, Thermo Scientific # 32430), HRP-labeled anti-guinea pig (1:10,000, Jackson ImmunoResearch #706-035-148) or HRP-labeled anti-rabbit (1:2,000, Thermo Scientific # 32460). Finally, protein detection was assessed with ECL Western Blotting Substrate (Thermo Scientific # 34106).

2.8. Solubility assay

Cell lysis was performed with Lysis buffer (15 mM Hepes pH=7.5, 250 mM NaCl, 0.5% (v/v) NP-40, 10% (v/v) Glycerol and protease inhibitors (Roche Diagnostic # 11836170001)). Subsequently, cells were sonicated for 10 minutes at the highest potency. The total amount of proteins in each sample was quantified by Bradford assay using Biorad reagent (Biorad # 500-0006). 250 µg of cell lysates were centrifuged at 33,000 rpm for 1 hr at 25°C. The supernatant was collected as the soluble fraction and the pellet was resuspended in Urea buffer (7 M urea, 4% CHAPS, 30 mM Tris pH 8.5). 10% of each fraction was loaded on SDS-PAGE followed by western blotting.

2.9. RNA extraction

To perform RNA extraction, cultured cells were washed once with PBS 1X and then harvested. Subsequently, centrifugation at room temperature at 0,1 x g for 5 minutes was performed. The cellular pellet was suspended in 500 µl of TRIzol reagent (Invitrogen # 15596-026) and incubated for 3-5 minutes at RT. RNA extraction was performed by adding 100 µl of chloroform to each sample and after 2-3 minutes of incubation at room temperature, samples were further centrifuged for 15 minutes at 13,4 x g at 4°C. The upper phase, containing the RNA was transferred into a new tube and RNA was precipitated by adding 250 µl of isopropanol. After 10 minutes of incubation at room temperature, the samples were centrifuged again for 15 minutes at 13,4 x g at 4°C. Finally, RNA pellet was washed with 70% (v/v) ethanol and resuspended in water.

2.10. cDNA synthesis

The cDNA synthesis was performed with 1µg of total RNA. To start with, RNA was treated with DNAse (Promega RQ1 # M610A). The mixture was incubated at 37°C for 30 minutes and then DNAse stop solution was added and incubated at 65°C for 10 minutes to inactivate the DNAse enzyme.

The RNA was subsequently retrotranscribed with Moloney murine leukemia virus reverse transcriptase (M-MVL RT) (Invitrogen # M1701) using random primers at a final concentration of 2.5 mM (Pharmacia # 27-2166-01). First, RNA denaturation was carried out at 70°C for 3 minutes. After denaturation, the following reagents were added: 5X RT Buffer, DTT 0.1 M, dNTPs 5mM, M-MVL RT and H_2O. Samples were then incubated for 1 hours at 37°C to allow cDNA synthesis.

2.11. POLDIP3 splicing assay

For *POLDIP3* splicing assay, cells with and without drug treatment were harvested and RNA was extracted using Trifast reagent (Euroclone # EMR507100), according to manufacturer instructions (see section x). After retrotrascription with M-MLV Reverse Transcriptase (Invitrogen # M1701), total cDNA was analyzed by PCR using the following primers: *POLDIP3* exon 3 forward: 5'gcttaatgccagaccgggagttgga3' and *POLDIP3* exon 3 reverse: 5' tcatcttcatccaggtcatataaatt3'. PCR was performed using DNA Polymerase (Biolabs # M0273L) with the following settings: 95°C for 5

minutes, 95°C for 30 seconds, 50°C for 30 seconds, 72°C for 1 minute, 72°C for 7 minutes, repeated 35 times from step 2 to 5. All PCR products were analyzed on 2% (w/v) agarose gels with ethidium bromide (Sigma # E1510).

3. A *Drosophila* model for TDP-43 aggregation

3.1. Generation of transgenic fly lines

3.1.1. Generation of constructs

In order to generate the transgenic fly model used in this work, the FLAG-TDPF4L12xQ/N construct (Budini, Romano et al. 2015) was cloned in a pUASTattB vector. pUASTattB is highly used in the field as it allows site specific insertion of the transgene of interest in the *Drosophila* genome. The plasmid (figure 21) is 8.4 Kb long (Gene Bank accession number EF362409). It contains the white gene (coding for the red colour of the eye) as a genetic marker, a region with 5 UAS binding sites upstream of the hsp70 promoter, loxP sequences, a multiple cloning site, the sequence attB and ampicillin resistance. The attB site allows the integration of the transgene in the attP-landing platform in the fly genome, taking advantage of the phage ΦC31 integrase system (Bischof et al., 2007) (figure 21). Both FLAG-TDPF4L12xQ/N and EGFP constructs were cloned in pUASTattB and specifically inserted in *Drosophila*'s third chromosome.

a)

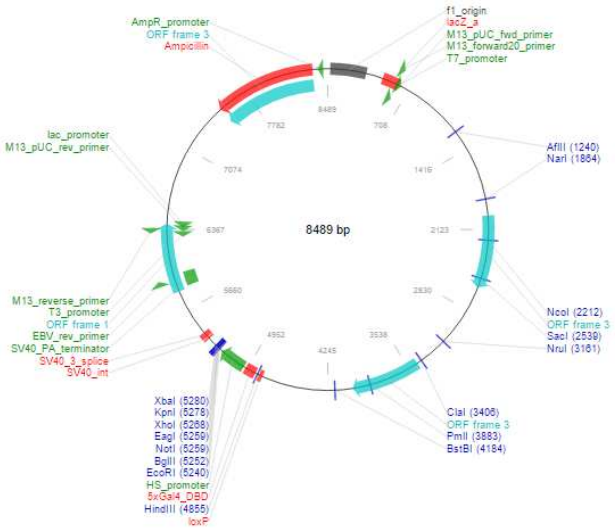

b)

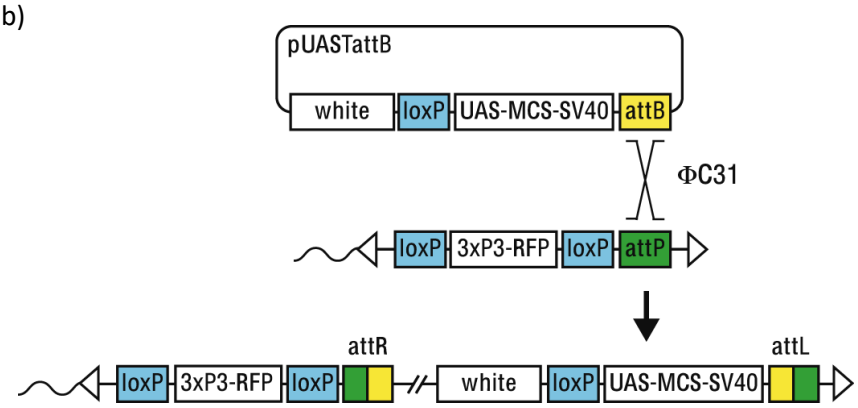

Figure 21. Schematic representation of the pUASTattB plasmid and its integration mechanism into attP landing sites. The ΦC31 integrase mediates recombination between attB and attP sites, resulting in the integration of pUASTattB into the landing site, thereby creating the two hybrid sites attL and attR, which are refractory to the ΦC31 integrase. Adapted from Bischof et al. 2007.

3.1.2. S2 cells transfection

The S2 cells derive from primary culture of late stage (20-24 hours) *Drosophila melanogaster* embryos (Schneider, 1972). They form semi adherent monolayer when grown in culture flasks at room temperature, without CO_2. Insect Express medium (Lonza # BE12-730F) supplemented with 10% (v/v) heat-inactivated fetal bovine serum and 1X antibiotic/antimycotic (Sigma # A5955) was used to maintain the cells in culture. Before sending the constructs to BestGene Company for the generation of the transgenic flies, the expression level and the potential toxicity of the exogenous protein were tested in S2 cells. Transfection was performed using Effectene transfection reagent kit (Qiagen # 301425), a non-liposomal lipid reagent for DNA transfection. S2 cells were plated at a concentration of $1.8x10^6$ cells/mL. The transfection reaction was prepared as follows: 300 ng of DNA plasmid containing the construct of interest, 500 ng of plasmid harboring Gal4 factor and 4 µl of Enhancer were added to the Condensation buffer (buffer EC) up to a total volume of 150 µl and incubated at room temperature for 5 minutes. 12,5 µl of Effectene reagent were subsequently added to the mixture, mixed by vortexing and incubated at room temperature for 10 minutes to allow formation of the transfection complex. Then, the transfection complex was added to 300 µl of medium and finally it was transferred to the dish containing the cells. The cells were incubated at 25°C for at least 48 hours in order to obtain the expression of the recombinant protein.

3.1.3. Transgenic flies

FLAG-TDPF4L12xQ/N (12 repetitions of the TDP-43 331-369 sequence) and EGFP constructs were cloned in the pUASTattB vector (Bischof et al., 2007). All the constructs have been sequenced and subsequently used to create transgenic flies by standard embryo injections (Best Gene Inc.). A specific insertion using strain 24486 was chosen for FLAG-TDPF4L12xQ/N and EGFP. All transgenic flies have been subsequently balanced on the required chromosome. *Drosophila* stocks W1118, GMR-Gal4 and ELAV-Gal4 were obtained from Bloomington *Drosophila* Stock Centre at Indiana University (http://flystocks.bio.indiana.edu/). Additional stocks were kindly provided by colleagues or were generated as part of this study.

3.1.4. Balancing of transgenic flies to avoid loss of the transgene

Balancer chromosomes are modified chromosomes used for genetically screening a population of organisms to select for heterozygotes. Balancer chromosomes can be used as a genetic tool to prevent genetic recombination between homologous chromosomes during meiosis. Balancers are often used in *Drosophila melanogaster* genetics to allow populations of flies carrying heterozygous mutations to be maintained without constantly screening for the mutations. Balancer chromosomes have three important properties: they suppress recombination with their homologs, carry dominant markers that allow you to tell which progeny inherit the balancer in crosses, and negatively affect reproductive fitness when carried homozygously.

Transgene insertion could be in any of the fly's chromosomes: X, II or III. Transgenes inserted on the fourth chromosome are very rare as this chromosome is very small and it is mainly formed by heterochromatin. Since the FLAG-TDPF4L12xQ/N construct was inserted on the third chromosome, transgenic flies obtained from Best Gene Company were directly crossed with the specific balancer on the third chromosome to avoid loss of the transgene. To do so, an individual male carrying the transgene (which contains the white gene coding for the red colour of the eye, marked as w+) is crossed with a balancer female. Since, the insertion has been made in the third chromosome, Apc/TM3Sb female balancer flies are used (carrying the dominant morphological marker stubble hair). To create the final stock, males and females, carrying both the transgene (marked with w+) and TM3Sb balancer, are crossed again.

3.2. *Drosophila* techniques

3.2.1. *Drosophila* stocks handling

Flies were fed on standard cornmeal (2,9% (w/v)), sugar (4,2% (w/v)), yeast (6,3% (w/v)) fly food and maintained in a humidified incubator at 25°C with a 12 hours-12 hours light-dark cycle. Experimental crosses were performed at 25°C with the same conditions of humidity and light/dark cycle as stock flies. To allow the identification of the sex and genotype, the flies were anaesthetized on a pad with CO_2 gas. The constant gas flow provided, allows the immediate and continuous anaesthetization.

3.2.2. *Drosophila* crossing techniques

Experimental crosses were established by adding males to virgin females. Females less than 8 hours old reject countership and, therefore, are considered as virgins. On this basis, all adults from a vial were removed and after 7-8 hours the newly eclosed females were harvested. They were kept in a separate vial for up to one week in order to collect a considerable number of females to proceed with the crosses. Virgin females were then combined with males in a 10:3 female:male ratio, placed in a fresh tube and stored at 25°C for up to 5 days. Flies were then removed to allow the collection of the progeny.

3.2.3. Drug feeding

Fly food was melted in the microwave. Once the food was properly melted, it was left on the stir to cool down until the T was below 40°C; subsequently, the selected drug, previously dissolved in either water or ethanol accordingly, was added to the food to obtain the final concentration and mixed. Thioridazine was dissolved in water, while compound B, C, D, E, F and G were dissolved in ethanol 100%. Based on previous experiments, a final concentration of 5% ethanol in the fly food was found to be non-toxic for the adult flies; as for the larvae, the concentration had to be decreased to 1% due to a strong toxic effect observed with higher doses. For the feeding of the larvae, the compounds were suspended in 1.2 ml of ethanol 100%, vortexed and put at 48 °C for 3-5 minutes. Finally, the compound was added to 120 mL of fly food (the final percentage of ethanol in the food was 1%). For the feeding of adult flies, the compounds were suspended in 7.5 mL of ethanol 100%, vortexed and put at 48°C for 3-5 minutes. The compound was then added to 142.5 ml of food (the final percentage of ethanol in the food was 5%). The mixture was subsequently aliquoted in each tube and let it solidify. Crosses were set directly in tubes containing food with the compound or water/ethanol alone. After 5 days, males and females were discarded to let the larvae eat the food. Five to six days later new flies hatched from the pupal case. One-day-old flies were collected for 2 days and put in tubes with the drug or water/ethanol alone in a male:female 1:1 ratio. The food was changed every second day and after 10 days of treatment the climbing ability of the flies was tested. The final concentrations used for each of the compounds tested in the fly model are reported in the table below (table 4).

Compounds	Larvae	Adults
Thioridazine	50 µM	0.4 mM
B	165 µM	800 µM
C	400 µM	1 mM
D	80 µM	1 mM
E	500 µM	1 mM
F	/	500 µM
G	143 µM	700 µM

Table 4. Final concentrations used for all the compounds tested to feed the TDPF4L12xQ/N fly model.

3.3. *Drosophila* phenotypic analysis

3.3.1. Climbing assay

The negative geotaxis (movement against gravity) is an innate characteristic of *Drosophila* (Benzer, 1967). Thus, flies were transferred without anaesthesia to a 50 ml glass-cylinder, tapped to the bottom of the tube and their subsequent climbing activity was quantified as number of flies that reached the top of the tube in 15 seconds. This behaviour is stable during the first three weeks of adult life, but progressively declines with age. Therefore, the climbing ability of control EGFP and transgenic TDPF4L12xQ/N flies was measured at 3, 7, 11 and 14 days after eclosion. At least 100 flies for each genotype were tested. In each set of experiments 20 flies (1:1 male:female ratio) were introduced in the cylinder and tested in triplicate. The number of top climbing flies was converted into % value, and the mean % value (±SEM) was calculated for at least 5 experiments. One-way ANOVA followed by Bonferroni's multiple comparison was used to compare measures among four groups. Unpaired t-test analysis was used to compare measures between two groups. The significance between the variables was shown based on the p-value obtained (ns indicates $p>0.05$, *indicates $p<0.05$, **indicates $p<0.01$, ***indicates $p<0.001$ and ****indicates $p<0.0001$).

3.3.2. Life span

Adult flies were collected for 2 days and transferred to tubes with food. Each tube contained 20 flies in a proportion 1:1 male:female ratio. The lifespan trials were conducted in humidity and temperature controlled conditions. Every third day, flies were transferred, without anesthetization to a fresh tube and deaths were scored. Survival rate was plotted as percentage of survival flies against day. Approximately 100 flies were tested for each genotype. Long rank test was performed to compare survival distribution between genotypes. The significance between the variables was shown based on the p-value obtained (ns indicates $p>0.05$, *indicates $p<0.05$, **indicates $p<0.01$, ***indicates $p<0.0001$).

3.3.3. Larval movement

Drosophila larvae show natural peristaltic movements, characterized by a wave, which starts at one end of the larvae, passes through all the body, and ends in the mouth. In physiological conditions, the movement is interrupted by pausing, turning and head swinging (Rodriguez Moncalvo and Campos, 2009). Evaluation of peristaltic waves has been done testing the movement of third instar larvae. Wandering third instar larvae were selected, washed and transferred to a Petri dish with a layer of 0.7% (w/v) agarose. After a period of adaptation, the peristaltic waves within 2 minutes were counted. At least 20 larvae from each genotype were counted, and the mean was calculated. One-way ANOVA followed by Bonferroni's multiple comparison was used to compare measures among four groups. Unpaired t-test analysis was used to compare measures between two groups. The significance between the variables was shown based on the p-value obtained (ns indicates $p>0.05$, *indicates $p<0.05$, **indicates $p<0.01$, ***indicates $p<0.0001$). Values are presented as a mean and error bars indicate standard error means (SEM).

3.4. Biochemical techniques

3.4.1. Protein extraction

Transfected S2 cells were transferred to 1.5 ml tubes, collected by centrifugation at 16,000 x g and resuspended in 100 µl of Lysis Buffer (50 mM Tris-HCl pH 7.6, 750 mM NaCl, 1% (v/v) Triton X-100 and protease inhibitors (Roche Diagnostic # 11836170001)). Regarding flies, total proteins were extracted from the head. Whole flies were frozen in liquid nitrogen and then vortexed to separate the head from the body. Drosophila heads were homogenized in lysis buffer (10 µl/head) (10 mM Tris-HCl, pH 7,4, 150 mM NaCl, 5 mM EDTA, 5 mM EGTA, 10% (v/v) Glycerol, 50 mM NaF, 5 mM DTT, 4 M Urea, and protease inhibitors (Roche Diagnostic # 11836170001)). After homogenization, samples were left on ice for 20 minutes followed by centrifugation at 2000 rmp for 7 minutes at 4°C. Supernatants were collected, used and/or stored at -80°C.

3.4.2. *Drosophila* Immunoblotting

Proteins were separated by 8% SDS-PAGE, transferred to nitrocellulose membranes (Whatman # NBA083C) and probed with primary antibodies: mouse anti-FLAG (1:1,000, Sigma # F1804), mouse anti-GFP (1:1000, Roche # 11814460001), rabbit anti-TBPH (1:1,500, home-made), and mouse anti-tubulin (1:4,000, Calbiochem # CP06). The membranes were incubated with the secondary antibodies: HRP-labeled anti-mouse (1:2000, Thermo Scientific # 32430) or HRP-labeled anti-rabbit (1:2000, Thermo Scientific # 32460). Finally, protein detection was assessed with Femto Super Signal substrate (Thermo Scientific # 34095). Protein bands were quantified using NIH ImageJ. The intensity of the band of interest was normalized with tubulin.

3.4.3. Solubility test

24 adult fly heads were dissected and homogenized in 240 µl of lysis buffer (10 µl/head) (10 mM Tris-HCl, pH 7,4, 150 mM NaCl, 5 mM EDTA, 5 mM EGTA, 10% (v/v) Glycerol, 50 mM NaF, 5 mM DTT, 4 M Urea, and protease inhibitors (Roche Diagnostic # 11836170001)). The samples were incubated under agitation for 1 h at 4˚C and then centrifuged at 1,000 x g for 10 minutes at 4˚C. An aliquot was

taken at this point as the input, and after a further centrifugation step at 100,000 x g for 30 minutes at 4˚C, the supernatant was collected as the soluble fraction. The remaining pellet was re-extracted in 60 µl of urea buffer (9 M urea, 50 mM Tris-HCl, pH 8, 1% (w/v) CHAPS and a cocktail of protease inhibitors (Roche # 04693159001)) and spun down to remove any precipitate, while the 9 M urea soluble material was collected as the insoluble fraction. Proteins were separated by 8% SDS-PAGE. The different samples were loaded in a proportion 1:1:1 for the input, soluble and insoluble fractions. Proteins were electro-blotted to a nitrocellulose membrane (Whatman # NBA083C) and probed with the following primary antibodies: mouse anti-GFP (1:1000, Roche # 11814460001) mouse anti-FLAG (1:1,000, Sigma # F1804), and mouse anti-tubulin (1:4,000, Calbiochem # CP06). The membranes were incubated with the secondary antibody HRP-labeled anti-mouse (1:2000, Thermo Scientific # 32430). Finally, protein detection was assessed with Femto Super Signal substrate (Thermo Scientific # 34095).

Results

1. A cellular model of TDP-43 aggregation

1.1. Creation and characterization of EGFP-TDPF4L12xQ/N stable cell line

In order to create a solid cell-based model of TDP-43 proteinopathies that may serve as a tool for the study of the mechanisms of TDP-43 pathology and eventual identification of compounds capable of reducing TDP-43 inclusions, I created a tetracycline-inducible cell line expressing a construct composed of TDP-43 linked to tandem repeats of the glutamine/asparagine region, which is known to be involved in the self-aggregation process (Fuentealba, Udan et al. 2010). As mutations of phenylalanine 147 and 149 into leucine in both the RNA recognition motifs have been shown to abolish its ability to bind nucleic acids (Budini, Romano et al. 2015), these were also introduced into the construct used to create the cell line. In fact in this way due to its inability to bind RNA the protein produced will be unable to down regulate the levels of soluble endogenous TDP-43 through the negative feedback loop (Ayala, De Conti et al. 2011, Avendaño-Vázquez, Dhir et al. 2012) as well as regulate RNA splicing, the principle process I use in this thesis to monitor TDP-43 functionality. An EGFP tag was chosen over the previously used FLAG (Budini, Romano et al. 2015) due to ease of kinetic monitoring and intrinsic fluorescent nature that are essential features in eventual high throughput screening assay development.

Transgene expression is blocked by the tetracycline repressor (R). Hence, only when tetracycline is added to the cells, the EGFP-TDPF4L12xQ/N transgene expression is induced (figure 22a for the cartoon showing the construct used to create the cell line). Immunofluorescence analysis of the cells upon induction with tetracycline, shows the formation of aggregates (green) localized in both the nucleus and cytoplasm (figure 22b lower panel). Interestingly, endogenous TDP-43 (red) which is normally diffused in the nucleus (figure 22b upper panel), was found to aggregate and to co-localize with the EGFP-TDPF4L12xQ/N aggregates (yellow dots, figure 22b lower panel), indicating sequestration of the endogenous protein by the aggregates.

a)

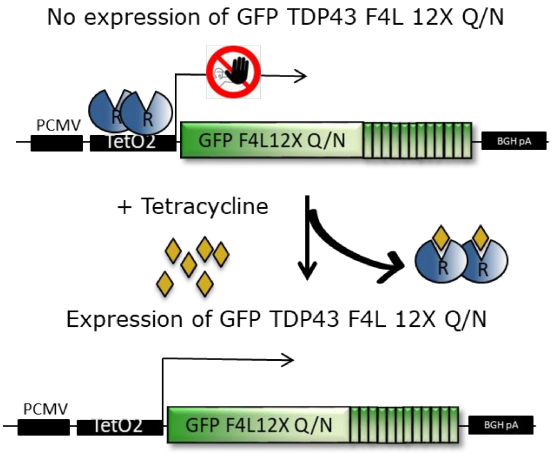

b)

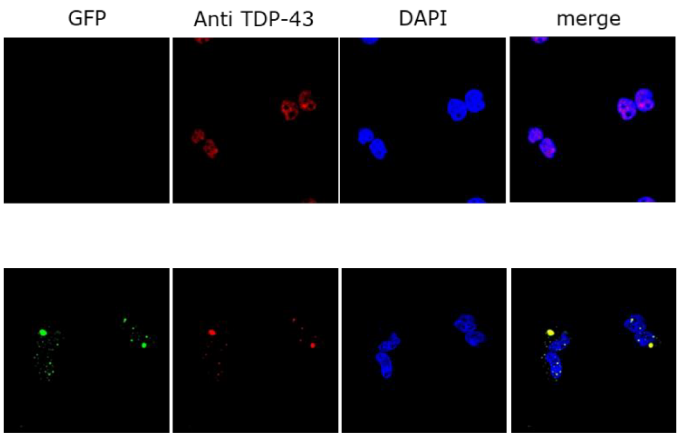

Figure 22. Tetracycline inducible cell line of EGFP-TDPF4L12xQ/N.

(a) Cartoon of the construct used to create the EGFP-TDPF4L12xQ/N cell line. Tetracycline binds to the repressor inducing the expression of the transgene. (b) Immunofluorescence of EGFP-TDPF4L12xQ/N stable cells showing sequestration of endogenous TDP-43 into the aggregates. Anti-GFP (green), anti-TDP-43 (red) antibodies were used. The cell nuclei were stained using the reagent TOPRO-3.

1.2. Sequestration of endogenous TDP-43 by the EGFP-TDPF4L12xQ/N aggregates reduces the amount of soluble TDP-43

To further confirm the ability of the EGFP-TDPF4L12xQ/N aggregates to sequester endogenous TDP-43, total protein extraction was performed after 24h following induction of the EGFP-TDPF4L12xQ/N construct. Subsequently, a fractionation of soluble and insoluble fractions was performed (see section 2.8 of Materials and Methods), and the presence of endogenous TDP-43 and exogenous (EGFP-TDPF4L12xQ/N) proteins in each fraction was analysed by western blot using an anti-TDP-43 antibody. As can be seen in figure 23, a clear shift in the solubility of endogenous TDP-43 occurs upon induction of EGFP-TDPF4L12xQ/N. In fact, in conditions where the transgene is not induced (-Tet), the endogenous TDP-43 is distributed in the soluble fraction (lane 1 and 2). Interestingly, upon EGFP-TDPF4L12xQ/N expression (+Tet), the endogenous TDP-43 protein shifts into the insoluble fraction together with the aggregates, confirming the sequestration and aggregation of the endogenous TDP-43 (lane 3 and 4).

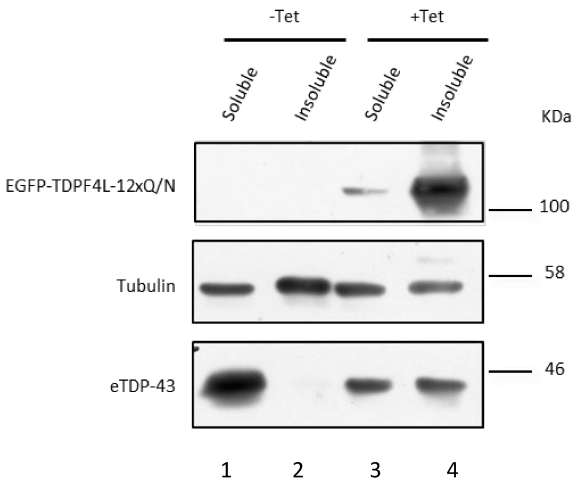

Figure 23. Endogenous TDP-43 solubility upon EGFP-TDPF4L12xQ/N expression.

Western blot of fractionated proteins obtained from EGFP-TDPF4L12xQ/N stable cells induced or not induced with tetracycline. In normal conditions, endogenous TDP-43 is mainly soluble (lane 1 and 2, lower panel), however, when the aggregates are formed upon tetracycline induction, there is a shift of the protein from the soluble to the insoluble fraction (lane 3 and 4, lower panel). Soluble

and insoluble fractions were separated by SDS-PAGE, followed by western blotting with anti-TDP-43. Tubulin was used as loading control.

1.3. Sequestration of endogenous TDP-43 results in a loss of function in its role in mRNA processing

I then analysed if the reduction of soluble TDP-43, due to its entrapment in the aggregates, would result in a concomitant loss of endogenous TDP-43 cellular functions. To do this, I analysed POLDIP3 alternative splicing of exon 3, that is regulated by TDP-43, which binds to the UG-rich sequences placed downstream of exon 3 (Buratti and Baralle 2001). As explained in section 2.1.1 of the introduction, when TDP-43 is present, it favours the inclusion of exon 3 in the mRNA of POLDIP3. On the contrary, when TDP-43 is silenced using a siRNA, exon 3 is skipped giving rise to a shorter transcript (figure 24, upper panel). Interestingly, upon EGFP-TDPF4L12xQ/N expression following induction with tetracycline, POLDIP3 exon 3 splicing pattern is similar to the one obtained after TDP-43 silencing (figure 24, lower panel), confirming that the aggregates are sequestering endogenous TDP-43, preventing it from regulating POLDIP3 alternative splicing, and causing loss-of-function.

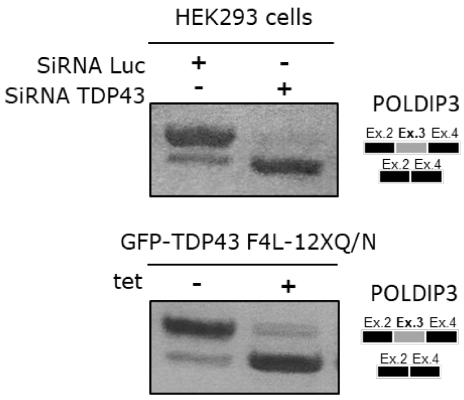

Figure 24. POLDIP3 alternative splicing is affected in cells expressing EGFP-TDPF4L12xQ/N.
Upper panel: representative agarose gel of RT-PCR products using POLDIP3 specific primers spanning exon 3 from cells treated with TDP-43 siRNA. Lower panel: representative agarose gel of RT-PCR products using POLDIP3 specific primers spanning exon 3 from cells expressing EGFP-

TDPF4L12xQ/N transgene upon tetracycline induction. On the right side of the gels, a schematic representation of the amplicons is shown.

2. EGFP-TDPF4L12xQ/N cell line as a tool for screening compounds able to promote aggregate clearance

2.1. Tricyclic compounds and their effect on aggregate clearance

The results presented thus far indicate that the cell line described above represents a good model to trigger endogenous TDP-43 aggregation. The aggregates produced by EGFP-TDPF4L12xQ/N act as a sink for the newly formed TDP-43, which results in a concomitant loss of TDP-43 function in regards to mRNA splicing. To our knowledge, this is the only existing experimental system that can mimic TDP-43 aggregation without altering directly the endogenous gene expression levels, a design that imitates the pathogenic mechanism acting in the human disease. As we hypothesize that a reduction of these inclusions could restore the normal TDP-43 levels and therefore its functions, providing a potential therapeutic approach for TDP-43 proteinopathies, this cell line represents an ideal substrate to be used in a high throughput screen; clearing aggregates by inducing cellular proteolysis could be a way to restore normal TDP-43 levels inside the nucleus and recover its functionality.

For this reason, I used the EGFP-TDPF4L12xQ/N cellular model to analyse aggregate clearance after treatment with five FDA approved drugs: Chlorpromazine, Fluphenazine, Thioridazine, Clomipramine and Nortriptyline. These drugs have been shown to have an effect on autophagy (Tsvetkov, Miller et al. 2010). Moreover, they are able to cross the blood brain barrier and were shown to be neuroprotective (see section 3.4 of Introduction).

The clearance assay was performed by inducing EGFP-TDPF4L12xQ/N expression with tetracycline for 24 hours. After aggregate formation, tetracycline was washed away with PBS, and cells were treated with the chosen compound for 48 hours. Different concentrations were used: Chlorpromazine 10 µM, Fluphenazine 5 µM, Thioridazine 4 µM, Clomipramine 10 µM and Nortriptyline 10 µM. All the compounds were tested at a maximum concentration of 10 µM, however, Thioridazine and Fluphenazine showed a toxic effect on the cells and were reduced. As a control, I performed the experiment without compound.

After the treatment, cells were harvested and proteins were extracted and separated by SDS-PAGE. The total amount of EGFP-TDPF4L12xQ/N was assessed using an anti-GFP antibody while GAPDH was used as loading control (figure 25, middle panel).

As shown in figure 25, the treatment with each of the five compounds significantly reduced the total level of EGFP-TDPF4L12xQ/N (upper panel).

In order to evaluate if the clearance of TDP-43 aggregates upon drug treatment correlates with a recovery of protein functionality, we induced EGFP-TDPF4L12xQ/N cells with tetracycline for 24 hours, and analysed the splicing pattern of POLDIP3 exon 3 before and after the treatment with the compounds. As shown in figure 25, tetracycline induction of EGFP-TDPF4L12xQ/N generates a switch in the exon 3 splicing pattern towards variant-2 (exon 3 skipping), similarly to that which occurs when TDP-43 is silenced. However, after drug treatment there is a shift towards variant-1 (exon 3 inclusion), which is comparable to the wild-type condition, confirming that the recovery of TDP-43 functionality is linked to aggregate clearance for all the compounds tested (figure 25, lower panel).

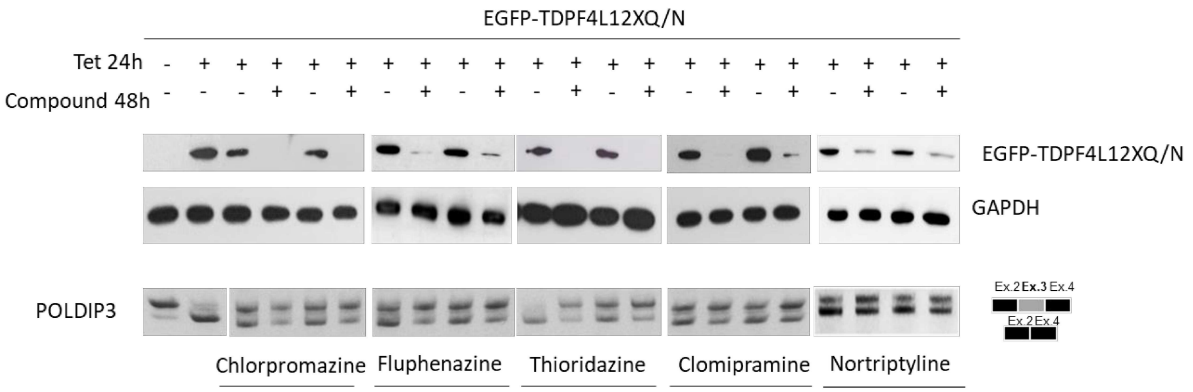

Figure 25. Clearance assay and POLDIP3 splicing pattern in cells expressing EGFP-TDPF4L12xQ/N before and after the treatment with FDA approved drugs. Upper panel: representative western blots showing the clearance of EGFP-TDPF4L12xQ/N aggregates after the treatment with five different FDA approved compounds. Middle panel: western blot showing GAPDH as loading control. Lower panel: representative agarose gel of RT-PCR products using POLDIP3 specific primers spanning exon 3 from EGFP-TDPF4L12xQ/N cells treated and non-treated with the compounds.

2.1.1. Aggregate clearance and TDP-43 functional recovery by Nortriptyline and Thioridazine is linked to a recovery of TDP-43 solubility

In order to assess if the recovery of functionality upon drug treatment was due to the fact that endogenous TDP-43 was no longer sequestered into the aggregates, I analysed the percentage of soluble TDP-43 before and after the treatment with either Nortriptyline 10 µM (figure 26a) or Thioridazine 4 µM (figure 26b). This experiment was performed with only two compounds as the previous results indicated that they were behaving in a similar manner.

As previously observed (see section 1.2 of results), in normal conditions, TDP-43 is mainly soluble, however, when aggregates are formed, there is a shift of the protein from the soluble to the insoluble fraction, together with the aggregates. Forty-eight hours after aggregate induction is stopped due to the removal of tetracycline, there is a partial increase in the soluble TDP-43, which follows the natural clearance of the aggregates that occurs due to degradation by the normal pathways of proteolysis (figure 26a and 26b, compare lane 5/6 with 3/4). However, this is significantly increased after the treatment with the compounds tested (figure 26a and 26b, lane 7/8), further demonstrating the ability of the compounds to enhance aggregate clearance that consequently results in less sequestration of endogenous TDP-43.

a)

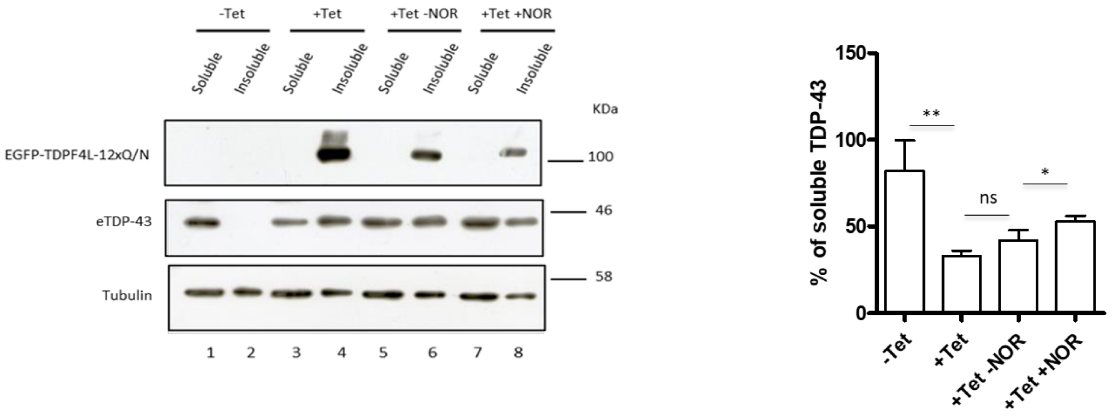

b)

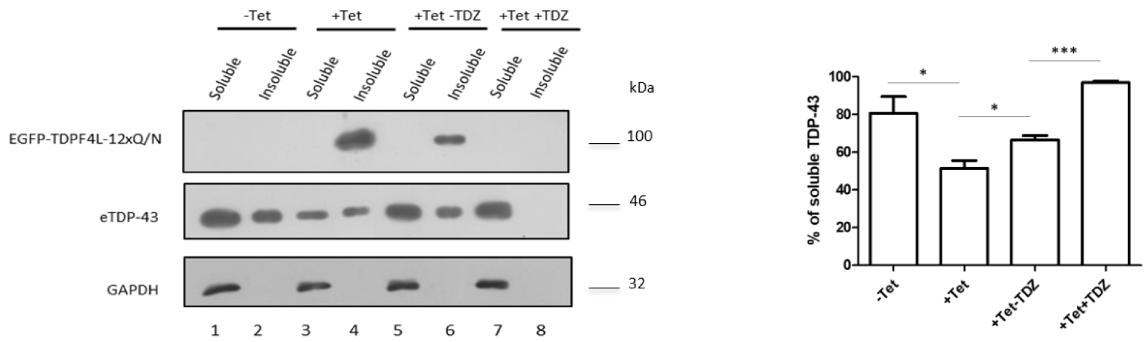

Figure 26. Endogenous TDP-43 solubility is recovered upon Nortriptyline and Thioridazine treatment. Western blot of fractionated proteins obtained from EGFP-TDPF4L12xQ/N stable cells treated or not treated with (a) Nortriptyline and (b) Thioridazine. Soluble and insoluble fractions were separated by SDS-PAGE, followed by western blotting with anti-TDP-43. Tubulin and GAPDH were used as loading controls. Quantification of soluble TDP-43 normalized against the respective loading controls is shown on the right-hand side of each panel (unpaired t-test analysis). ns indicates $p>0,05$ (not significant), ** and * indicate $p<0,05$ (significant). Error bars indicate SEM.

2.1.2. The effect of Nortriptyline and Thioridazine on aggregate clearance is independent of autophagy

To understand the proteolytic pathway involved in the degradation of the aggregates, I initially analysed aggregate clearance in cells treated with the compounds in presence of two different autophagy inhibitors: chloroquine and ammonium chloride (NH_4Cl), that act by changing the pH inside of the lysosome inhibiting the fusion with the autophagosome, thus blocking the autophagic flux. After 24 hours of tetracycline induction, cells were treated with Nortriptyline 10 μM or Thioridazine 4 μM together with either chloroquine or NH_4Cl for 48 hours. Cells were then harvested and proteins were extracted and separated by SDS-PAGE.

To confirm that autophagy was actually blocked, I analysed LC3 conversion and p62 accumulation upon chloroquine and NH_4Cl treatment. As previously explained, LC3 is a soluble protein that during autophagy is converted from its soluble form (LC3I) to the LC3-phosphatidylethanolamine conjugated form (LC3II) and is recruited to the autophagosomal membrane. Therefore, LC3-II levels directly correlate with the amount of autophagosomes inside the cell. As shown in figure 27a and 27b, after treatment with NH_4Cl and chloroquine, an increase in the conversion of LC3I into LC3II was observed (lanes 3/4 and 5/6).

However, this could be a consequence of either increased autophagosome formation, due to an enhancement of autophagy, or a reduced turnover of autophagosomes due to an impairment in the degradation pathway. Therefore, the use of autophagy markers such as LC3-II needs to be complemented by other markers that will help understanding the overall autophagic flux. One approach could be to measure p62 levels. p62 acts as a link between ubiquitinated substrates and LC3 and it is degraded by autophagy, thus, it accumulates when autophagy is blocked. Therefore, I analysed the amount of p62 after the treatment with NH_4Cl and chloroquine. As shown in the western blot analysis (figure 27a and 27b lanes 3/4 and 5/6), p62 accumulates after the treatment with both the inhibitors, confirming that autophagy is indeed blocked.

a)

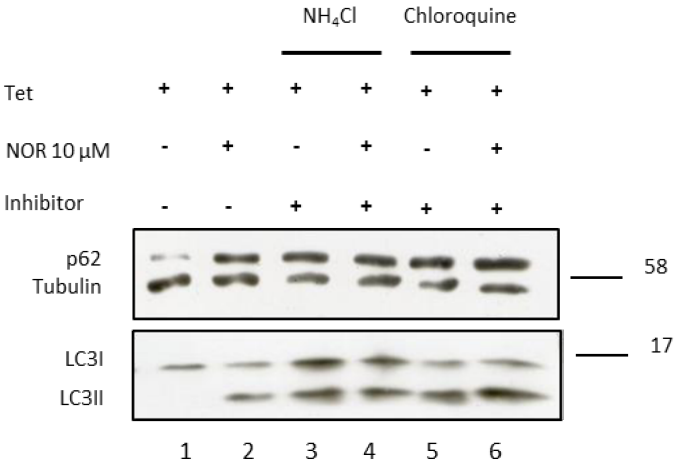

b)

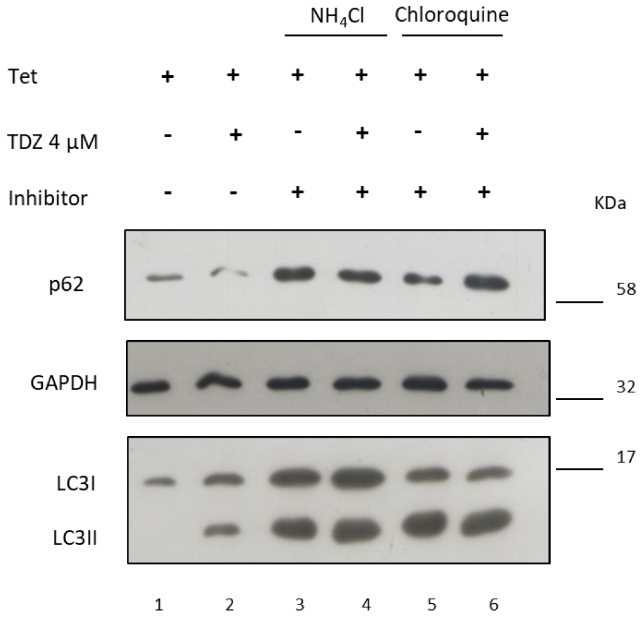

Figure 27. NH_4Cl and chloroquine effectively block autophagy.

Western blots of LC3 conversion and p62 accumulation after treatment of EGFP-TDPF4L12xQ/N cells with (a) Nortriptyline and (b) Thioridazine in presence of NH_4Cl and chloroquine for 48 hours. GAPDH and tubulin were used as loading controls.

Once I confirmed that both NH_4Cl and chloroquine could effectively block autophagy, I performed a western blot with anti-GFP antibody to analyse the levels of EGFP-TDPF4L12xQ/N before and after the treatment with Nortriptyline or Thioridazine on the same protein extracts. Interestingly, as shown in figure 28a and 28b, even in the presence of the autophagy inhibitors, Nortriptyline and Thioridazine are still able to clear the aggregates, indicating that autophagy is not involved in the clearance mechanism (compare lane 3 with lane 4 and lane 5 with lane 6).

a)

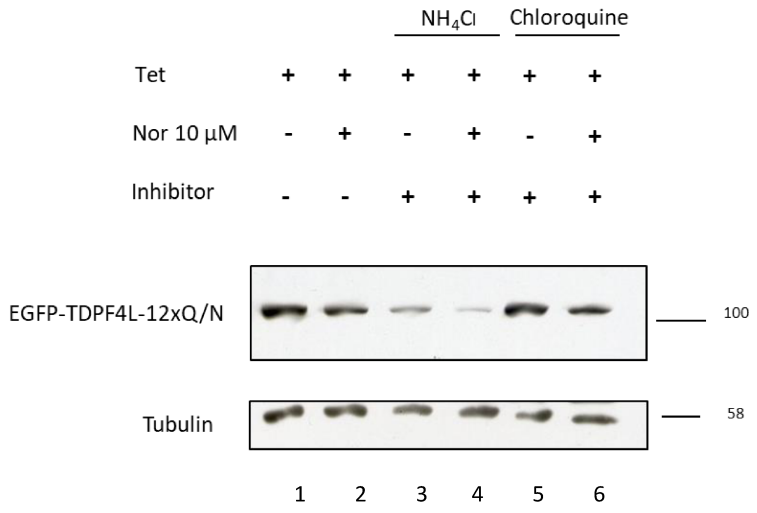

b)

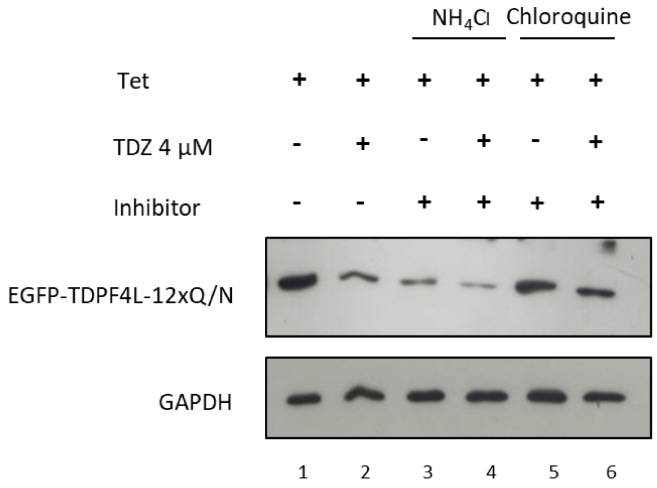

Figure 28. Clearance assay of EGFP-TDPF4L12xQ/N in presence of NH_4Cl and chloroquine.

Western blots of EGFP-TDPF4L12xQ/N levels after cells were treated for 48 hours with either (a) Nortriptyline or (b) Thioridazine in presence of the autophagy inhibitors NH_4Cl and chloroquine. GAPDH and tubulin were used as loading controls.

Subsequently, I analysed the splicing pattern of POLDIP3 before and after the compound treatment in presence of the inhibitors. As expected when taking into account the results above (figure 28), after 48 hours of treatment with either Nortriptyline 10 µM (figure 29a) or Thioridazine 4 µM (figure 29b), I observed that TDP-43 loss-of-function is still recovered when cells are treated with the selected compound together with either chloroquine or ammonium chloride; there is indeed a shift of POLDIP3 mRNA to variant-1 (exon 3 inclusion), which is comparable to the control (Figure 29a and 29b, lane 5/6 and 7/8).

a)

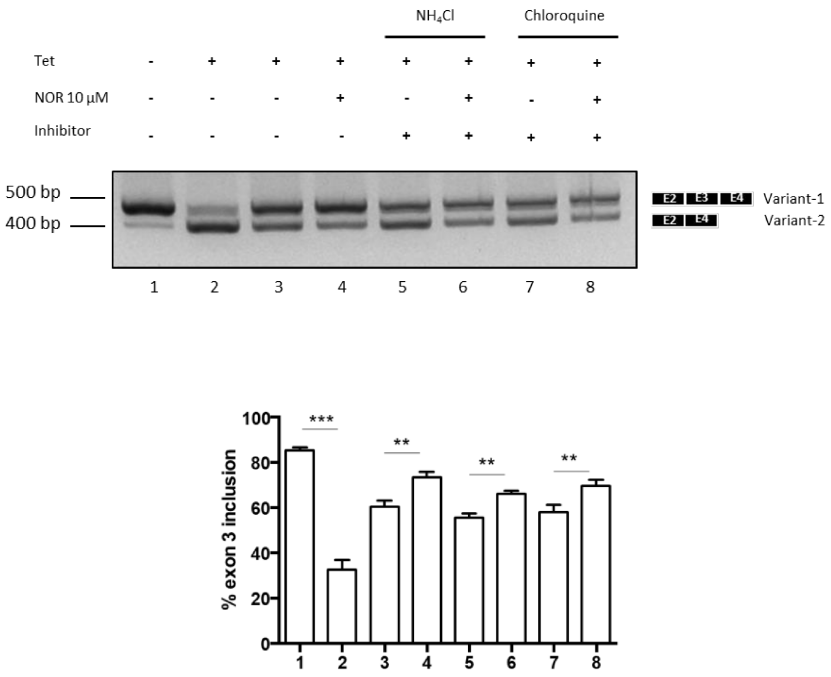

b)

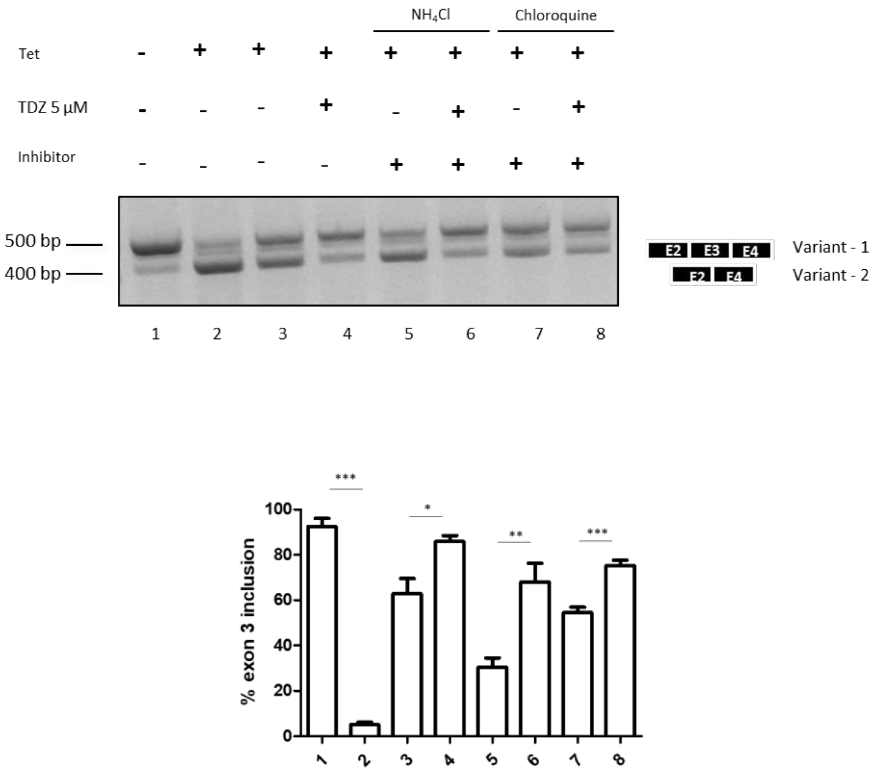

Figure 29. POLDIP3 alternative splicing in EGFP-TDPF4L12xQ/N stable cells. POLDIP3 exon 3 alternative splicing was analysed by RT-PCR after the treatment with (a) Nortriptyline and (b) Thioridazine in presence of the autophagy inhibitors NH_4Cl and chloroquine. On the right side of the gels, a schematic representation of the amplicons is shown. Unpaired t-test analysis was used to compare measures between 2 groups. * indicates $p<0,05$, ** indicates $p<0,01$ and *** indicates $p<0,0001$.

2.1.3. Aggregate clearance by Nortriptyline and Thioridazine needs a functional ubiquitin-proteasome system

To investigate whether aggregate clearance occurs through the ubiquitin-proteasome system (UPS), we treated cells with either Nortriptyline 10 µM or Thioridazine 4 µM in presence of the proteasome inhibitor Bortezomib. As for the autophagy inhibitors, Bortezomib was added to the media 1 hour before the drug treatment. After 48 hours, cells were harvested and proteins were extracted. The

lysates were separated by SDS-PAGE and then analysed by western blot. Remarkably, neither Nortriptyline (figure 30a) nor Thioridazine (figure 30b) were able to degrade the aggregates in presence of the proteasome inhibitor.

As already mentioned, cells were induced with tetracycline for 24 hours and after induction, tetracycline was washed out to block EGFP-TDPF4L12xQ/N expression and stop aggregate formation. Control cells were further cultured for 48 hours in the absence of the compounds. It is important to notice that, during this time, EGFP-TDPF4L12xQ/N is usually degraded, up to some extent, by the normal protein degradation pathways within the cell. However, upon UPS inhibition, cells are no longer able to clear EGFP-TDPF4L12xQ/N aggregates leading to their accumulation (figure 30a and 30b lane 3 and 4). Anti-ubiquitin was used to check whether the proteasome was inhibited upon treatment with Bortezomib (figure 30a and 30b lane 3 and 4, right-hand side); ubiquitinated proteins are normally degraded by the proteasome, thus as an increase in ubiquitin signal is an indication of an impairment in the UPS pathway.

a)

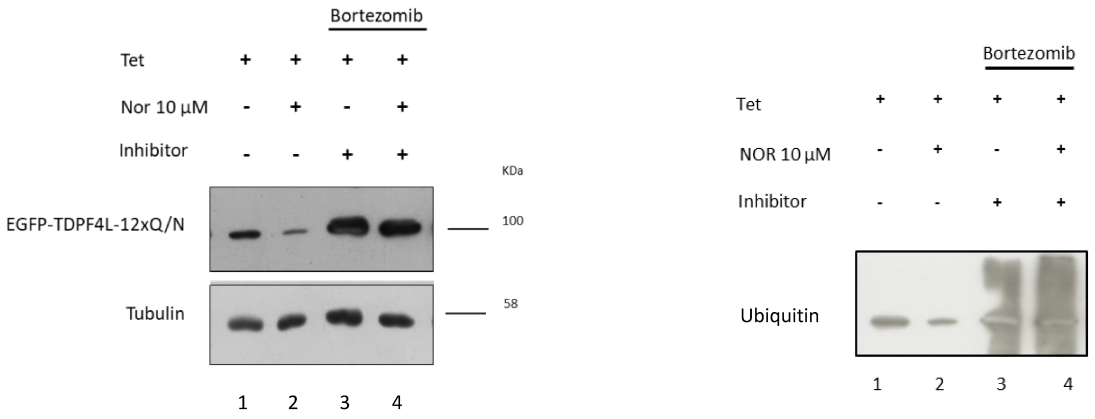

b)

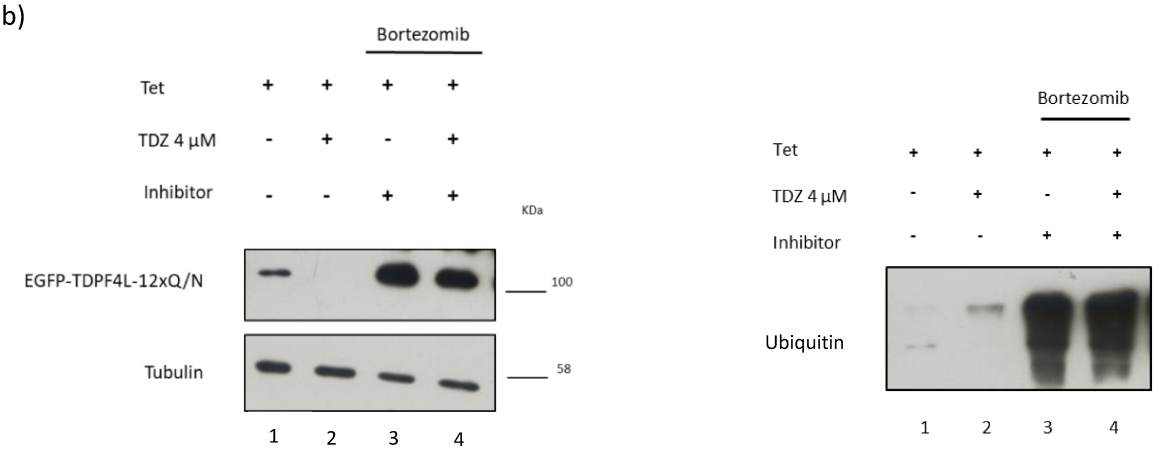

Figure 30. Clearance assay of EGFP-TDPF4L12xQ/N in presence of Bortezomib.

Western blots of EGFP-TDPF4L12xQ/N levels after cells were treated for 48 hours with either (a) Nortriptyline or (b) Thioridazine in presence of the proteasome inhibitor Bortezomib. GAPDH and tubulin were used as loading controls. Western blots with anti-ubiquitin showing the inhibition of the proteasome after treatment with Bortezomib are shown on the right-hand side.

I then analysed POLDIP3 exon 3 alternative splicing in presence of the proteasome inhibitor. As shown in figure 31, when the proteasome is inhibited, there is no recovery of protein functionality upon compound treatment as shown by the increase of variant-2 over variant-1 of POLDIP3 mRNA (figure 31a and 31b lane 5/6). This could be a consequence of the defective degradation of the aggregates upon UPS inhibition.

a)

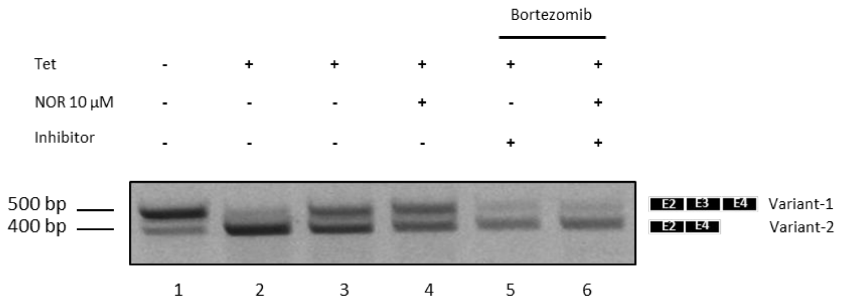
Bortezomib
Tet - + + + + +
NOR 10 µM - - - + - +
Inhibitor - - - - + +
500 bp
400 bp
E2 E3 E4 Variant-1
E2 E4 Variant-2
1 2 3 4 5 6

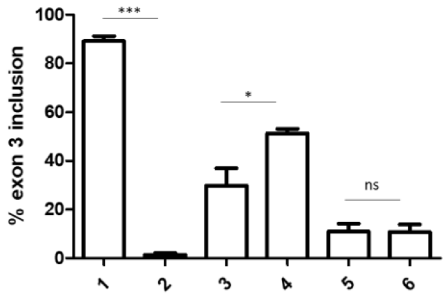
% exon 3 inclusion
100
80
60
40
20
0
***
*
ns
1 2 3 4 5 6

b)

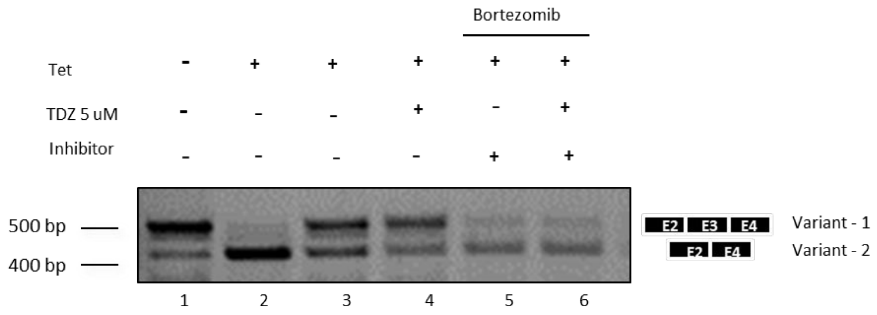
Bortezomib
Tet - + + + + +
TDZ 5 uM - - - + - +
Inhibitor - - - - + +
500 bp
400 bp
E2 E3 E4 Variant - 1
E2 E4 Variant - 2
1 2 3 4 5 6

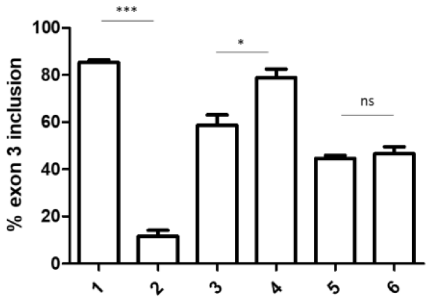
% exon 3 inclusion
100
80
60
40
20
0
***
*
ns
1 2 3 4 5 6

Figure 31. POLDIP3 alternative splicing in EGFP-TDPF4L12xQ/N stable cells. POLDIP3 exon 3 alternative splicing was analysed by RT-PCR after the treatment with (a) Nortriptyline and (b) Thioridazine in presence of the proteasome inhibitor Bortezomib. On the right side of the gels, a schematic representation of the amplicons is shown. Unpaired t-test analysis was used to compare measures between 2 groups. ns indicates p>0,05 (not significant), * indicates p<0,05, ** indicates p<0,01 and *** indicates p<0,0001 (significant).

3. A *Drosophila* model for TDP-43 aggregation

3.1. Creation of TDPF4L12xQ/N *Drosophila* lines

In order to study the effects of these compounds on TDP-43 aggregation *in vivo*, as well as those eventually deriving from the high-throughput screen that was simultaneously undertaken by collaborators (see section 5 of Results), I created a *Drosophila* model expressing the identical aggregate inducer as the cell line. This was done by cloning the TDPF4L12xQ/N sequence linked to a FLAG tag under the control of an upstream activating sequence (UAS) in a pUASTattb vector and sequenced it. A FLAG tag was chosen over the previously used EGFP as shorter thus easier to clone into the fly. After the sequencing analysis, I tested the expression of the protein FLAG-TDPF4L12xQ/N in S2 *Drosophila* cells that derive from primary culture of late stage (20-24 hours) *Drosophila melanogaster* embryos. To do so, I co-transfected s2 cells with a pUAST- FLAG-TDPF4L12xQ/N plasmid and a plasmid containing Gal4 in order to induce the expression of the gene under the control of the UAS sequence. After 48 hours, cells were collected and proteins were extracted and separated with SDS-PAGE. Subsequently, a western blot with anti-FLAG antibody was performed. As shown in figure 32, the expression of the transgene is activated when Gal4 is present (lane 2).

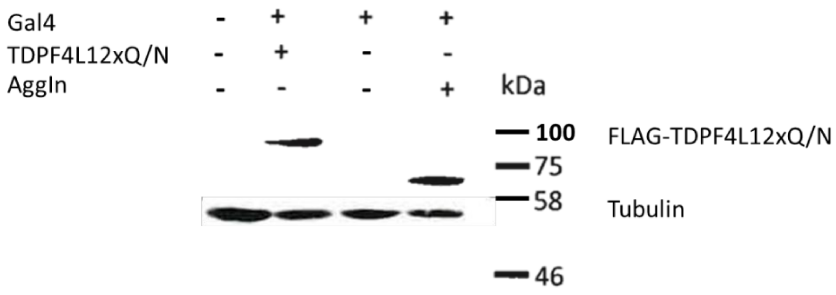

Figure 32. FLAG-TDPF4L12xQ/N is correctly expressed in S2 cells. Western blot of proteins obtained from S2 cells transfected with a plasmid containing Gal4 together with pUAST-FLAG-TDPF4L12xQ/N (lane 2) or pUAST-AggIn (lane 4) used as positive control. Tubulin was used as loading control.

After confirming the correct expression of the FLAG-TDPF4L12xQ/N construct, transgenic *Drosophila* lines were created by site-specific insertion (Best Gene Inc.). Five different transgenic lines were obtained through micro-injection in the posterior pole of *Drosophila* embryos.

The expression of FLAG-TDPF4L12xQ/N transgene in all the 5 transgenic lines sent by Best Gene Inc. was evaluated by crossing each line with GMR-Gal4 driver flies to drive the expression of FLAG-TDPF4L12xQ/N specifically in the eye tissue. After obtaining the progeny, I extracted the proteins from the heads and separated them with SDS-PAGE. Using an anti-FLAG antibody, I assessed the expression level of FLAG-TDPF4L12xQ/N in each of the five lines. As shown in figure 33, transgenic line 1 and 5 respectively under and overexpressed the protein. The other three lines (2, 3 and 4) expressed comparable levels of FLAG-TDPF4L12xQ/N protein, which can be observed below 100 kDa. Line 3 has been chosen arbitrarily for the rest of the experiments.

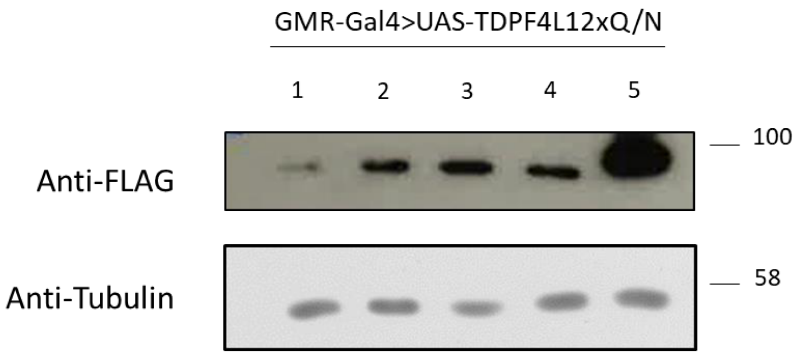

Figure 33. *Drosophila* FLAG-TDPF4L12xQ/N transgenic lines. Western blot of proteins obtained from adult heads of five different FLAG-TDPF4L12xQ/N transgenic lines crossed with GMR-Gal4 driver flies. Tubulin was used as loading control. Line 3 has been chosen arbitrarily for the rest of the experiments.

3.2. FLAG-TDPF4L12xQ/N expression promotes endogenous TDP-43 aggregation in flies

I then assessed whether the FLAG-TDPF4L12xQ/N protein was able to aggregate and sequester endogenous TDP-43 in the transgenic fly. For this purpose, I performed a biochemical fractionation of proteins extracted from adult heads of flies expressing TBPH (*Drosophila* homologue of TDP-43) together with either EGFP or FLAG-TDPF4L12xQ/N. Three fractions were loaded in the SDS-PAGE: the input, the soluble and the insoluble fraction. As shown in figure 34, the FLAG-TDPF4L12xQ/N protein is aggregating, being present in the insoluble fraction (lane 3). Moreover, when EGFP is expressed, TBPH is mainly present in the soluble fraction (lane 5); however, there is a shift of TBPH into the insoluble fraction when FLAG-TDPF4L12xQ/N is expressed, confirming the capability of the aggregates to sequester TBPH (lane 3).

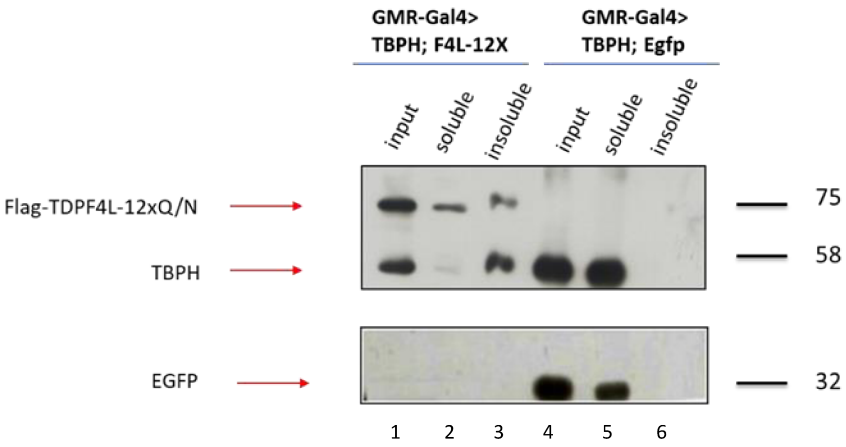

Figure 34. FLAG-TDPF4L12xQ/N promotes TBPH aggregation in *Drosophila* retinal cells.

Western blot of fractionated proteins obtained from flies expressing TBPH together with either TDPF4L12xQ/N or EGFP. Co-expression of TBPH and TDPF4L12xQ/N leads to the formation of TBPH insoluble aggregates, whereas TBPH remains soluble when co-expressed with EGFP.

3.3. FLAG-TDPF4L12xQ/N aggregates are not toxic and are able to rescue TBPH-induced degeneration

Subsequently, I assessed if aggregates could have any detrimental effect on the tissue. For this purpose, I crossed UAS-FLAG-TDPF4L12xQ/N flies with GMR-Gal4 driver flies, to drive the expression of the transgene in the eye (figure 35). The *Drosophila* eye is indeed a powerful tool to detect toxicity due to its delicate and precise structure. In our case, despite the formation of aggregates upon FLAG-TDPF4L12xQ/N expression, we could not observe any modification in the external structure of the eye, suggesting that aggregates are not toxic *per se* (figure 35a). As a control, I expressed EGFP protein (figure 35b).

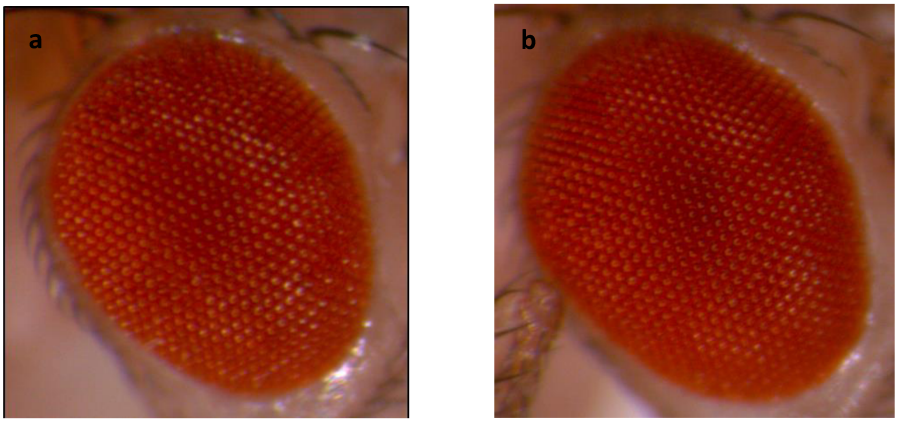

GMR-Gal4>UAS-TDPF4L12xQ/N GMR-Gal4>UAS-EGFP

Figure 35. FLAG-TDPF4L12xQ/N expression in the *Drosophila* eye does not affect its structure. External eye phenotype of (a) GMR-Gal4>UAS-TDPF4L12xQ/N and (b) GMR-Gal4>UAS-EGFP flies.

In order to further confirm that the sequestration of the endogenous TDP-43 by the aggregates was occurring as observed in the cellular model (section 1.2 of Results), I first over expressed TBPH in the eye tissue using GMR-Gal4 driver flies. As already reported by others, TBPH overexpression induces a strong degeneration in the eye structure, with loss of pigmentation and formation of necrotic areas (Miguel, Frébourg et al. 2011).

I then analysed the effect of the expression of TBPH together with FLAG-TDPF4L12xQ/N. If the aggregates are formed and sequester TBPH, the toxic effect caused by the overexpression of TBPH previously observed in the fly eye, should be at least partially reduced. This was indeed the case. As can be seen, the strong degeneration induced by TBPH is completely recovered, as it can be appreciated in figure 36b where the structure of the eye is comparable to the wild type (figure 36a). In order to confirm that the recovery of the degeneration was dependent on the expression of FLAG-TDPF4L12xQ/N, TBPH was overexpressed also in presence of EGFP alone. However, in this case we were still able to visualize a strong degeneration (figure 36c).

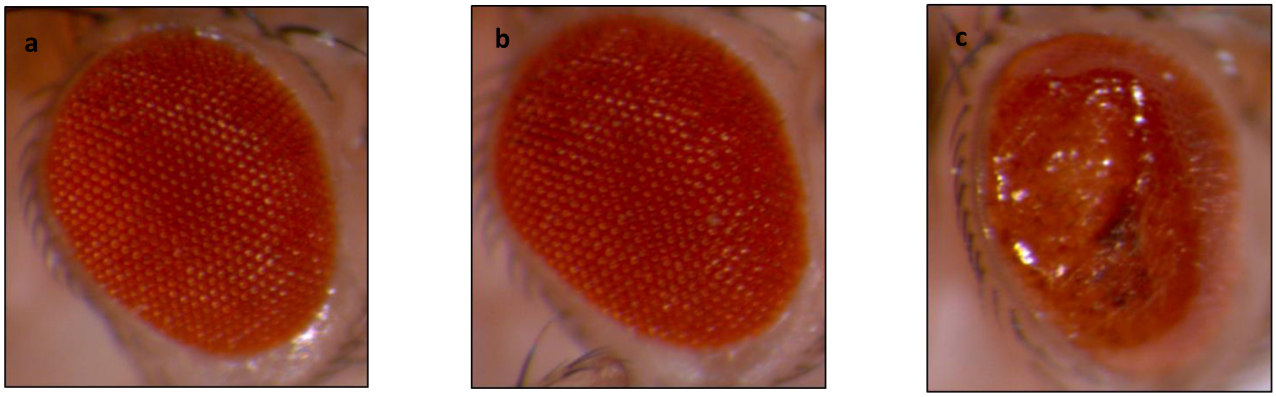

Figure 36. TDPF4L12xQ/N expression rescues TBPH-induced degeneration.

External eye phenotype of (a) wild-type flies and flies expressing TBPH together with either (b) TDPF4L12xQ/N or (c) EGFP. The co-expression of TBPH and the transgene rescues TBPH-induced eye degeneration (b), whereas the co-expression of TBPH with EGFP does not recover the phenotype (c).

3.4. Phenotype analysis of FLAG-TDPF4L12xQ/N neuronal expression

Once I assessed that aggregates were not toxic *per se*, and that they were able to entrap TBPH, I analysed whether the aggregates could induce an ALS-like motor phenotype, due to endogenous TBPH sequestration. In order to do so, FLAG-TDPF4L12xQ/N expression was induced in neurons by crossing FLAG-TDPF4L12xQ/N flies with Elav-Gal4 driver flies. UAS-EGFP flies were used as control. Progeny expressing FLAG-TDPF4L12xQ/N was then analysed for a motor phenotype at third instar larval stage and adulthood.

3.4.1. Motor phenotype analysis of third instar larvae expressing FLAG-TDPF4L12xQ/N

Drosophila larvae naturally show peristaltic movements characterized by a wave, which starts at the tail of the larva and ends in the mouth, passing throughout the body. To analyse the movement of the transgenic fly, peristaltic waves performed by the larvae in two minutes were counted. As shown in the graph (figure 37), the number of peristaltic waves performed by TDPF4L12xQ/N expressing larvae was comparable to that observed in EGFP control flies.

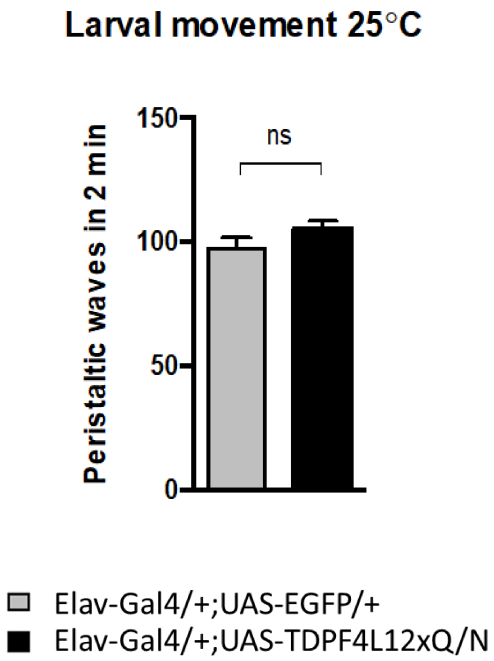

Figure 37. TDPF4L12xQ/N expression in neurons does not affect larval movement.

Number of peristaltic waves performed by third instar larvae expressing either EGFP or TDPF4L12xQ/N in the nervous system. More than 20 larvae per genotype were tested and the mean was calculated. p>0,05 (not significant) was calculated by unpaired t-test. Error bars indicate SEM.

3.4.2. Phenotype analysis of adult flies expressing FLAG-TDPF4L12xQ/N

The adult phenotype was examined by analysing the climbing ability of transgenic FLAG-TDPF4L12xQ/N flies and EGFP control flies at day 3, 7, 11 and 14. As can be observed in figure 38a, starting from day 7 TDPF4L12xQ/N expressing flies show a significant decrease in their climbing ability when compared to control flies (77% of top climbing flies vs 87% for EGFP flies). Interestingly, locomotion defects get worse with aging with only 35% of TDPF4L12xQ/N flies reaching the top at day 11, becoming less than 10% at day 14. On the contrary, 85% of control EGFP flies were still able to climb to the top at day 14. Moreover, the lifespan of FLAG-TDPF4L12xQ/N expressing flies was severely impaired with a median survival of 25 days against a median survival of 50 days for flies expressing EGFP (figure 38b). These results confirmed that TDP-43 aggregation is able to trigger an ALS-like age-related motor phenotype *in vivo*.

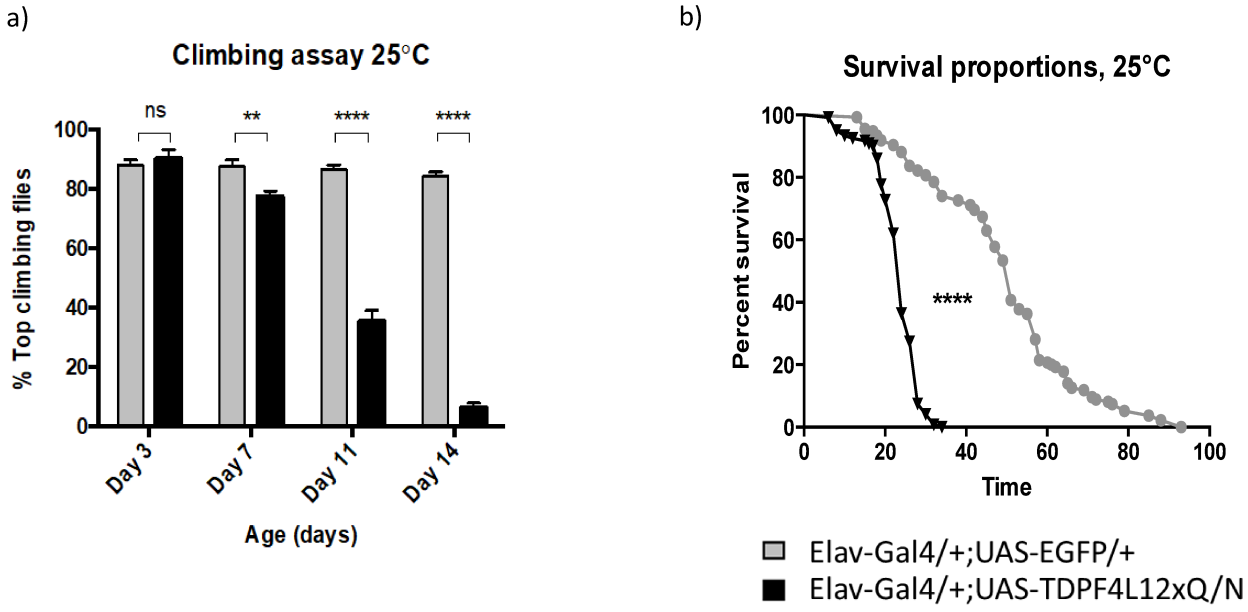

Figure 38. TDPF4L12xQ/N expression in neurons triggers an age-related motor phenotype in *Drosophila* adult flies. (a) Climbing assay and (b) lifespan of FLAG-TDPF4L12xQ/N expressing flies compared with EGFP control flies. For each time point, 100 flies per genotype were tested. Unpaired t-test analysis was used to compare measures between the two groups. Long rank test was

performed to compare survival distribution between genotypes. ns indicates p>0,05 (not significant), ** indicates p<0,05 (significant) and **** indicates p<0,0001. Error bars indicate SEM.

4. Thioridazine testing in the TDPF4L12xQ/N *Drosophila* model

Once I assessed the presence of an age-related motor phenotype in the fly expressing the TDPF4L12xQ/N construct, I used the same model to test if Thioridazine could improve the locomotive defects. Thioridazine was chosen over Nortriptyline as in the cellular model this compound appeared to clear aggregates more efficiently. The protocol to treat the flies was based on analysing the climbing ability of flies after 10 days of treatment with the compound. This time period was chosen as it seemed, based on previous experiments (see figure 38), to be an optimal compromise between the appearance of locomotive defects and the survival. In fact, 10 days after hatching from the pupal case, a motor phenotype is visible but not too severe, and the majority of the flies are still alive (they start to significantly die at day 12/14). Regarding the feeding of the compound to the flies, this was performed by dissolving the compound in the fly food; flies were thus fed for 10 days starting from day 1 after hatching from the pupal case. After 10 days of treatment, the climbing ability of the flies was tested (see section 3.3.1 of Materials and Methods).

To find a dose of Thioridazine that was not toxic, EGFP control flies were treated with different concentrations of the compound. An initial testing was performed, and a scale of concentrations ranging from 2 mM to 0.4 mM were tested. As can be seen in figure 39, a 2 mM final concentration of Thioridazine dissolved in the food was found to be lethal and flies died before the end of the treatment (column 2). 1 mM Thioridazine resulted in a slightly impaired locomotion when compared with the climbing performance of EGFP flies treated with water (column 3). Flies treated with Thioridazine 0.4 mM on the other hand did not show any adverse effect in the climbing assay (column 4).

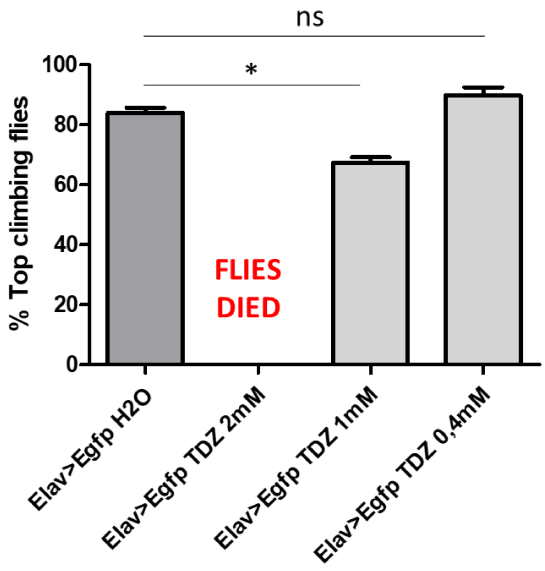

Figure 39. Climbing assay after treatment with Thioridazine. Climbing assay of EGFP control flies treated and non-treated with Thioridazine 2 mM, 1 mM and 0.4 mM for 10 days. 100 flies per condition were tested. One-way anova analysis was used to compare measures between four groups. ns indicates p>0,05 (not significant), * indicates p<0,05. Error bars indicate SEM.

Since Thioridazine 0.4 mM was found to be non-toxic, this dose was chosen to treat TDPF4L12xQ/N expressing flies to test if the locomotive defects could be improved. Briefly, one-day-old flies expressing EGFP or TDPF4L12xQ/N were collected and transferred to tubes with either the compound or water as control (100 flies per group were tested putting 20 flies per tube in a female:male 1:1 ratio). Interestingly, after 10 days of treatment with Thioridazine, the climbing ability of TDPF4L12xQ/N expressing flies was found to be significantly improved when compared with TDPF4L12xQ/N non-treated flies (figure 40, compare column 3 and 4).

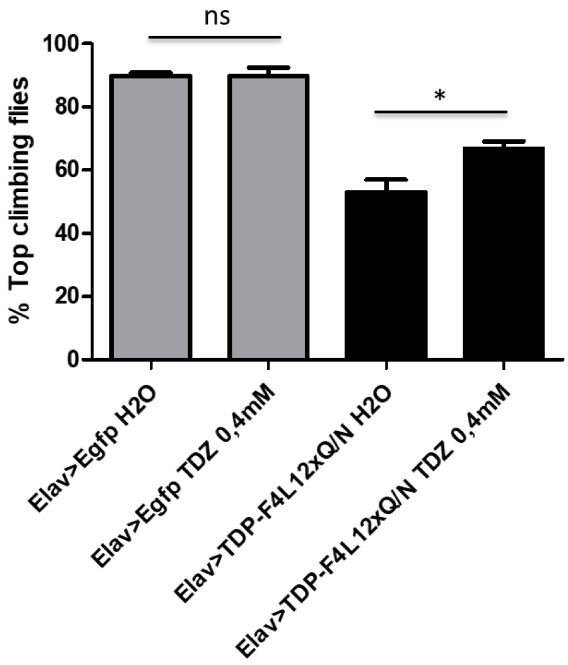

Figure 40. Rescue of climbing deficit in TDPF4L12xQ/N flies by feeding Thioridazine.

Climbing assay of TDPF4L12xQ/N expressing flies and EGFP control flies treated and non-treated with Thioridazine 0.4 mM for 10 days. 100 flies per condition were tested. One-way anova analysis was used to compare measures between four groups. ns indicates $p>0,05$ (not significant), * indicates $p<0,05$. Error bars indicate SEM.

Even though TDPF4L12xQ/N expressing larvae did not harbour locomotion deficits, albeit the fact that the aggregates are already being formed at this stage due to the Gal4-UAS system, which activates the expression of the transgene (see section 5.2 of Introduction), I decided to investigate if feeding the flies with Thioridazine starting from the larval stage could improve the recovery of the motor defects in the adult fly. The protocol followed was to set the crosses between Elav-Gal4 driver flies and flies carrying the transgene in tubes with or without the compound dissolved in the food. After five days, the larval movement of treated and non-treated third instar larvae was assayed. To find a dose that was not toxic, I treated wild-type larvae with different concentrations of Thioridazine: 100 µM, 50 µM and 20 µM. As shown from the graph, none of the doses tested was found to be toxic for the larvae. The number of peristaltic waves performed by the larvae treated with Thioridazine was indeed comparable to the one performed by the controls, which were treated with water (figure 41).

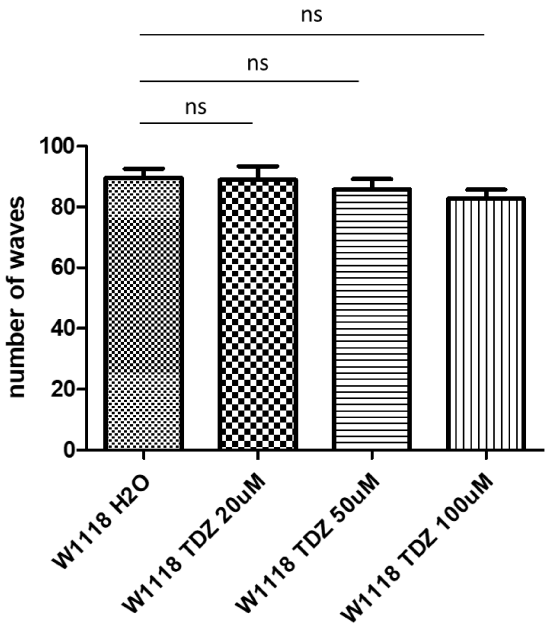

Figure 41. Thioridazine dose testing in wild-type larvae. Larval movement performed by third instar wild-type larvae treated with Thioridazine 20 µM, 50 µM and 100 µM. Twenty larvae per condition were tested. P>0,05 (not significant).

Subsequently, the adult flies coming from the larvae treated with Thioridazine 50 µM and 100 µM were collected and fed with Thioridazine 0.4 mM. After 10 days of treatment, the climbing ability was tested. As shown in figure 42, none of the doses tested caused a significant reduction in the percentage of top climbing flies when compared with control flies treated with water. However, although not significant, there was a slightly visible motor deficit in flies treated with a combination of Thioridazine 100 µM and 0.4 mM (column 3).

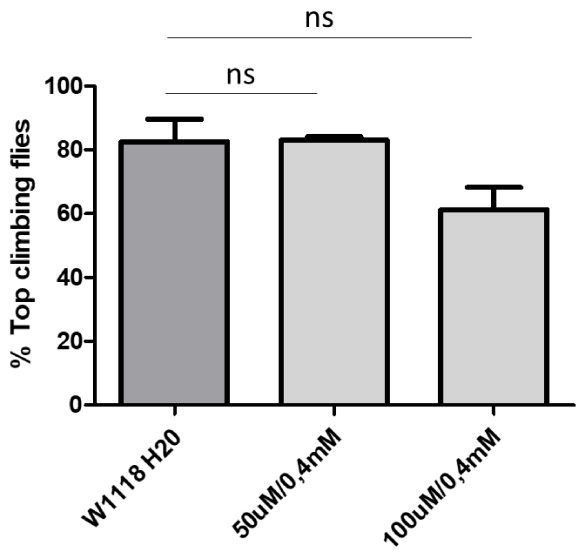

Figure 42. Thioridazine dose testing in wild-type flies. Climbing assay performed by wild-type flies treated with different doses of Thioridazine during the larval and adult stage until day 10. Sixty flies per condition were tested. ns p>0,05 (not significant).

Due to the lower climbing ability observed in flies treated with 100µM/0.4mM Thioridazine, for the treatment of TDPF4L12xQ/N flies I chose the combination of Thioridazine 50 µM to feed the larvae and 0.4 mM to feed the adults. Crosses between UAS-TDPF4L12xQ/N flies (or EGFP flies in case of the controls) and Elav-Gal4 driver flies were set in tubes with or without Thioridazine 50 µM. After 10 days, one-day-old flies expressing the transgene were collected and placed in new tubes (20 flies/each in a 1:1 female:male ratio). After 10 days of treatment with Thioridazine 0.4 mM, the climbing ability of EGFP control flies and TDPF4L12xQ/N flies was assayed. About 100 flies per condition were tested. Interestingly, transgenic flies treated with Thioridazine showed a significant improvement in their climbing ability when compared with non-treated flies (figure 43, compare column 3 and 4). Moreover, the significance between the percentage of top climbing EGFP flies and TDPF4L12xQ/N flies decreased after the treatment with Thioridazine (figure 43, compare column 1 with 3 and column 2 with 4).

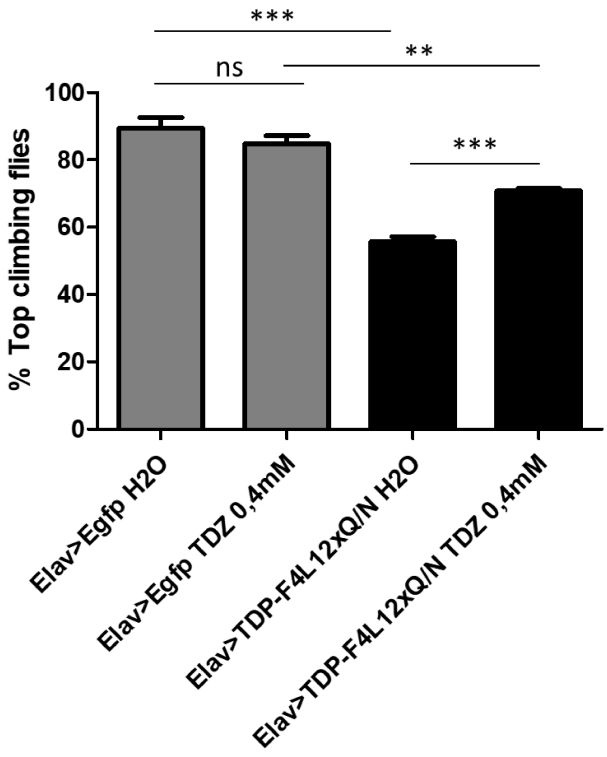

Figure 43. Rescue of climbing deficit in TDPF4L12xQ/N flies by feeding Thioridazine.

Climbing assay performed by TDPF4L12xQ/N expressing flies and EGFP control flies treated and non-treated with Thioridazine during the larval (50 µM) and adult stage (0,4 mM) for 10 days. 100 flies per condition were tested. One-way anova analysis was used to compare measures between four groups. ns indicates $p>0,05$ (not significant), * and ** indicate $p<0,05$ *** indicate $p<0,0001$. Error bars indicate SEM.

5. High throughput testing of compounds using the cellular EGFP-TDPF4L12xQ/N system

In collaboration with LifeArc, a high-throughput compound screening using the EGFP-TDPF4L12xQ/N cell model described in section 1.1 of Results was performed to identify new compounds able to clear aggregates and recover TDP-43 functionality. The screen was performed on the LifeArc discovery set, made up of about 10,640 unique compounds. This set is a subset of the LifeArc in-house library, which consists of about 250,000 molecules. Approximately 80% of this library has been cherry-picked from commercial sources to cover a wide structural diversity while sampling suitable drug-like physicochemical properties.

The screen was performed using IN Cell Developer and images were analysed using the toolbox 1.9.2 software (GE Healthcare). Imaging read-outs were: total number of aggregates per well (green fluorescent tag, measure of aggregate clearance), total number of cells per well and average nuclear diameter (Hoechst staining, measure of cell viability), and TMRM intensity (measure of mitochondrial toxicity). Dose response curve analysis were generated using the High Content Analysis module of the Genedata Screener® software.

Typical full curves for each compound could principally be grouped into five compound profiles (figure 44). “Active” compounds are compounds that decrease the total number of aggregates per well without affecting the cell count (EC_{50} for cell count >30 uM). “Differential” compounds affect both the aggregate count and the cell count, with EC_{50} at least half a log unit apart. “Partial toxic” compounds have a similar EC_{50} for the cell count and aggregate count; the cell count curve does not reach 100% (partial toxicity) and is at least 20% apart from the bottom of the aggregate count curve. “Toxic” compounds are compounds where all curves have a similar EC_{50} (aggregate count decreases because of a decrease in cell count). “Inactive” compounds are those compounds where all curves do not show any decrease in comparison to DMSO controls.

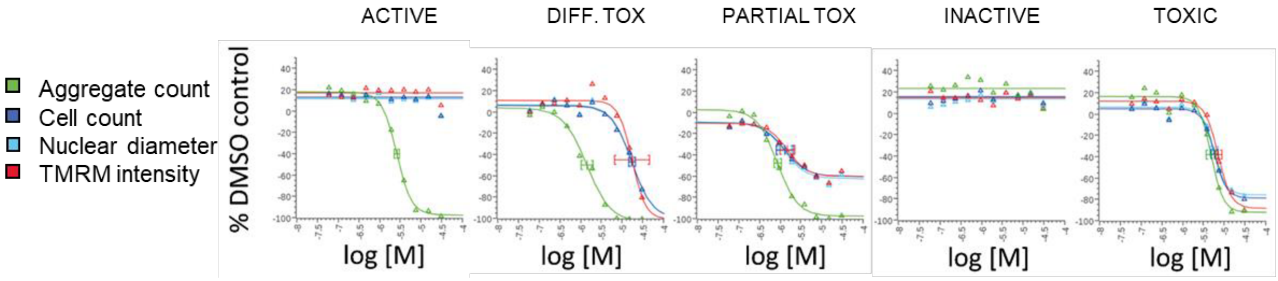

Figure 44. Distribution of the different compound profiles across different subsets within the Annotated Bioactive Set. The compounds were divided into 5 different classes, based on different parameters: aggregate count, cell count, nuclear diameter and TMRM intensity. Dose response curve analysis were generated using the High Content Analysis module of the Genedata Screener® software.

293 compounds selected from the original hit compounds and the analogues were tested in the POLDIP3 splicing recovery assay to ensure whether aggregate clearance was linked to a recovery in TDP-43 functionality. 47 out of the 56 "active" compounds (which reduce aggregate count without cell toxicity in the clearance assay) tested in the POLDIP3 assay, led to splicing recovery in a dose dependent manner. In the case of "partial" or "differential" compounds, a given toxic dose of the compound in the aggregate clearance assay usually led to no amplification of exon 3 in the POLDIP3 splicing assay, however, the relationship between how much effect on cell count is needed to overcome POLDIP3 splicing recovery, still needs to be established and might be variable from one compound cluster to the other. In the end, the best representatives for each of the five profiles were chosen to be tested *in vivo* as well as a negative control (figure 45).

Compound B

EC50= 0 μM

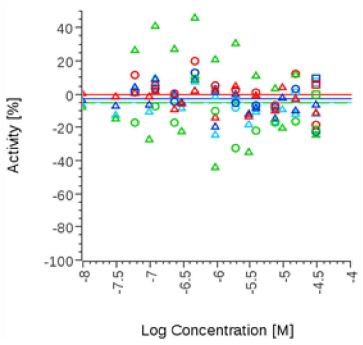

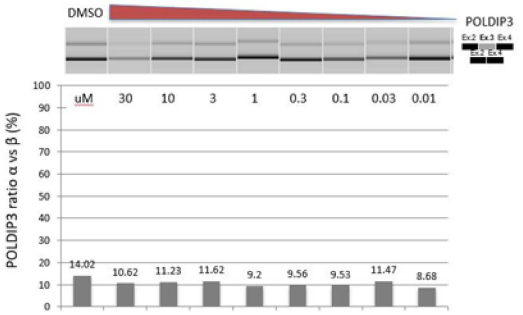

Compound C

EC50=0.07 μM

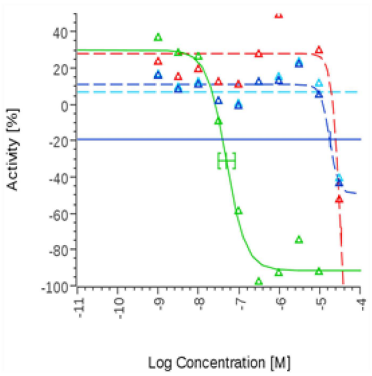

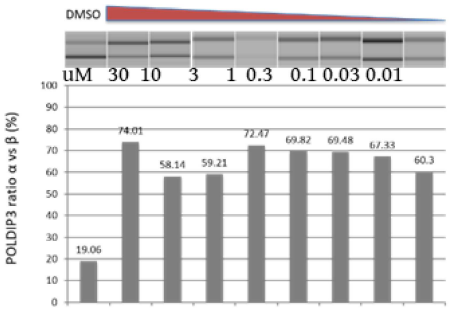

Compound D

EC50=0.02 μM

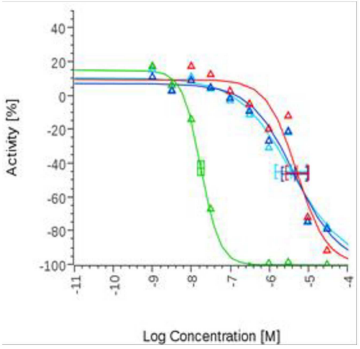

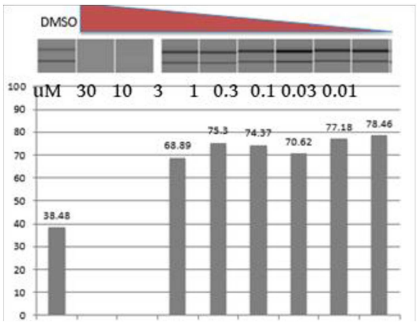

Compound E

EC50=2.48 μM

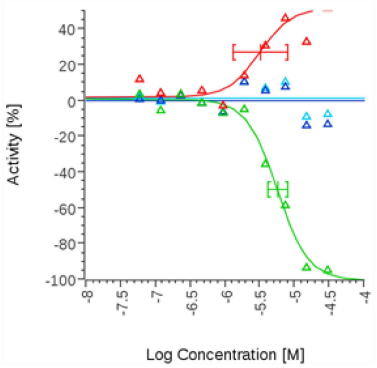

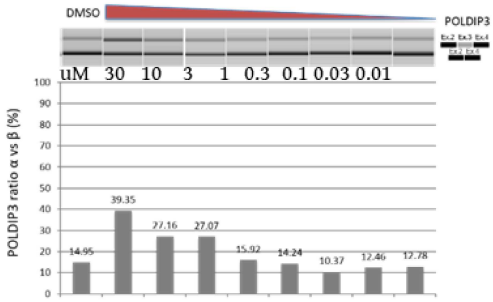

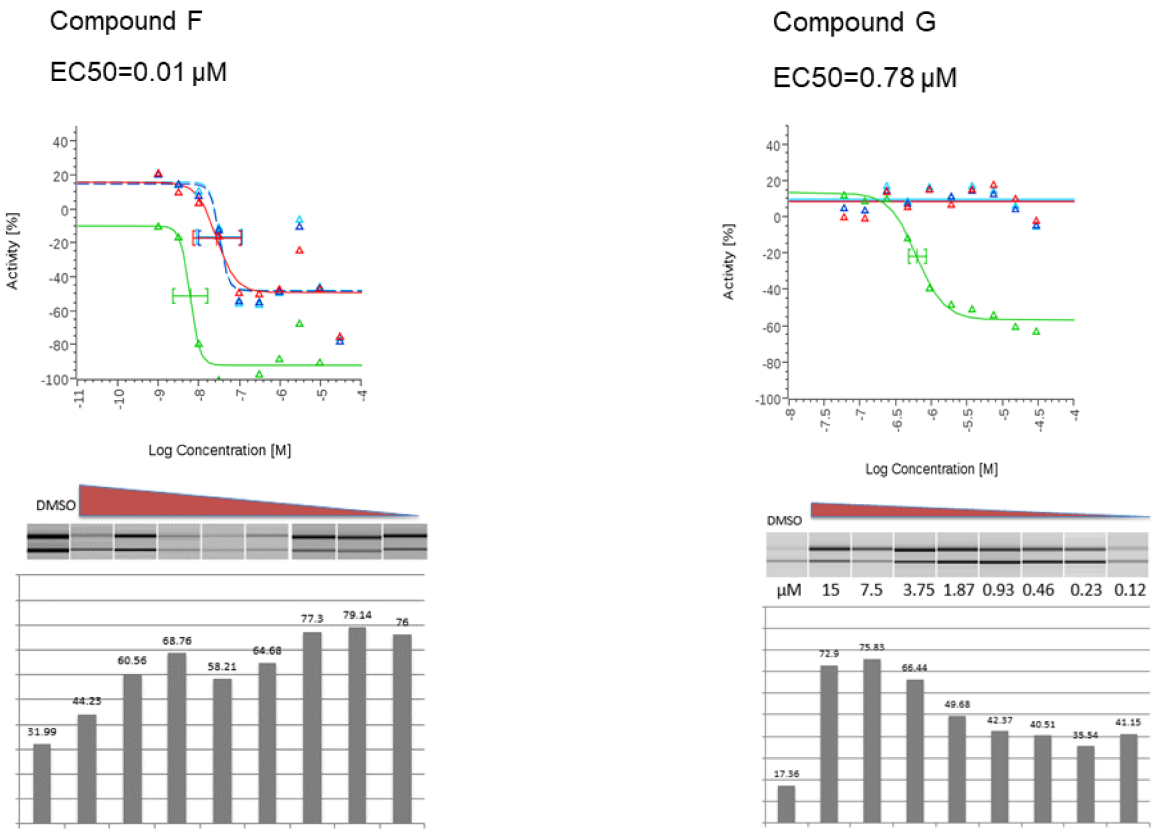

Figure 45. Top hit compounds. Dose response curves showing the ability of each compound to decrease the number of aggregates as well as their degree of toxicity measured taking into account cell count, nuclear diameter and TMRM intensity. POLDIP3 splicing assay analysis indicating the percentage of exon 3 inclusion as a measure of TDP-43 functionality for each compound is also shown.

6. Testing of top hit compounds from the high throughput screen in the TDPF4L12xQ/N *Drosophila* model

In order to study whether the effect seen in the EGFP-TDPF4L12xQ/N cell model would translate into a rescue of the motor phenotype observed in the *Drosophila* model expressing the same TDPF4L12xQ/N construct, a compound of interest from each profile was selected (see figure 45). The compounds were chosen to cover all clusters with an EC_{50} < 5µM in the aggregate clearance assay, and display good POLDIP3 splicing recovery, i.e. recovery of TDP-43 function. I received these compounds together with a negative control and worked blind during the process of experimentation. From a practical point of view, the compounds needed to be soluble and stable in ethanol in fly food. The compounds were initially dissolved in ethanol 100% and subsequently added to the fly food (see section 3.2.3 of Materials and Methods). The amount used was based on the maximum solubility in ethanol 5% with a roof of 1 mM. This was because of the sourceability of the compounds and the fact that previous experiments in the laboratory showed, a final concentration of 5% ethanol in the fly food to be non-toxic for the adult flies; for the larvae, the concentration had to be decreased to 1% due to a strong toxic effect observed with higher doses. Taking into account the limitation on the amount of compound that could be used (1 mM), and considering that the compound dissolved in ethanol had to be added to the fly food at a final concentration of 5% for the adult flies and 1% for the larvae, a compromise had to be made, for each compound, regarding the treatment of the adult flies and the larvae separately. The final concentration of the compound that was given to the adult flies was normally higher than the one used to feed larvae also due to a difference in the amount of food eaten (adults eat less food than the larvae).

In order to treat the larvae, crosses between Elav-Gal4 driver flies and TDPF4L12xQ/N flies were set in tubes with or without the compound; ethanol alone was used as a control. After 10 days, one-day-old flies expressing the transgene were collected and transferred to tubes with or without the compound. After 10 days of treatment, the climbing ability of EGFP control flies and TDPF4L12xQ/N flies (treated and non-treated with the compound) was tested. As can be seen from figure 46, feeding of compound B, tested at 165 µM in the larvae and 800 µM in the adults, showed no significant improvement in the motor phenotype (figure 46a). This was also the case for compound E, tested at 500 µM during the larval phase and 1 mM in the adult, and compound G, tested at 143 µM during the larval phase and 700 µM in the adults (figure 46b and 46c). On the other hand, the treatment with compound C, tested at 400 µM during the larval phase and 1 mM in the adult phase,

gave a significant recovery of the locomotion defects of TDPF4L12xQ/N expressing flies (figure 46d). Compound D and F were toxic at the doses tested; compound D, which was first tested at 165 µM for the larvae and 1mM for the adults, caused a significant decrease in the climbing ability of EGFP control flies (figure 46e). After testing different doses to avoid toxicity both in the larvae and in the adult flies separately, compound D was subsequently tested at a lower concentration (80 µM to feed the larvae and 1 mM for the adults). Notwithstanding the testing of the doses to be used, the climbing ability of EGFP control flies was still compromised, however, there was a slight but significant recovery in the climbing ability of TDPF4L12xQ/N expressing flies (figure 46f). The toxicity in this experiment may derive from the fact that the testing of toxicity was performed in wild-type flies rather than the transgenic flies. Compound F, which was first tested at 50 µM during the larval phase, caused the death of all the larvae. Subsequently, flies were treated with compound F at 500 µM during the adult phase only. The climbing ability of control flies was not impaired, however, the treatment with compound F of TDPF4L12xQ/N flies did not show a significant improvement in the motor phenotype when compared with non-treated flies (figure 46g).

a)

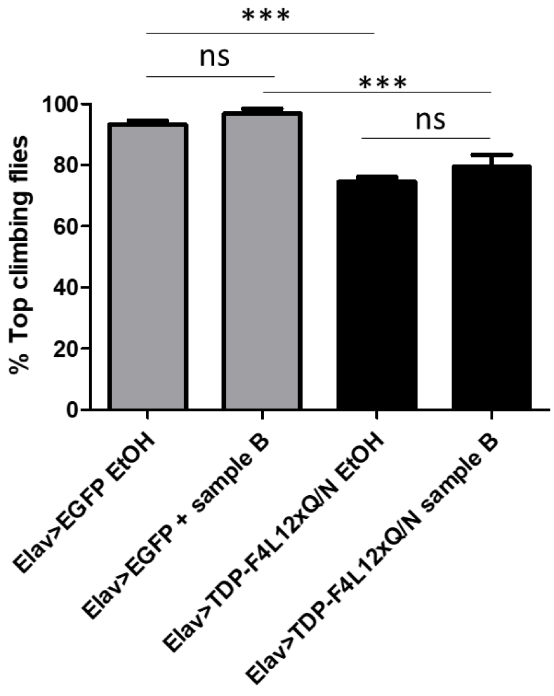

b)

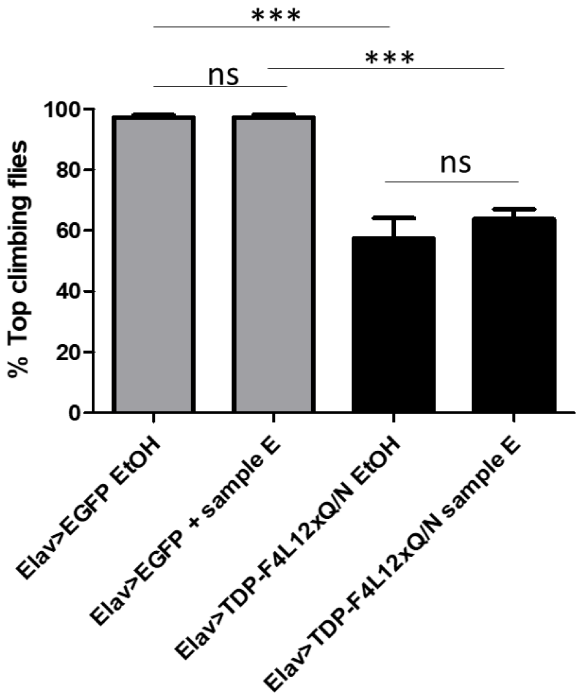

c)

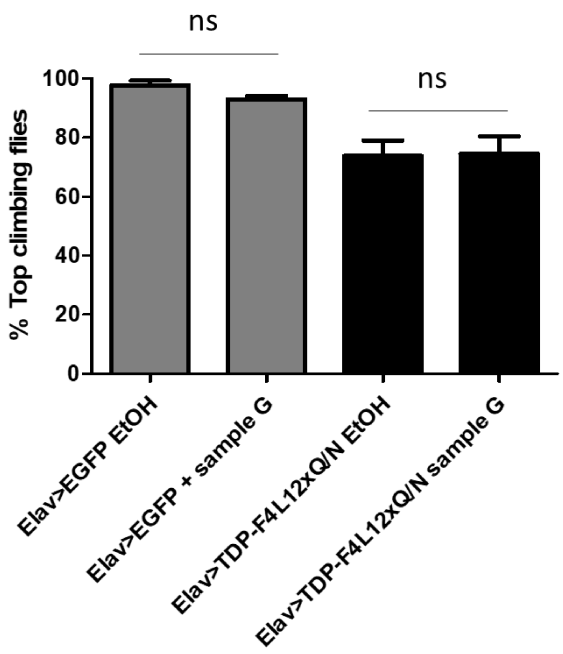
ns
ns
% Top climbing flies
100
80
60
40
20
0
Elav>EGFP EtOH
Elav>EGFP + sample G
Elav>TDP-F4L12xQ/N EtOH
Elav>TDP-F4L12xQ/N sample G

d)

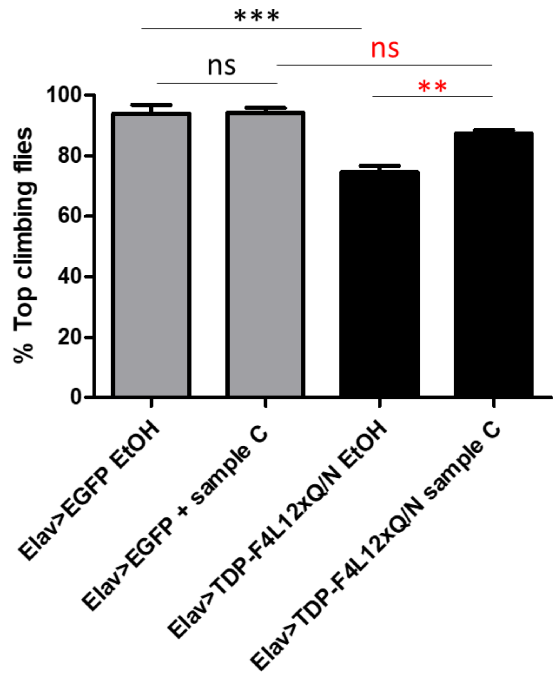
***
ns
ns
**
% Top climbing flies
100
80
60
40
20
0
Elav>EGFP EtOH
Elav>EGFP + sample C
Elav>TDP-F4L12xQ/N EtOH
Elav>TDP-F4L12xQ/N sample C

e)

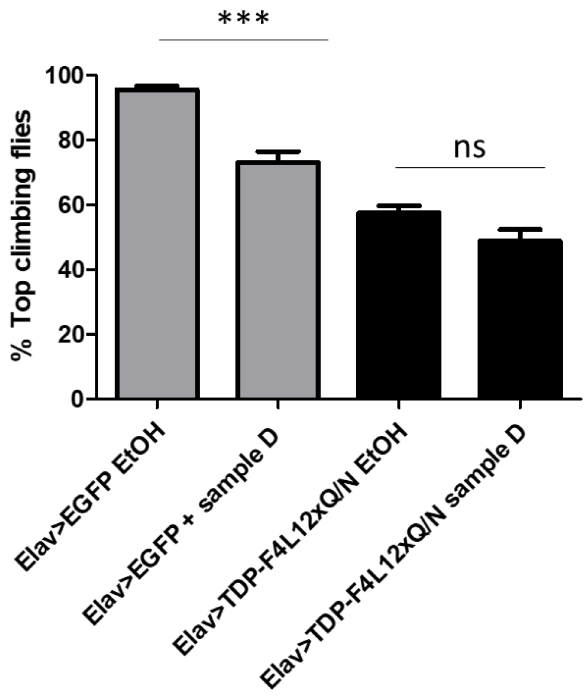
***
ns
% Top climbing flies
100
80
60
40
20
0
Elav>EGFP EtOH
Elav>EGFP + sample D
Elav>TDP-F4L12xQ/N EtOH
Elav>TDP-F4L12xQ/N sample D

f)

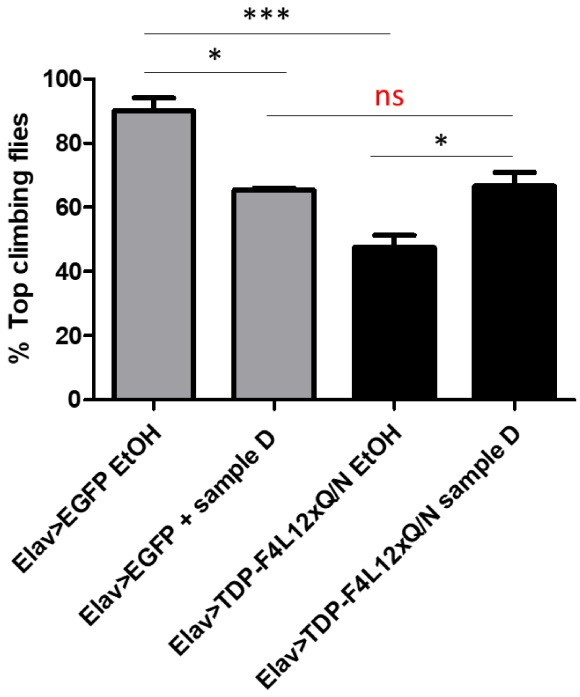
***
*
ns
*
% Top climbing flies
100
80
60
40
20
0
Elav>EGFP EtOH
Elav>EGFP + sample D
Elav>TDP-F4L12xQ/N EtOH
Elav>TDP-F4L12xQ/N sample D

g)

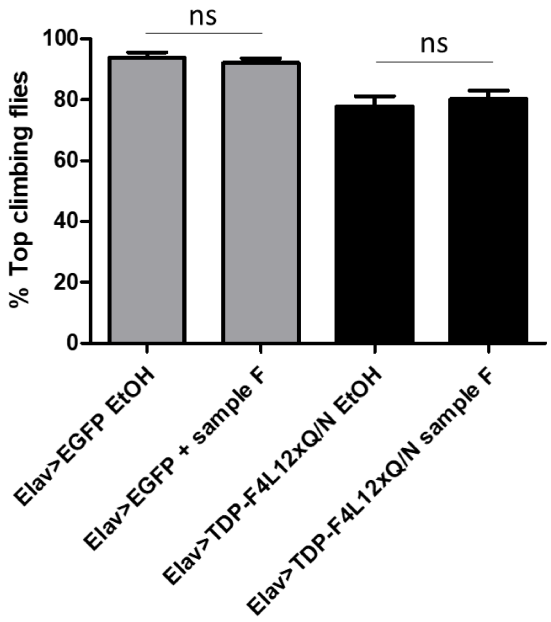

Figure 46. Climbing ability of TDPF4L12xQ/N flies upon treatment with top hit compounds.

Climbing assay performed by TDPF4L12xQ/N expressing flies and EGFP control flies treated and non-treated with top hit compounds during the larval and adult stage for 10 days. 100 flies per condition were tested. One-way anova analysis was used to compare measures between four groups. ns indicates p>0,05 (not significant), * and ** indicate p<0,05 *** indicate p<0,0001. Error bars indicate SEM.

Discussion

Today no treatment that blocks the progression of ALS significantly exists. This is likely due to the fact that several factors are involved in the disease (section 1.1.3 of Introduction), and therapeutic approaches were mainly based around targeting one or more of these cellular mechanisms. Since its approval by the FDA in 1995, Riluzole (by Sanofi-Aventis), was the only disease-modifying therapy available for ALS patients offering a very modest survival benefit of 2 to 3 months. Riluzole's mechanism of action is not fully understood, but it has been shown to modulate glutamate neurotransmission by inhibiting both presynaptic glutamate release and postsynaptic glutamate receptor signalling. In addition, it has also been reported to inhibit voltage-gated sodium channels (Carbone, Duty et al. 2012). Subsequently, in May 2017, the FDA approved Edaravone (Radicava, Mitsubishi Tanabe Pharma America), a novel neuroprotective agent indicated to slow the advance of ALS. Although the exact mechanism of action of Edaravone in the treatment of ALS is unknown, its therapeutic effect may be due to its known antioxidant properties; oxidative stress is indeed a part of the process that kills neurons in patients with ALS (Cruz 2018).

The main hallmark of ALS is TDP-43 protein misfolding and aggregation in motor neurons. The exact pathological significance of these aggregates is currently unknown, and possibilities range from inherent toxicity of the aggregates to loss of function effects induced by the sequestration of TDP-43 by the aggregates resulting in a lack of its soluble form (both possibilities do not exclude each other). However, it is certainly true that loss of function of TDP-43 results in a deleterious phenotype in all the animal models tested. For example, a complete knock out of TDP-43 in *Drosophila* results in locomotion deficits with spastic, uncoordinated, movements, incapacity to fly or walk normally and reduced lifespan (Feiguin, Godena et al. 2009). This, as already mentioned, is likely due to the disturbance of the myriad of biological pathways TDP-43 has been shown to play a role in (section 2 of Introduction).

Consequently the essential role played by TDP-43 and its likely loss of function in ALS, several studies have looked for ways to target this abnormality as a therapeutic strategy. Arimoclomol (Orphazyme ApS) for example, is a compound that increases the production of a group of proteins called heat-shock proteins (HSPs), and is currently in clinical trials as a potential treatment for ALS patients with SOD1 mutations and other diseases. HSPs work to counteract protein aggregation, in part by

improving the function of lysosomes, cellular organelles that act as the waste disposal system of cells and work to remove undesirable materials.

Rapamycin, a known inducer of autophagy, has been observed to rescue motor function disorders in a mouse model with TDP-43 inclusions (Wang, Guo et al. 2012). Moreover, a recent study has used human iPSC-derived neurons to perform a high throughput screen for molecules that increased LC3 II, the lipidated form of LC3I, which is incorporated into developing autophagosomes, confirming their efficacy in stimulating autophagy. The top candidates, fluphenazine, methotrimeprazine and 4'(N-diethylamino)butyl)-2-chlorophenoxazine, were subsequently shown to improve TDP-43 clearance/localization and enhanced survival of human stem cell derived neurons over-expressing a mutant TDP-43 (Barmada, Serio et al. 2014).

Notwithstanding this and other ongoing studies, there is still concrete need for the discovery of novel compounds to treat patients suffering from ALS. This is particularly important considering the recent data that demonstrate that it may be possible to reverse the neurological phenotype caused by TDP-43 loss of function, by restoring TDP-43 functionality. For example, it has been shown that late re-introduction of TDP-43 in TBPH knock out flies is actually able to rescue the anatomical and locomotion defects caused by the loss of functionality of TDP-43 (Romano, Klima et al. 2014), indicating that late corrections of TDP-43 activity in neurons are possible and sufficient to recover the neurological defects. Furthermore, in a recent study in which expression of human TDP-43 without the nuclear localization signal in mice resulted in the formation of TDP-43 aggregates, with the concomitant loss of nuclear TDP-43, resulting in a severe motor phenotype, it was shown that the phenotype could be reverted when the expression of the mutated TDP-43 was halted; this caused a dramatic reduction in TDP-43 aggregation and, more importantly, an increase in nuclear TDP-43 (Walker, Spiller et al. 2015). These data further confirm that even after disease onset the pathological phenotype may be recovered by restoring TDP-43 functionality.

Thus, therapeutic strategies aimed to re-establish or compensate TDP-43 functionality could successfully correct the neurological phenotype providing a pathway to reversibility that can be explored in the therapy of human ALS patients.

The aim of this study was to create a model to be used in a phenotypic high throughput screening which would enable the identification of compounds leading to TDP-43 aggregate clearance regardless of their putative mode of action. This last point is important if for example we consider that TDP-43 loss of function activates autophagosome formation but at the same time inhibits

autophagosome-lysosome fusion (Xia, Wang et al. 2016). In this context, it becomes evident that a generalized activation of autophagy might not be the best strategy to reduce protein aggregation. Instead, a better therapeutic approach could be for example a more specific enhancement of autophagosome maturation to achieve cargo degradation. Irrespectively, a phenotypic screen would by-pass these issues and only identify compounds that clear aggregates.

One of the main difficulties in performing a compound screen is the development of appropriate disease models. From the point of view of the pathology, it is important to keep in mind that many activities are regulated by TDP-43 (section 2 of Introduction). There are several ways to trigger TDP-43 aggregation, however the majority of these depend on the overexpression of TDP-43 (Igaz, Kwong et al. 2009, Zhang, Xu et al. 2009). Triggering TDP-43 aggregation just by artificially increasing its expression within any model system of interest may not be the best choice. In fact, the exogenous TDP-43 expression may directly affect the normal regulation of the processes in which TDP-43 is involved in unpredictable manners. It has been shown both in cells and *in vivo* that increasing TDP-43 levels is highly deleterious, leading to degeneration. Indeed, TDP-43 levels are tightly regulated through an auto regulatory feedback mechanism in order to guarantee cell function and survival (section 2.2.2 of Introduction).

The cellular model I developed by-passes these issues as it relies on tandem repetitions of the prion like Q/N region of TDP-43 (residues 331–366) which was shown to play a role in the self-aggregation process (Budini et al. 2012; Fuentealba et al. 2010). We have observed that tandem repetitions of the Q/N region linked to the TDP-43 molecule itself (or fragments of it) induce, in a highly reproducible and efficient manner, aggregate formation and TDP-43 nuclear depletion, as a result of the recruitment of the native protein into the inactive aggregates (Budini et al. 2014; Langellotti et al. 2016; Romano et al. 2015). This leads to a clearly visible splicing loss of function, both in endogenous and exogenous (transfected) genes. Based on this information, I have created an inducible cellular model based on this aggregate-inducer (EGFP-TDPF4L-12XQ/N) (section 1 of Results), that could be used in a high content live imaging screen due to the EGFP tag. The two phenylalanine residues in both the RNA recognition motifs (RRM) were mutated thus abolishing TDP-43 ability to bind RNA, in order to produce an inactive protein (TDPF4L12xQ/N). In fact in this way, due to its inability to bind RNA, the protein produced will be unable to down regulate the levels of soluble endogenous TDP-43 through the negative feedback loop (Ayala, De Conti et al. 2011, Avendaño-Vázquez, Dhir et al. 2012) as well as regulate RNA splicing, the principle process I use in this thesis to monitor TDP 43 functionality.

Expression of this construct in the cells, results in the formation of aggregates with the consequent sequestration of soluble TDP-43 into the insoluble aggregates (figure 22b and figure 23). More importantly, the entrapment of the endogenous protein caused a loss of splicing functionality of TDP-43 that I confirmed through the analysis of POLDIP3 exon 3 alternative splicing. It has already been shown by two different groups that when TDP-43 is silenced, POLDIP3 isoform-1 decreases while isoform-2 increases (POLDIP3 exon 3 is skipped) (Fiesel, Weber et al. 2012, Shiga, Ishihara et al. 2012). Indeed, our results show that upon induction of the TDPF4L12xQ/N transgene, POLDIP3 exon 3 is skipped, as when TDP-43 is silenced, confirming that the endogenous protein is being sequestered by the aggregates preventing it from regulating RNA splicing causing loss-of-function (figure 24).

The innovative approach of our cell model lies in the fact that it is centred on tandem repeats of the prion like Q/N-rich region of TDP-43. The TDPF4L12xQ/N aggregates have the capacity of sequestering endogenous wild-type TDP-43 without altering the expression levels of the endogenous gene. Therefore, the compounds screened in our system will have the advantage of working in a more ALS pathological-like scenario where the molecular pathways will be unaltered and do not have to deal with all the additional changes/alterations that have been described to occur when TDP-43 is artificially overexpressed.

The compounds we initially chose to screen in our system belong to the tricyclic family, and are considered to be neuroprotective. Moreover, there is evidence that these compounds could trigger aggregate clearance (Tsvetkov, Miller et al. 2010).

Upon compound treatment, I observed that all the compounds tested enhanced aggregate clearance. More importantly, the degradation of these aggregates is linked to the recovery of TDP-43 functionality, as confirmed through the analysis of POLDIP3 exon 3 alternative splicing (figure 25). The recovery of TDP-43 functionality was furthermore shown to be a consequence of an increased solubility of the protein, most probably due to the elimination of self-templeting conformers that act as a sink for the newly synthetized TDP-43 (figure 26a and 26b).

Regarding the mechanism of action of the compounds, I observed that the clearance is occurring through the ubiquitin proteasome system (UPS) as the degradation of the aggregates is impaired upon treatment with the proteasome inhibitor Bortezomib (figure 30). Moreover, I show that aggregates degradation is independent of autophagy, at least beyond the autophagosome-

lysosome fusion. In fact, in presence of two different autophagy inhibitors, chloroquine and ammonium chloride, compound treatment is still able to induce aggregate clearance (figure 28).

These data are partly in contrast with previous studies that show that tricyclic compounds (Thioridazine among others) act by enhancing the autophagy pathway (Tsvetkov, Miller et al. 2010). I observed that upon compound treatment, although the LC3II/I ratio is increasing, which usually indicates an increased number of autophagosomes, there is an increase in p62, which is usually degraded through autophagy, indicating a block in the pathway (figure 27). On the other hand, in line with our results, tricyclic compounds have also been shown to accumulate in lysosomes and behave as autophagy inhibitors by increasing the pH of lysosomes thus impairing lysosomal hydrolases. This process results in the inhibition of the cargo degradation (Nadanaciva, Lu et al. 2011, Ashoor, Yafawi et al. 2013).

Regarding the proteasome degradation of TDP-43 inclusions, a study conducted by Zhang et al. demonstrated that TDP-43 aggregates could be eliminated from the cell by the UPS, as proteasome inhibition but not autophagy prevented aggregate clearance (Zhang, Gendron et al. 2010).

Since proteasomes can only accommodate single unfolded polypeptide chains and not large aggregates, it has been assumed that the proteasome cannot degrade larger aggregates. However, it has been demonstrated that the proteasome can clear aggregates through a UBQLN2-HSP70 pathway. According to this study, aggregates are first solubilized by HSP70-HSP110 disaggregase activity; subsequently, UBQLN2 acts as a proteasome shuttle connecting ubiquitylated misfolded proteins to the proteasome for degradation (Hjerpe, Bett et al. 2016).

Interestingly, mutations in ubiquilin-2 gene have been described to be responsible of a fraction of familial ALS cases, and functional analysis showed that mutations in ubiquilin-2 gene lead to an impairment of protein degradation (Deng, Chen et al. 2011).

In conclusion, the results pertaining to the mechanism of action of the tricyclic compounds on aggregate clearance thus far obtained and future analysis of the compounds identified in the high throughput assay to clear aggregates at the phenotypic level (section 5 of Results), have and will identify mechanisms that increase aggregate clearance and soluble TDP-43 possibly reverting this phenotype and help advance the understanding of TDP-43 proteinopathies.

Regarding this last aspect, in order to study whether the effect seen in the EGFP-TDPF4L12xQ/N cell line would translate into a phenotype, I created a *Drosophila* model expressing the same aggregate

inducer TDPF4L12XQ/N and tested a compound from the tricyclic set as well as compounds deriving from the high throughput screen.

Expression of the aggregates in the eye showed no toxicity, and the ability to rescue TBPH-induced degeneration by the sequestration of the endogenous protein into the aggregates (figure 34 and 36). Pan-neuronal expression of TDPF4L12xQ/N resulted in flies that developed an age-related motor phenotype characterized by a deficient locomotive behaviour. Of particular interest was the age-related appearance of the phenotype; in fact, while during the larval stage, flies expressing TDPF4L12xQ/N did not have any impairment in locomotion (figure 37), at day 7 flies start to present deficits in climbing which get worse with aging. Moreover, their lifespan was observed to be severely compromised with a median survival that was about the half of that of control flies (figure 38). This is in line with the age related onset of the disease in human.

Previous studies have indicated the presence of a physiological reduction in the endogenous levels of TDP-43 in wild-type mice during aging (Huang, Xia et al. 2010, Liu, Atkinson et al. 2015). Moreover, a study carried out by our group demonstrated a drop in TDP-43 levels, both at mRNA and protein level, in wild-type *Drosophila* as well (Cragnaz, Klima et al. 2015). Interestingly, it was observed that aggregates, when combined with a decrease in TDP-43 levels, due to the physiological age drop, could trigger a locomotive defect in a fly model of TDP-43 aggregation (Cragnaz, Klima et al. 2015). This age-related drop was observed starting from day 7, which is in line with our results showing an impaired climbing in TDPF4L12xQ/N adult flies at the same time point.

It is thus tempting to speculate that the combination of a physiological reduction of TDP-43 during aging and the presence of aggregates that act as a sink for the remaining soluble functional TDP-43 could be responsible for the pathogenesis of ALS.

As a preliminary approach, TDPF4L12xQ/N flies were first treated with Thioridazine, which was shown to clear the aggregates and rescue TDP-43 functionality (section 2 of Results). After 10 days of treatment with Thioridazine, the climbing ability of transgenic flies was found significantly improved when compared with non-treated flies (figure 40). This improvement was even more marked when the flies were fed from the larval stage (figure 43). This is most likely due to the fact that the time the compound has to act on aggregate clearance is longer. In fact, notwithstanding that TDPF4L12xQ/N expressing larvae did not harbour locomotion deficits, aggregates are present also during the larval stage. It may also be the case that the aggregates in the larvae are of smaller size and thus the mechanism of action enhanced by the compounds can clear these easier.

Testing of 5 compounds deriving from the high throughput screen, shown to clear aggregates and revert POLDIP3 splicing pattern to wildtype levels, as well as one compound that did not (section 5 of Results), identified two compounds that also improved the phenotype observed in our fly model. In fact, treatment with compound C and D significantly improved the climbing ability of TDPF4L12xQ/N expressing flies (figure 46d and 46f), albeit the latter of these showed toxicity to some extent at the dose used. Compound B, as expected, due to the data derived from the cellular assay did not revert the phenotype (figure 46a).

As for the lack of effect of the other compounds, a higher dose than the one tested might be needed to have a visible effect on the phenotype. It may also be the case that the compounds that did not show a recovery in the flies' phenotype are not able to cross the blood brain barrier and did not reach the nervous system. These are areas of further studies.

In conclusion, these results confirm that the neurological phenotype caused by TDP-43 loss of function can be reverted by clearing the aggregates and therefore restoring TDP-43 functionality, providing a new therapeutic approach for ALS patients harbouring TDP-43 proteinopathy and also confirm the validity of the cellular model of TDP-43 aggregation. Further follow up studies in regards of the mechanism of action and target deconvolution studies focusing on these pathways, will help characterizing the compound's mode of action and will strengthen this proof of concept study and prove beneficial to advance research on a variety of neurodegenerative diseases where aggregate formation occurs.

Concluding remarks

- Clearance of the aggregates in a cell model of TDP-43 aggregation is associated with the recovery of TDP-43 functionality

- TDP-43 aggregate clearance by Nortriptyline and Thioridazine is independent of autophagy, beyond the chloroquine and NH_4Cl block

- TDP-43 aggregate clearance by Nortriptyline and Thioridazine needs a functional ubiquitin-proteasome system

- Thioridazine treatment can improve the motor phenotype in a *Drosophila* model expressing the aggregate inducer TDPF4L12xQ/N

- Treatment with two of the compounds coming from the high-throughput screen (compound C and D) significantly improve the climbing ability of TDPF4L12xQ/N expressing flies

- The neurological phenotype caused by TDP-43 loss of function can be reverted restoring TDP-43 functionality following aggregate clearance

Bibliography

Ajroud-Driss, S. and T. Siddique (2015). "Sporadic and hereditary amyotrophic lateral sclerosis (ALS)." Biochim Biophys Acta **1852**(4): 679-684.

Al-Chalabi, A. and O. Hardiman (2013). "The epidemiology of ALS: a conspiracy of genes, environment and time." Nat Rev Neurol **9**(11): 617-628.

Al-Chalabi, A., O. Hardiman, M. C. Kiernan, A. Chiò, B. Rix-Brooks and L. H. van den Berg (2016). "Amyotrophic lateral sclerosis: moving towards a new classification system." Lancet Neurol **15**(11): 1182-1194.

Alfieri, J. A., N. S. Pino and L. M. Igaz (2014). "Reversible behavioral phenotypes in a conditional mouse model of TDP-43 proteinopathies." J Neurosci **34**(46): 15244-15259.

Aman, P., I. Panagopoulos, C. Lassen, T. Fioretos, M. Mencinger, H. Toresson, M. Höglund, A. Forster, T. H. Rabbitts, D. Ron, N. Mandahl and F. Mitelman (1996). "Expression patterns of the human sarcoma-associated genes FUS and EWS and the genomic structure of FUS." Genomics **37**(1): 1-8.

Andersson, M. K., A. Ståhlberg, Y. Arvidsson, A. Olofsson, H. Semb, G. Stenman, O. Nilsson and P. Aman (2008). "The multifunctional FUS, EWS and TAF15 proto-oncoproteins show cell type-specific expression patterns and involvement in cell spreading and stress response." BMC Cell Biol **9**: 37.

Arai, T., M. Hasegawa, H. Akiyama, K. Ikeda, T. Nonaka, H. Mori, D. Mann, K. Tsuchiya, M. Yoshida, Y. Hashizume and T. Oda (2006). "TDP-43 is a component of ubiquitin-positive tau-negative inclusions in frontotemporal lobar degeneration and amyotrophic lateral sclerosis." Biochem Biophys Res Commun **351**(3): 602-611.

Arnold, E. S., S. C. Ling, S. C. Huelga, C. Lagier-Tourenne, M. Polymenidou, D. Ditsworth, H. B. Kordasiewicz, M. McAlonis-Downes, O. Platoshyn, P. A. Parone, S. Da Cruz, K. M. Clutario, D. Swing, L. Tessarollo, M. Marsala, C. E. Shaw, G. W. Yeo and D. W. Cleveland (2013). "ALS-linked TDP-43 mutations produce aberrant RNA splicing and adult-onset motor neuron disease without aggregation or loss of nuclear TDP-43." Proc Natl Acad Sci U S A **110**(8): E736-745.

Ashoor, R., R. Yafawi, B. Jessen and S. Lu (2013). "The contribution of lysosomotropism to autophagy perturbation." PLoS One **8**(11): e82481.

Avendaño-Vázquez, S. E., A. Dhir, S. Bembich, E. Buratti, N. Proudfoot and F. E. Baralle (2012). "Autoregulation of TDP-43 mRNA levels involves interplay between transcription, splicing, and alternative polyA site selection." Genes Dev **26**(15): 1679-1684.

Ayala, Y. M., L. De Conti, S. E. Avendaño-Vázquez, A. Dhir, M. Romano, A. D'Ambrogio, J. Tollervey, J. Ule, M. Baralle, E. Buratti and F. E. Baralle (2011). "TDP-43 regulates its mRNA levels through a negative feedback loop." EMBO J **30**(2): 277-288.

Ayala, Y. M., S. Pantano, A. D'Ambrogio, E. Buratti, A. Brindisi, C. Marchetti, M. Romano and F. E. Baralle (2005). "Human, Drosophila, and C.elegans TDP43: nucleic acid binding properties and splicing regulatory function." J Mol Biol **348**(3): 575-588.

Ayala, Y. M., P. Zago, A. D'Ambrogio, Y. F. Xu, L. Petrucelli, E. Buratti and F. E. Baralle (2008). "Structural determinants of the cellular localization and shuttling of TDP-43." J Cell Sci **121**(Pt 22): 3778-3785.

Balch, W. E., R. I. Morimoto, A. Dillin and J. W. Kelly (2008). "Adapting proteostasis for disease intervention." Science **319**(5865): 916-919.

Barmada, S. J., A. Serio, A. Arjun, B. Bilican, A. Daub, D. M. Ando, A. Tsvetkov, M. Pleiss, X. Li, D. Peisach, C. Shaw, S. Chandran and S. Finkbeiner (2014). "Autophagy induction enhances TDP43 turnover and survival in neuronal ALS models." Nat Chem Biol **10**(8): 677-685.

Barth, S., D. Glick and K. F. Macleod (2010). "Autophagy: assays and artifacts." J Pathol **221**(2): 117-124.

Bedford, L., D. Hay, A. Devoy, S. Paine, D. G. Powe, R. Seth, T. Gray, I. Topham, K. Fone, N. Rezvani, M. Mee, T. Soane, R. Layfield, P. W. Sheppard, T. Ebendal, D. Usoskin, J. Lowe and R. J. Mayer (2008). "Depletion of 26S proteasomes in mouse brain neurons causes neurodegeneration and Lewy-like inclusions resembling human pale bodies." J Neurosci **28**(33): 8189-8198.

Bjørkøy, G., T. Lamark, A. Brech, H. Outzen, M. Perander, A. Overvatn, H. Stenmark and T. Johansen (2005). "p62/SQSTM1 forms protein aggregates degraded by autophagy and has a protective effect on huntingtin-induced cell death." J Cell Biol **171**(4): 603-614.

Blokhuis, A. M., E. J. Groen, M. Koppers, L. H. van den Berg and R. J. Pasterkamp (2013). "Protein aggregation in amyotrophic lateral sclerosis." Acta Neuropathol **125**(6): 777-794.

Boillée, S., C. Vande Velde and D. W. Cleveland (2006). "ALS: a disease of motor neurons and their nonneuronal neighbors." Neuron **52**(1): 39-59.

Bosco, D. A., G. Morfini, N. M. Karabacak, Y. Song, F. Gros-Louis, P. Pasinelli, H. Goolsby, B. A. Fontaine, N. Lemay, D. McKenna-Yasek, M. P. Frosch, J. N. Agar, J. P. Julien, S. T. Brady and R. H. Brown (2010). "Wild-type and mutant SOD1 share an aberrant conformation and a common pathogenic pathway in ALS." Nat Neurosci **13**(11): 1396-1403.

Braak, H., K. Del Tredici, U. Rüb, R. A. de Vos, E. N. Jansen Steur and E. Braak (2003). "Staging of brain pathology related to sporadic Parkinson's disease." Neurobiol Aging **24**(2): 197-211.

Brooks, B. R., R. G. Miller, M. Swash, T. L. Munsat and W. F. o. N. R. G. o. M. N. Diseases (2000). "El Escorial revisited: revised criteria for the diagnosis of amyotrophic lateral sclerosis." Amyotroph Lateral Scler Other Motor Neuron Disord **1**(5): 293-299.

Bruijn, L. I., M. W. Becher, M. K. Lee, K. L. Anderson, N. A. Jenkins, N. G. Copeland, S. S. Sisodia, J. D. Rothstein, D. R. Borchelt, D. L. Price and D. W. Cleveland (1997). "ALS-linked SOD1 mutant G85R mediates damage to astrocytes and promotes rapidly progressive disease with SOD1-containing inclusions." Neuron **18**(2): 327-338.

Bruijn, L. I., M. K. Houseweart, S. Kato, K. L. Anderson, S. D. Anderson, E. Ohama, A. G. Reaume, R. W. Scott and D. W. Cleveland (1998). "Aggregation and motor neuron toxicity of an ALS-linked SOD1 mutant independent from wild-type SOD1." Science **281**(5384): 1851-1854.

Budini, M., E. Buratti, C. Stuani, C. Guarnaccia, V. Romano, L. De Conti and F. E. Baralle (2012). "Cellular model of TAR DNA-binding protein 43 (TDP-43) aggregation based on its C-terminal Gln/Asn-rich region." J Biol Chem **287**(10): 7512-7525.

Budini, M., V. Romano, S. E. Avendaño-Vázquez, S. Bembich, E. Buratti and F. E. Baralle (2012). "Role of selected mutations in the Q/N rich region of TDP-43 in EGFP-12xQ/N-induced aggregate formation." Brain Res **1462**: 139-150.

Budini, M., V. Romano, Z. Quadri, E. Buratti and F. E. Baralle (2015). "TDP-43 loss of cellular function through aggregation requires additional structural determinants beyond its C-terminal Q/N prion-like domain." Hum Mol Genet **24**(1): 9-20.

Buratti, E. (2015). "Functional Significance of TDP-43 Mutations in Disease." Adv Genet **91**: 1-53.

Buratti, E. and F. E. Baralle (2001). "Characterization and functional implications of the RNA binding properties of nuclear factor TDP-43, a novel splicing regulator of CFTR exon 9." J Biol Chem **276**(39): 36337-36343.

Buratti, E. and F. E. Baralle (2010). "The multiple roles of TDP-43 in pre-mRNA processing and gene expression regulation." RNA Biol **7**(4): 420-429.

Buratti, E. and F. E. Baralle (2011). "TDP-43: new aspects of autoregulation mechanisms in RNA binding proteins and their connection with human disease." FEBS J **278**(19): 3530-3538.

Cairns, N. J., M. Neumann, E. H. Bigio, I. E. Holm, D. Troost, K. J. Hatanpaa, C. Foong, C. L. White, J. A. Schneider, H. A. Kretzschmar, D. Carter, L. Taylor-Reinwald, K. Paulsmeyer, J. Strider, M. Gitcho, A. M. Goate, J. C. Morris, M. Mishra, L. K. Kwong, A. Stieber, Y. Xu, M. S. Forman, J. Q. Trojanowski, V. M. Lee and I. R. Mackenzie (2007). "TDP-43 in familial and sporadic frontotemporal lobar degeneration with ubiquitin inclusions." Am J Pathol **171**(1): 227-240.

Carbone, M., S. Duty and M. Rattray (2012). "Riluzole elevates GLT-1 activity and levels in striatal astrocytes." Neurochem Int **60**(1): 31-38.

Carra, S., V. Crippa, P. Rusmini, A. Boncoraglio, M. Minoia, E. Giorgetti, H. H. Kampinga and A. Poletti (2012). "Alteration of protein folding and degradation in motor neuron diseases: Implications and protective functions of small heat shock proteins." Prog Neurobiol **97**(2): 83-100.

Chiang, P. M., J. Ling, Y. H. Jeong, D. L. Price, S. M. Aja and P. C. Wong (2010). "Deletion of TDP-43 down-regulates Tbc1d1, a gene linked to obesity, and alters body fat metabolism." Proc Natl Acad Sci U S A **107**(37): 16320-16324.

Chien, P., J. S. Weissman and A. H. DePace (2004). "Emerging principles of conformation-based prion inheritance." Annu Rev Biochem **73**: 617-656.

Chiò, A., G. Logroscino, B. J. Traynor, J. Collins, J. C. Simeone, L. A. Goldstein and L. A. White (2013). "Global epidemiology of amyotrophic lateral sclerosis: a systematic review of the published literature." Neuroepidemiology **41**(2): 118-130.

Ciura, S., S. Lattante, I. Le Ber, M. Latouche, H. Tostivint, A. Brice and E. Kabashi (2013). "Loss of function of C9orf72 causes motor deficits in a zebrafish model of Amyotrophic Lateral Sclerosis." Ann Neurol.

Collier, T. J., K. R. Srivastava, C. Justman, T. Grammatopoulous, B. Hutter-Paier, M. Prokesch, D. Havas, J. C. Rochet, F. Liu, K. Jock, P. de Oliveira, G. L. Stirtz, U. Dettmer, C. E. Sortwell, M. B. Feany, P. Lansbury, L. Lapidus and K. L. Paumier (2017). "Nortriptyline inhibits aggregation and neurotoxicity of alpha-synuclein by enhancing reconfiguration of the monomeric form." Neurobiol Dis **106**: 191-204.

Conicella, A. E., G. H. Zerze, J. Mittal and N. L. Fawzi (2016). "ALS Mutations Disrupt Phase Separation Mediated by α-Helical Structure in the TDP-43 Low-Complexity C-Terminal Domain." Structure **24**(9): 1537-1549.

Cragnaz, L., R. Klima, L. De Conti, G. Romano, F. Feiguin, E. Buratti, M. Baralle and F. E. Baralle (2015). "An age-related reduction of brain TBPH/TDP-43 levels precedes the onset of locomotion defects in a Drosophila ALS model." Neuroscience **311**: 415-421.

Crippa, V., S. Carra, P. Rusmini, D. Sau, E. Bolzoni, C. Bendotti, S. De Biasi and A. Poletti (2010). "A role of small heat shock protein B8 (HspB8) in the autophagic removal of misfolded proteins responsible for neurodegenerative diseases." Autophagy **6**(7): 958-960.

Cruz, M. P. (2018). "Edaravone (Radicava): A Novel Neuroprotective Agent for the Treatment of Amyotrophic Lateral Sclerosis." P T **43**(1): 25-28.

Cudkowicz, M. E., D. McKenna-Yasek, P. E. Sapp, W. Chin, B. Geller, D. L. Hayden, D. A. Schoenfeld, B. A. Hosler, H. R. Horvitz and R. H. Brown (1997). "Epidemiology of mutations in superoxide dismutase in amyotrophic lateral sclerosis." Ann Neurol **41**(2): 210-221.

Cushman, M., B. S. Johnson, O. D. King, A. D. Gitler and J. Shorter (2010). "Prion-like disorders: blurring the divide between transmissibility and infectivity." J Cell Sci **123**(Pt 8): 1191-1201.

D'Ambrogio, A., E. Buratti, C. Stuani, C. Guarnaccia, M. Romano, Y. M. Ayala and F. E. Baralle (2009). "Functional mapping of the interaction between TDP-43 and hnRNP A2 in vivo." Nucleic Acids Res **37**(12): 4116-4126.

Dal Canto, M. C. and M. E. Gurney (1995). "Neuropathological changes in two lines of mice carrying a transgene for mutant human Cu,Zn SOD, and in mice overexpressing wild type human SOD: a model of familial amyotrophic lateral sclerosis (FALS)." Brain Res **676**(1): 25-40.

De Vos, K. J. and M. Hafezparast (2017). "Neurobiology of axonal transport defects in motor neuron diseases: Opportunities for translational research?" Neurobiol Dis **105**: 283-299.

DeJesus-Hernandez, M., I. R. Mackenzie, B. F. Boeve, A. L. Boxer, M. Baker, N. J. Rutherford, A. M. Nicholson, N. A. Finch, H. Flynn, J. Adamson, N. Kouri, A. Wojtas, P. Sengdy, G. Y. Hsiung, A. Karydas, W. W. Seeley, K. A. Josephs, G. Coppola, D. H. Geschwind, Z. K. Wszolek, H. Feldman, D. S. Knopman, R. C. Petersen, B. L. Miller, D. W. Dickson, K. B. Boylan, N. R. Graff-Radford and R. Rademakers (2011). "Expanded GGGGCC hexanucleotide repeat in noncoding region of C9ORF72 causes chromosome 9p-linked FTD and ALS." Neuron **72**(2): 245-256.

Deng, H. X., W. Chen, S. T. Hong, K. M. Boycott, G. H. Gorrie, N. Siddique, Y. Yang, F. Fecto, Y. Shi, H. Zhai, H. Jiang, M. Hirano, E. Rampersaud, G. H. Jansen, S. Donkervoort, E. H. Bigio, B. R. Brooks, K. Ajroud, R. L. Sufit, J. L. Haines, E. Mugnaini, M. A. Pericak-Vance and T. Siddique (2011). "Mutations in UBQLN2 cause dominant X-linked juvenile and adult-onset ALS and ALS/dementia." Nature **477**(7363): 211-215.

Deng, H. X., Y. Shi, Y. Furukawa, H. Zhai, R. Fu, E. Liu, G. H. Gorrie, M. S. Khan, W. Y. Hung, E. H. Bigio, T. Lukas, M. C. Dal Canto, T. V. O'Halloran and T. Siddique (2006). "Conversion to the amyotrophic lateral sclerosis phenotype is associated with intermolecular linked insoluble aggregates of SOD1 in mitochondria." Proc Natl Acad Sci U S A **103**(18): 7142-7147.

Diaper, D. C., Y. Adachi, L. Lazarou, M. Greenstein, F. A. Simoes, A. Di Domenico, D. A. Solomon, S. Lowe, R. Alsubaie, D. Cheng, S. Buckley, D. M. Humphrey, C. E. Shaw and F. Hirth (2013). "Drosophila TDP-43 dysfunction in glia and muscle cells cause cytological and behavioural phenotypes that characterize ALS and FTLD." Hum Mol Genet **22**(19): 3883-3893.

Diaper, D. C., Y. Adachi, B. Sutcliffe, D. M. Humphrey, C. J. Elliott, A. Stepto, Z. N. Ludlow, L. Vanden Broeck, P. Callaerts, B. Dermaut, A. Al-Chalabi, C. E. Shaw, I. M. Robinson and F. Hirth (2013). "Loss and gain of

Drosophila TDP-43 impair synaptic efficacy and motor control leading to age-related neurodegeneration by loss-of-function phenotypes." Hum Mol Genet **22**(8): 1539-1557.

DiFiglia, M., E. Sapp, K. O. Chase, S. W. Davies, G. P. Bates, J. P. Vonsattel and N. Aronin (1997). "Aggregation of huntingtin in neuronal intranuclear inclusions and dystrophic neurites in brain." Science **277**(5334): 1990-1993.

Dormann, D., A. Capell, A. M. Carlson, S. S. Shankaran, R. Rodde, M. Neumann, E. Kremmer, T. Matsuwaki, K. Yamanouchi, M. Nishihara and C. Haass (2009). "Proteolytic processing of TAR DNA binding protein-43 by caspases produces C-terminal fragments with disease defining properties independent of progranulin." J Neurochem **110**(3): 1082-1094.

Estes, P. S., A. Boehringer, R. Zwick, J. E. Tang, B. Grigsby and D. C. Zarnescu (2011). "Wild-type and A315T mutant TDP-43 exert differential neurotoxicity in a Drosophila model of ALS." Hum Mol Genet **20**(12): 2308-2321.

Ezzi, S. A., M. Urushitani and J. P. Julien (2007). "Wild-type superoxide dismutase acquires binding and toxic properties of ALS-linked mutant forms through oxidation." J Neurochem **102**(1): 170-178.

Feiguin, F., V. K. Godena, G. Romano, A. D'Ambrogio, R. Klima and F. E. Baralle (2009). "Depletion of TDP-43 affects Drosophila motoneurons terminal synapsis and locomotive behavior." FEBS Lett **583**(10): 1586-1592.

Fiesel, F. C., S. S. Weber, J. Supper, A. Zell and P. J. Kahle (2012). "TDP-43 regulates global translational yield by splicing of exon junction complex component SKAR." Nucleic Acids Res **40**(6): 2668-2682.

Fuentealba, R. A., M. Udan, S. Bell, I. Wegorzewska, J. Shao, M. I. Diamond, C. C. Weihl and R. H. Baloh (2010). "Interaction with polyglutamine aggregates reveals a Q/N-rich domain in TDP-43." J Biol Chem **285**(34): 26304-26314.

Furukawa, Y., R. Fu, H. X. Deng, T. Siddique and T. V. O'Halloran (2006). "Disulfide cross-linked protein represents a significant fraction of ALS-associated Cu, Zn-superoxide dismutase aggregates in spinal cords of model mice." Proc Natl Acad Sci U S A **103**(18): 7148-7153.

Furukawa, Y., K. Kaneko, S. Watanabe, K. Yamanaka and N. Nukina (2011). "A seeding reaction recapitulates intracellular formation of Sarkosyl-insoluble transactivation response element (TAR) DNA-binding protein-43 inclusions." J Biol Chem **286**(21): 18664-18672.

Gendron, T. F., R. Rademakers and L. Petrucelli (2013). "TARDBP mutation analysis in TDP-43 proteinopathies and deciphering the toxicity of mutant TDP-43." J Alzheimers Dis **33 Suppl 1**: S35-45.

Geser, F., M. Martinez-Lage, J. Robinson, K. Uryu, M. Neumann, N. J. Brandmeir, S. X. Xie, L. K. Kwong, L. Elman, L. McCluskey, C. M. Clark, J. Malunda, B. L. Miller, E. A. Zimmerman, J. Qian, V. Van Deerlin, M. Grossman, V. M. Lee and J. Q. Trojanowski (2009). "Clinical and pathological continuum of multisystem TDP-43 proteinopathies." Arch Neurol **66**(2): 180-189.

Giacomelli, C., S. Daniele and C. Martini (2017). "Potential biomarkers and novel pharmacological targets in protein aggregation-related neurodegenerative diseases." Biochem Pharmacol **131**: 1-15.

Giordana, M. T., M. Piccinini, S. Grifoni, G. De Marco, M. Vercellino, M. Magistrello, A. Pellerino, B. Buccinnà, E. Lupino and M. T. Rinaudo (2010). "TDP-43 redistribution is an early event in sporadic amyotrophic lateral sclerosis." Brain Pathol **20**(2): 351-360.

Gitcho, M. A., E. H. Bigio, M. Mishra, N. Johnson, S. Weintraub, M. Mesulam, R. Rademakers, S. Chakraverty, C. Cruchaga, J. C. Morris, A. M. Goate and N. J. Cairns (2009). "TARDBP 3'-UTR variant in autopsy-confirmed frontotemporal lobar degeneration with TDP-43 proteinopathy." Acta Neuropathol **118**(5): 633-645.

Glickman, M. H. and V. Maytal (2002). "Regulating the 26S proteasome." Curr Top Microbiol Immunol **268**: 43-72.

Goedert, M., F. Clavaguera and M. Tolnay (2010). "The propagation of prion-like protein inclusions in neurodegenerative diseases." Trends Neurosci **33**(7): 317-325.

Guo, W., Y. Chen, X. Zhou, A. Kar, P. Ray, X. Chen, E. J. Rao, M. Yang, H. Ye, L. Zhu, J. Liu, M. Xu, Y. Yang, C. Wang, D. Zhang, E. H. Bigio, M. Mesulam, Y. Shen, Q. Xu, K. Fushimi and J. Y. Wu (2011). "An ALS-associated mutation affecting TDP-43 enhances protein aggregation, fibril formation and neurotoxicity." Nat Struct Mol Biol **18**(7): 822-830.

Gurney, M. E. (1994). "Transgenic-mouse model of amyotrophic lateral sclerosis." N Engl J Med **331**(25): 1721-1722.

Hara, T., K. Nakamura, M. Matsui, A. Yamamoto, Y. Nakahara, R. Suzuki-Migishima, M. Yokoyama, K. Mishima, I. Saito, H. Okano and N. Mizushima (2006). "Suppression of basal autophagy in neural cells causes neurodegenerative disease in mice." Nature **441**(7095): 885-889.

Hardiman, O., A. Al-Chalabi, A. Chio, E. M. Corr, G. Logroscino, W. Robberecht, P. J. Shaw, Z. Simmons and L. H. van den Berg (2017). "Amyotrophic lateral sclerosis." Nat Rev Dis Primers **3**: 17085.

Hasegawa, M., T. Arai, T. Nonaka, F. Kametani, M. Yoshida, Y. Hashizume, T. G. Beach, E. Buratti, F. Baralle, M. Morita, I. Nakano, T. Oda, K. Tsuchiya and H. Akiyama (2008). "Phosphorylated TDP-43 in frontotemporal lobar degeneration and amyotrophic lateral sclerosis." Ann Neurol **64**(1): 60-70.

Hjerpe, R., J. S. Bett, M. J. Keuss, A. Solovyova, T. G. McWilliams, C. Johnson, I. Sahu, J. Varghese, N. Wood, M. Wightman, G. Osborne, G. P. Bates, M. H. Glickman, M. Trost, A. Knebel, F. Marchesi and T. Kurz (2016). "UBQLN2 Mediates Autophagy-Independent Protein Aggregate Clearance by the Proteasome." Cell **166**(4): 935-949.

Huang, C., P. Y. Xia and H. Zhou (2010). "Sustained expression of TDP-43 and FUS in motor neurons in rodent's lifetime." Int J Biol Sci **6**(4): 396-406.

Huisman, M. H., S. W. de Jong, P. T. van Doormaal, S. S. Weinreich, H. J. Schelhaas, A. J. van der Kooi, M. de Visser, J. H. Veldink and L. H. van den Berg (2011). "Population based epidemiology of amyotrophic lateral sclerosis using capture-recapture methodology." J Neurol Neurosurg Psychiatry **82**(10): 1165-1170.

Igaz, L. M., L. K. Kwong, A. Chen-Plotkin, M. J. Winton, T. L. Unger, Y. Xu, M. Neumann, J. Q. Trojanowski and V. M. Lee (2009). "Expression of TDP-43 C-terminal Fragments in Vitro Recapitulates Pathological Features of TDP-43 Proteinopathies." J Biol Chem **284**(13): 8516-8524.

Igaz, L. M., L. K. Kwong, E. B. Lee, A. Chen-Plotkin, E. Swanson, T. Unger, J. Malunda, Y. Xu, M. J. Winton, J. Q. Trojanowski and V. M. Lee (2011). "Dysregulation of the ALS-associated gene TDP-43 leads to neuronal death and degeneration in mice." J Clin Invest **121**(2): 726-738.

Igaz, L. M., L. K. Kwong, Y. Xu, A. C. Truax, K. Uryu, M. Neumann, C. M. Clark, L. B. Elman, B. L. Miller, M. Grossman, L. F. McCluskey, J. Q. Trojanowski and V. M. Lee (2008). "Enrichment of C-terminal fragments in TAR DNA-binding protein-43 cytoplasmic inclusions in brain but not in spinal cord of frontotemporal lobar degeneration and amyotrophic lateral sclerosis." Am J Pathol **173**(1): 182-194.

Iguchi, Y., M. Katsuno, J. Niwa, S. Takagi, S. Ishigaki, K. Ikenaka, K. Kawai, H. Watanabe, K. Yamanaka, R. Takahashi, H. Misawa, S. Sasaki, F. Tanaka and G. Sobue (2013). "Loss of TDP-43 causes age-dependent progressive motor neuron degeneration." Brain **136**(Pt 5): 1371-1382.

Iko, Y., T. S. Kodama, N. Kasai, T. Oyama, E. H. Morita, T. Muto, M. Okumura, R. Fujii, T. Takumi, S. Tate and K. Morikawa (2004). "Domain architectures and characterization of an RNA-binding protein, TLS." J Biol Chem **279**(43): 44834-44840.

Ip, P., V. K. Mulligan and A. Chakrabartty (2011). "ALS-causing SOD1 mutations promote production of copper-deficient misfolded species." J Mol Biol **409**(5): 839-852.

Jellinger, K. A. (2010). "Basic mechanisms of neurodegeneration: a critical update." J Cell Mol Med **14**(3): 457-487.

Jentsch, S. (1992). "Ubiquitin-dependent protein degradation: a cellular perspective." Trends Cell Biol **2**(4): 98-103.

Jiang, L. L., M. X. Che, J. Zhao, C. J. Zhou, M. Y. Xie, H. Y. Li, J. H. He and H. Y. Hu (2013). "Structural transformation of the amyloidogenic core region of TDP-43 protein initiates its aggregation and cytoplasmic inclusion." J Biol Chem **288**(27): 19614-19624.

Johnson, B. S., J. M. McCaffery, S. Lindquist and A. D. Gitler (2008). "A yeast TDP-43 proteinopathy model: Exploring the molecular determinants of TDP-43 aggregation and cellular toxicity." Proc Natl Acad Sci U S A **105**(17): 6439-6444.

Johnson, B. S., D. Snead, J. J. Lee, J. M. McCaffery, J. Shorter and A. D. Gitler (2009). "TDP-43 is intrinsically aggregation-prone, and amyotrophic lateral sclerosis-linked mutations accelerate aggregation and increase toxicity." J Biol Chem **284**(30): 20329-20339.

Johnston, J. A., M. J. Dalton, M. E. Gurney and R. R. Kopito (2000). "Formation of high molecular weight complexes of mutant Cu, Zn-superoxide dismutase in a mouse model for familial amyotrophic lateral sclerosis." Proc Natl Acad Sci U S A **97**(23): 12571-12576.

Kabashi, E., P. N. Valdmanis, P. Dion, D. Spiegelman, B. J. McConkey, C. Vande Velde, J. P. Bouchard, L. Lacomblez, K. Pochigaeva, F. Salachas, P. F. Pradat, W. Camu, V. Meininger, N. Dupre and G. A. Rouleau (2008). "TARDBP mutations in individuals with sporadic and familial amyotrophic lateral sclerosis." Nat Genet **40**(5): 572-574.

Kandil, E. A., N. F. Abdelkader, B. M. El-Sayeh and S. Saleh (2016). "Imipramine and amitriptyline ameliorate the rotenone model of Parkinson's disease in rats." Neuroscience **332**: 26-37.

Kato, S., M. Takikawa, K. Nakashima, A. Hirano, D. W. Cleveland, H. Kusaka, N. Shibata, M. Kato, I. Nakano and E. Ohama (2000). "New consensus research on neuropathological aspects of familial amyotrophic lateral sclerosis with superoxide dismutase 1 (SOD1) gene mutations: inclusions containing SOD1 in neurons and astrocytes." Amyotroph Lateral Scler Other Motor Neuron Disord **1**(3): 163-184.

Kiernan, M. C., S. Vucic, B. C. Cheah, M. R. Turner, A. Eisen, O. Hardiman, J. R. Burrell and M. C. Zoing (2011). "Amyotrophic lateral sclerosis." Lancet **377**(9769): 942-955.

Kisselev, A. F., T. N. Akopian, K. M. Woo and A. L. Goldberg (1999). "The sizes of peptides generated from protein by mammalian 26 and 20 S proteasomes. Implications for understanding the degradative mechanism and antigen presentation." J Biol Chem **274**(6): 3363-3371.

Komatsu, M., S. Waguri, T. Chiba, S. Murata, J. Iwata, I. Tanida, T. Ueno, M. Koike, Y. Uchiyama, E. Kominami and K. Tanaka (2006). "Loss of autophagy in the central nervous system causes neurodegeneration in mice." Nature **441**(7095): 880-884.

Koyama, A., A. Sugai, T. Kato, T. Ishihara, A. Shiga, Y. Toyoshima, M. Koyama, T. Konno, S. Hirokawa, A. Yokoseki, M. Nishizawa, A. Kakita, H. Takahashi and O. Onodera (2016). "Increased cytoplasmic TARDBP mRNA in affected spinal motor neurons in ALS caused by abnormal autoregulation of TDP-43." Nucleic Acids Res **44**(12): 5820-5836.

Kraemer, B. C., T. Schuck, J. M. Wheeler, L. C. Robinson, J. Q. Trojanowski, V. M. Lee and G. D. Schellenberg (2010). "Loss of murine TDP-43 disrupts motor function and plays an essential role in embryogenesis." Acta Neuropathol **119**(4): 409-419.

Kuma, A., M. Hatano, M. Matsui, A. Yamamoto, H. Nakaya, T. Yoshimori, Y. Ohsumi, T. Tokuhisa and N. Mizushima (2004). "The role of autophagy during the early neonatal starvation period." Nature **432**(7020): 1032-1036.

Kuo, P. H., L. G. Doudeva, Y. T. Wang, C. K. Shen and H. S. Yuan (2009). "Structural insights into TDP-43 in nucleic-acid binding and domain interactions." Nucleic Acids Res **37**(6): 1799-1808.

Kwiatkowski, T. J., D. A. Bosco, A. L. Leclerc, E. Tamrazian, C. R. Vanderburg, C. Russ, A. Davis, J. Gilchrist, E. J. Kasarskis, T. Munsat, P. Valdmanis, G. A. Rouleau, B. A. Hosler, P. Cortelli, P. J. de Jong, Y. Yoshinaga, J. L. Haines, M. A. Pericak-Vance, J. Yan, N. Ticozzi, T. Siddique, D. McKenna-Yasek, P. C. Sapp, H. R. Horvitz, J. E. Landers and R. H. Brown (2009). "Mutations in the FUS/TLS gene on chromosome 16 cause familial amyotrophic lateral sclerosis." Science **323**(5918): 1205-1208.

Laaksovirta, H., T. Peuralinna, J. C. Schymick, S. W. Scholz, S. L. Lai, L. Myllykangas, R. Sulkava, L. Jansson, D. G. Hernandez, J. R. Gibbs, M. A. Nalls, D. Heckerman, P. J. Tienari and B. J. Traynor (2010). "Chromosome 9p21 in amyotrophic lateral sclerosis in Finland: a genome-wide association study." Lancet Neurol **9**(10): 978-985.

Lagier-Tourenne, C., M. Polymenidou and D. W. Cleveland (2010). "TDP-43 and FUS/TLS: emerging roles in RNA processing and neurodegeneration." Hum Mol Genet **19**(R1): R46-64.

Lecker, S. H., A. L. Goldberg and W. E. Mitch (2006). "Protein degradation by the ubiquitin-proteasome pathway in normal and disease states." J Am Soc Nephrol **17**(7): 1807-1819.

Lee, E. B., V. M. Lee and J. Q. Trojanowski (2011). "Gains or losses: molecular mechanisms of TDP43-mediated neurodegeneration." Nat Rev Neurosci **13**(1): 38-50.

Lee, J., S. J. Hyeon, H. Im, H. Ryu and Y. Kim (2016). "Astrocytes and Microglia as Non-cell Autonomous Players in the Pathogenesis of ALS." Exp Neurobiol **25**(5): 233-240.

Leigh, P. N., B. H. Anderton, A. Dodson, J. M. Gallo, M. Swash and D. M. Power (1988). "Ubiquitin deposits in anterior horn cells in motor neurone disease." Neurosci Lett **93**(2-3): 197-203.

Li, H. Y., P. A. Yeh, H. C. Chiu, C. Y. Tang and B. P. Tu (2011). "Hyperphosphorylation as a defense mechanism to reduce TDP-43 aggregation." PLoS One **6**(8): e23075.

Li, Y., P. Ray, E. J. Rao, C. Shi, W. Guo, X. Chen, E. A. Woodruff, K. Fushimi and J. Y. Wu (2010). "A Drosophila model for TDP-43 proteinopathy." Proc Natl Acad Sci U S A **107**(7): 3169-3174.

Liachko, N. F., C. R. Guthrie and B. C. Kraemer (2010). "Phosphorylation promotes neurotoxicity in a Caenorhabditis elegans model of TDP-43 proteinopathy." J Neurosci **30**(48): 16208-16219.

Lim, L., Y. Wei, Y. Lu and J. Song (2016). "ALS-Causing Mutations Significantly Perturb the Self-Assembly and Interaction with Nucleic Acid of the Intrinsically Disordered Prion-Like Domain of TDP-43." PLoS Biol **14**(1): e1002338.

Lin, H. Y., W. L. Yeh, B. R. Huang, C. Lin, C. H. Lai, H. Lin and D. Y. Lu (2012). "Desipramine protects neuronal cell death and induces heme oxygenase-1 expression in Mes23.5 dopaminergic neurons." PLoS One **7**(11): e50138.

Ling, S. C., M. Polymenidou and D. W. Cleveland (2013). "Converging mechanisms in ALS and FTD: disrupted RNA and protein homeostasis." Neuron **79**(3): 416-438.

Liu, Y., R. A. Atkinson, C. M. Fernandez-Martos, M. T. Kirkcaldie, H. Cui, J. C. Vickers and A. E. King (2015). "Changes in TDP-43 expression in development, aging, and in the neurofilament light protein knockout mouse." Neurobiol Aging **36**(2): 1151-1159.

Logroscino, G., B. J. Traynor, O. Hardiman, A. Chiò, D. Mitchell, R. J. Swingler, A. Millul, E. Benn, E. Beghi and EURALS (2010). "Incidence of amyotrophic lateral sclerosis in Europe." J Neurol Neurosurg Psychiatry **81**(4): 385-390.

Lu, Y., J. Ferris and F. B. Gao (2009). "Frontotemporal dementia and amyotrophic lateral sclerosis-associated disease protein TDP-43 promotes dendritic branching." Mol Brain **2**: 30.

Ma, X. M., S. O. Yoon, C. J. Richardson, K. Jülich and J. Blenis (2008). "SKAR links pre-mRNA splicing to mTOR/S6K1-mediated enhanced translation efficiency of spliced mRNAs." Cell **133**(2): 303-313.

Mackenzie, I. R., E. H. Bigio, P. G. Ince, F. Geser, M. Neumann, N. J. Cairns, L. K. Kwong, M. S. Forman, J. Ravits, H. Stewart, A. Eisen, L. McClusky, H. A. Kretzschmar, C. M. Monoranu, J. R. Highley, J. Kirby, T. Siddique, P. J. Shaw, V. M. Lee and J. Q. Trojanowski (2007). "Pathological TDP-43 distinguishes sporadic amyotrophic lateral sclerosis from amyotrophic lateral sclerosis with SOD1 mutations." Ann Neurol **61**(5): 427-434.

Mackenzie, I. R. and R. Rademakers (2008). "The role of transactive response DNA-binding protein-43 in amyotrophic lateral sclerosis and frontotemporal dementia." Curr Opin Neurol **21**(6): 693-700.

Mackenzie, I. R., R. Rademakers and M. Neumann (2010). "TDP-43 and FUS in amyotrophic lateral sclerosis and frontotemporal dementia." Lancet Neurol **9**(10): 995-1007.

Medinas, D. B., P. Rozas, F. Martínez Traub, U. Woehlbier, R. H. Brown, D. A. Bosco and C. Hetz (2018). "Endoplasmic reticulum stress leads to accumulation of wild-type SOD1 aggregates associated with sporadic amyotrophic lateral sclerosis." Proc Natl Acad Sci U S A **115**(32): 8209-8214.

Miguel, L., T. Frébourg, D. Campion and M. Lecourtois (2011). "Both cytoplasmic and nuclear accumulations of the protein are neurotoxic in Drosophila models of TDP-43 proteinopathies." Neurobiol Dis **41**(2): 398-406.

Mizushima, N. (2007). "Autophagy: process and function." Genes Dev **21**(22): 2861-2873.

Mompeán, M., E. Buratti, C. Guarnaccia, R. M. Brito, A. Chakrabartty, F. E. Baralle and D. V. Laurents (2014). ""Structural characterization of the minimal segment of TDP-43 competent for aggregation"." Arch Biochem Biophys **545**: 53-62.

Mompeán, M., R. Hervás, Y. Xu, T. H. Tran, C. Guarnaccia, E. Buratti, F. Baralle, L. Tong, M. Carrión-Vázquez, A. E. McDermott and D. V. Laurents (2015). "Structural Evidence of Amyloid Fibril Formation in the Putative Aggregation Domain of TDP-43." J Phys Chem Lett **6**(13): 2608-2615.

Mompeán, M., V. Romano, D. Pantoja-Uceda, C. Stuani, F. E. Baralle, E. Buratti and D. V. Laurents (2016). "The TDP-43 N-terminal domain structure at high resolution." FEBS J **283**(7): 1242-1260.

Mompeán, M., V. Romano, D. Pantoja-Uceda, C. Stuani, F. E. Baralle, E. Buratti and D. V. Laurents (2017). "Point mutations in the N-terminal domain of transactive response DNA-binding protein 43 kDa (TDP-43) compromise its stability, dimerization, and functions." J Biol Chem **292**(28): 11992-12006.

Mori, K., T. Arzberger, F. A. Grässer, I. Gijselinck, S. May, K. Rentzsch, S. M. Weng, M. H. Schludi, J. van der Zee, M. Cruts, C. Van Broeckhoven, E. Kremmer, H. A. Kretzschmar, C. Haass and D. Edbauer (2013). "Bidirectional transcripts of the expanded C9orf72 hexanucleotide repeat are translated into aggregating dipeptide repeat proteins." Acta Neuropathol **126**(6): 881-893.

Mori, K., S. Lammich, I. R. Mackenzie, I. Forné, S. Zilow, H. Kretzschmar, D. Edbauer, J. Janssens, G. Kleinberger, M. Cruts, J. Herms, M. Neumann, C. Van Broeckhoven, T. Arzberger and C. Haass (2013). "hnRNP A3 binds to GGGGCC repeats and is a constituent of p62-positive/TDP43-negative inclusions in the hippocampus of patients with C9orf72 mutations." Acta Neuropathol **125**(3): 413-423.

Mori, K., S. M. Weng, T. Arzberger, S. May, K. Rentzsch, E. Kremmer, B. Schmid, H. A. Kretzschmar, M. Cruts, C. Van Broeckhoven, C. Haass and D. Edbauer (2013). "The C9orf72 GGGGCC repeat is translated into aggregating dipeptide-repeat proteins in FTLD/ALS." Science **339**(6125): 1335-1338.

Muqit, M. M. and M. B. Feany (2002). "Modelling neurodegenerative diseases in Drosophila: a fruitful approach?" Nat Rev Neurosci **3**(3): 237-243.

Muyderman, H. and T. Chen (2014). "Mitochondrial dysfunction in amyotrophic lateral sclerosis - a valid pharmacological target?" Br J Pharmacol **171**(8): 2191-2205.

Nadanaciva, S., S. Lu, D. F. Gebhard, B. A. Jessen, W. D. Pennie and Y. Will (2011). "A high content screening assay for identifying lysosomotropic compounds." Toxicol In Vitro **25**(3): 715-723.

Nakai, A., O. Yamaguchi, T. Takeda, Y. Higuchi, S. Hikoso, M. Taniike, S. Omiya, I. Mizote, Y. Matsumura, M. Asahi, K. Nishida, M. Hori, N. Mizushima and K. Otsu (2007). "The role of autophagy in cardiomyocytes in the basal state and in response to hemodynamic stress." Nat Med **13**(5): 619-624.

Neumann, M. (2009). "Molecular neuropathology of TDP-43 proteinopathies." Int J Mol Sci **10**(1): 232-246.

Neumann, M., L. K. Kwong, E. B. Lee, E. Kremmer, A. Flatley, Y. Xu, M. S. Forman, D. Troost, H. A. Kretzschmar, J. Q. Trojanowski and V. M. Lee (2009). "Phosphorylation of S409/410 of TDP-43 is a consistent feature in all sporadic and familial forms of TDP-43 proteinopathies." Acta Neuropathol **117**(2): 137-149.

Neumann, M., R. Rademakers, S. Roeber, M. Baker, H. A. Kretzschmar and I. R. Mackenzie (2009). "A new subtype of frontotemporal lobar degeneration with FUS pathology." Brain **132**(Pt 11): 2922-2931.

Neumann, M., D. M. Sampathu, L. K. Kwong, A. C. Truax, M. C. Micsenyi, T. T. Chou, J. Bruce, T. Schuck, M. Grossman, C. M. Clark, L. F. McCluskey, B. L. Miller, E. Masliah, I. R. Mackenzie, H. Feldman, W. Feiden, H. A. Kretzschmar, J. Q. Trojanowski and V. M. Lee (2006). "Ubiquitinated TDP-43 in frontotemporal lobar degeneration and amyotrophic lateral sclerosis." Science **314**(5796): 130-133.

Newell, K., F. Paron, M. Mompean, J. Murrell, E. Salis, C. Stuani, G. Pattee, M. Romano, D. Laurents, B. Ghetti and E. Buratti (2018). "Dysregulation of TDP-43 intracellular localization and early onset ALS are associated with a TARDBP S375G variant." Brain Pathol.

Nonaka, T., T. Arai, E. Buratti, F. E. Baralle, H. Akiyama and M. Hasegawa (2009). "Phosphorylated and ubiquitinated TDP-43 pathological inclusions in ALS and FTLD-U are recapitulated in SH-SY5Y cells." FEBS Lett **583**(2): 394-400.

Nonaka, T., F. Kametani, T. Arai, H. Akiyama and M. Hasegawa (2009). "Truncation and pathogenic mutations facilitate the formation of intracellular aggregates of TDP-43." Hum Mol Genet **18**(18): 3353-3364.

Nonaka, T., M. Masuda-Suzukake, T. Arai, Y. Hasegawa, H. Akatsu, T. Obi, M. Yoshida, S. Murayama, D. M. Mann, H. Akiyama and M. Hasegawa (2013). "Prion-like properties of pathological TDP-43 aggregates from diseased brains." Cell Rep **4**(1): 124-134.

Nonaka, T., G. Suzuki, Y. Tanaka, F. Kametani, S. Hirai, H. Okado, T. Miyashita, M. Saitoe, H. Akiyama, H. Masai and M. Hasegawa (2016). "Phosphorylation of TAR DNA-binding Protein of 43 kDa (TDP-43) by Truncated Casein Kinase 1δ Triggers Mislocalization and Accumulation of TDP-43." J Biol Chem **291**(11): 5473-5483.

Nonaka, T., S. T. Watanabe, T. Iwatsubo and M. Hasegawa (2010). "Seeded aggregation and toxicity of {alpha}-synuclein and tau: cellular models of neurodegenerative diseases." J Biol Chem **285**(45): 34885-34898.

Onodera, J. and Y. Ohsumi (2005). "Autophagy is required for maintenance of amino acid levels and protein synthesis under nitrogen starvation." J Biol Chem **280**(36): 31582-31586.

Ou, S. H., F. Wu, D. Harrich, L. F. García-Martínez and R. B. Gaynor (1995). "Cloning and characterization of a novel cellular protein, TDP-43, that binds to human immunodeficiency virus type 1 TAR DNA sequence motifs." J Virol **69**(6): 3584-3596.

Pankiv, S., T. H. Clausen, T. Lamark, A. Brech, J. A. Bruun, H. Outzen, A. Øvervatn, G. Bjørkøy and T. Johansen (2007). "p62/SQSTM1 binds directly to Atg8/LC3 to facilitate degradation of ubiquitinated protein aggregates by autophagy." J Biol Chem **282**(33): 24131-24145.

Pesiridis, G. S., V. M. Lee and J. Q. Trojanowski (2009). "Mutations in TDP-43 link glycine-rich domain functions to amyotrophic lateral sclerosis." Hum Mol Genet **18**(R2): R156-162.

Polymenidou, M. and D. W. Cleveland (2011). "The seeds of neurodegeneration: prion-like spreading in ALS." Cell **147**(3): 498-508.

Prusiner, S. B. (1982). "Novel proteinaceous infectious particles cause scrapie." Science **216**(4542): 136-144.

Ramesh, N. and U. B. Pandey (2017). "Autophagy Dysregulation in ALS: When Protein Aggregates Get Out of Hand." Front Mol Neurosci **10**: 263.

Ratti, A. and E. Buratti (2016). "Physiological functions and pathobiology of TDP-43 and FUS/TLS proteins." J Neurochem **138 Suppl 1**: 95-111.

Reaume, A. G., J. L. Elliott, E. K. Hoffman, N. W. Kowall, R. J. Ferrante, D. F. Siwek, H. M. Wilcox, D. G. Flood, M. F. Beal, R. H. Brown, R. W. Scott and W. D. Snider (1996). "Motor neurons in Cu/Zn superoxide dismutase-deficient mice develop normally but exhibit enhanced cell death after axonal injury." Nat Genet **13**(1): 43-47.

Renton, A. E., A. Chiò and B. J. Traynor (2014). "State of play in amyotrophic lateral sclerosis genetics." Nat Neurosci **17**(1): 17-23.

Renton, A. E., E. Majounie, A. Waite, J. Simón-Sánchez, S. Rollinson, J. R. Gibbs, J. C. Schymick, H. Laaksovirta, J. C. van Swieten, L. Myllykangas, H. Kalimo, A. Paetau, Y. Abramzon, A. M. Remes, A. Kaganovich, S. W. Scholz, J. Duckworth, J. Ding, D. W. Harmer, D. G. Hernandez, J. O. Johnson, K. Mok, M. Ryten, D. Trabzuni, R. J. Guerreiro, R. W. Orrell, J. Neal, A. Murray, J. Pearson, I. E. Jansen, D. Sondervan, H. Seelaar, D. Blake, K. Young, N. Halliwell, J. B. Callister, G. Toulson, A. Richardson, A. Gerhard, J. Snowden, D. Mann, D. Neary, M. A. Nalls, T. Peuralinna, L. Jansson, V. M. Isoviita, A. L. Kaivorinne, M. Hölttä-Vuori, E. Ikonen, R. Sulkava, M. Benatar, J. Wuu, A. Chiò, G. Restagno, G. Borghero, M. Sabatelli, D. Heckerman, E. Rogaeva, L. Zinman, J. D. Rothstein, M. Sendtner, C. Drepper, E. E. Eichler, C. Alkan, Z. Abdullaev, S. D. Pack, A. Dutra, E. Pak, J. Hardy, A. Singleton, N. M. Williams, P. Heutink, S. Pickering-Brown, H. R. Morris, P. J. Tienari, B. J. Traynor and I. Consortium (2011). "A hexanucleotide repeat expansion in C9ORF72 is the cause of chromosome 9p21-linked ALS-FTD." Neuron **72**(2): 257-268.

Richardson, C. J., M. Bröenstrup, D. C. Fingar, K. Jülich, B. A. Ballif, S. Gygi and J. Blenis (2004). "SKAR is a specific target of S6 kinase 1 in cell growth control." Curr Biol **14**(17): 1540-1549.

Ringholz, G. M., S. H. Appel, M. Bradshaw, N. A. Cooke, D. M. Mosnik and P. E. Schulz (2005). "Prevalence and patterns of cognitive impairment in sporadic ALS." Neurology **65**(4): 586-590.

Robberecht, W. and T. Philips (2013). "The changing scene of amyotrophic lateral sclerosis." Nat Rev Neurosci **14**(4): 248-264.

Rock, K. L., C. Gramm, L. Rothstein, K. Clark, R. Stein, L. Dick, D. Hwang and A. L. Goldberg (1994). "Inhibitors of the proteasome block the degradation of most cell proteins and the generation of peptides presented on MHC class I molecules." Cell **78**(5): 761-771.

Romano, G., R. Klima, E. Buratti, P. Verstreken, F. E. Baralle and F. Feiguin (2014). "Chronological requirements of TDP-43 function in synaptic organization and locomotive control." Neurobiol Dis **71**: 95-109.

Rosen, D. R. (1993). "Mutations in Cu/Zn superoxide dismutase gene are associated with familial amyotrophic lateral sclerosis." Nature **364**(6435): 362.

Ross, C. A. and M. A. Poirier (2005). "Opinion: What is the role of protein aggregation in neurodegeneration?" Nat Rev Mol Cell Biol **6**(11): 891-898.

Rossbach, O., L. H. Hung, S. Schreiner, I. Grishina, M. Heiner, J. Hui and A. Bindereif (2009). "Auto- and cross-regulation of the hnRNP L proteins by alternative splicing." Mol Cell Biol **29**(6): 1442-1451.

Rotunno, M. S. and D. A. Bosco (2013). "An emerging role for misfolded wild-type SOD1 in sporadic ALS pathogenesis." Front Cell Neurosci **7**: 253.

Rowland, L. P. and N. A. Shneider (2001). "Amyotrophic lateral sclerosis." N Engl J Med **344**(22): 1688-1700.

Rubinsztein, D. C., J. E. Gestwicki, L. O. Murphy and D. J. Klionsky (2007). "Potential therapeutic applications of autophagy." Nat Rev Drug Discov **6**(4): 304-312.

Saric, T., C. I. Graef and A. L. Goldberg (2004). "Pathway for degradation of peptides generated by proteasomes: a key role for thimet oligopeptidase and other metallopeptidases." J Biol Chem **279**(45): 46723-46732.

Sasaguri, H., J. Chew, Y. F. Xu, T. F. Gendron, A. Garrett, C. W. Lee, K. Jansen-West, P. O. Bauer, E. A. Perkerson, J. Tong, C. Stetler and Y. J. Zhang (2016). "The extreme N-terminus of TDP-43 mediates the cytoplasmic aggregation of TDP-43 and associated toxicity in vivo." Brain Res **1647**: 57-64.

Sasaki, S. (2011). "Autophagy in spinal cord motor neurons in sporadic amyotrophic lateral sclerosis." J Neuropathol Exp Neurol **70**(5): 349-359.

Scotter, E. L., C. Vance, A. L. Nishimura, Y. B. Lee, H. J. Chen, H. Urwin, V. Sardone, J. C. Mitchell, B. Rogelj, D. C. Rubinsztein and C. E. Shaw (2014). "Differential roles of the ubiquitin proteasome system and autophagy in the clearance of soluble and aggregated TDP-43 species." J Cell Sci **127**(Pt 6): 1263-1278.

Shatunov, A., K. Mok, S. Newhouse, M. E. Weale, B. Smith, C. Vance, L. Johnson, J. H. Veldink, M. A. van Es, L. H. van den Berg, W. Robberecht, P. Van Damme, O. Hardiman, A. E. Farmer, C. M. Lewis, A. W. Butler, O. Abel, P. M. Andersen, I. Fogh, V. Silani, A. Chiò, B. J. Traynor, J. Melki, V. Meininger, J. E. Landers, P. McGuffin, J. D. Glass, H. Pall, P. N. Leigh, J. Hardy, R. H. Brown, J. F. Powell, R. W. Orrell, K. E. Morrison, P. J. Shaw, C. E. Shaw and A. Al-Chalabi (2010). "Chromosome 9p21 in sporadic amyotrophic lateral sclerosis in the UK and seven other countries: a genome-wide association study." Lancet Neurol **9**(10): 986-994.

Shiga, A., T. Ishihara, A. Miyashita, M. Kuwabara, T. Kato, N. Watanabe, A. Yamahira, C. Kondo, A. Yokoseki, M. Takahashi, R. Kuwano, A. Kakita, M. Nishizawa, H. Takahashi and O. Onodera (2012). "Alteration of POLDIP3 splicing associated with loss of function of TDP-43 in tissues affected with ALS." PLoS One **7**(8): e43120.

Soto, C. (2003). "Unfolding the role of protein misfolding in neurodegenerative diseases." Nat Rev Neurosci **4**(1): 49-60.

Sreedharan, J., I. P. Blair, V. B. Tripathi, X. Hu, C. Vance, B. Rogelj, S. Ackerley, J. C. Durnall, K. L. Williams, E. Buratti, F. Baralle, J. de Belleroche, J. D. Mitchell, P. N. Leigh, A. Al-Chalabi, C. C. Miller, G. Nicholson and C. E. Shaw (2008). "TDP-43 mutations in familial and sporadic amyotrophic lateral sclerosis." Science **319**(5870): 1668-1672.

Stallings, N. R., K. Puttaparthi, C. M. Luther, D. K. Burns and J. L. Elliott (2010). "Progressive motor weakness in transgenic mice expressing human TDP-43." Neurobiol Dis **40**(2): 404-414.

Stavrovskaya, I. G., M. V. Narayanan, W. Zhang, B. F. Krasnikov, J. Heemskerk, S. S. Young, J. P. Blass, A. M. Brown, M. F. Beal, R. M. Friedlander and B. S. Kristal (2004). "Clinically approved heterocyclics act on a mitochondrial target and reduce stroke-induced pathology." J Exp Med **200**(2): 211-222.

Swarup, V., D. Phaneuf, C. Bareil, J. Robertson, G. A. Rouleau, J. Kriz and J. P. Julien (2011). "Pathological hallmarks of amyotrophic lateral sclerosis/frontotemporal lobar degeneration in transgenic mice produced with TDP-43 genomic fragments." Brain **134**(Pt 9): 2610-2626.

Swinnen, B. and W. Robberecht (2014). "The phenotypic variability of amyotrophic lateral sclerosis." Nat Rev Neurol **10**(11): 661-670.

Tashiro, Y., M. Urushitani, H. Inoue, M. Koike, Y. Uchiyama, M. Komatsu, K. Tanaka, M. Yamazaki, M. Abe, H. Misawa, K. Sakimura, H. Ito and R. Takahashi (2012). "Motor neuron-specific disruption of proteasomes, but not autophagy, replicates amyotrophic lateral sclerosis." J Biol Chem **287**(51): 42984-42994.

Taylor, J. P., R. H. Brown and D. W. Cleveland (2016). "Decoding ALS: from genes to mechanism." Nature **539**(7628): 197-206.

Tokuda, E., T. Nomura, S. Ohara, S. Watanabe, K. Yamanaka, Y. Morisaki, H. Misawa and Y. Furukawa (2018). "A copper-deficient form of mutant Cu/Zn-superoxide dismutase as an early pathological species in amyotrophic lateral sclerosis." Biochim Biophys Acta Mol Basis Dis **1864**(6 Pt A): 2119-2130.

Tollervey, J. R., T. Curk, B. Rogelj, M. Briese, M. Cereda, M. Kayikci, J. König, T. Hortobágyi, A. L. Nishimura, V. Zupunski, R. Patani, S. Chandran, G. Rot, B. Zupan, C. E. Shaw and J. Ule (2011). "Characterizing the RNA targets and position-dependent splicing regulation by TDP-43." Nat Neurosci **14**(4): 452-458.

Tran, N. Q. V., A. N. Nguyen, K. Takabe, Z. Yamagata and K. Miyake (2017). "Pre-treatment with amitriptyline causes epigenetic up-regulation of neuroprotection-associated genes and has anti-apoptotic effects in mouse neuronal cells." Neurotoxicol Teratol **62**: 1-12.

Tsvetkov, A. S., J. Miller, M. Arrasate, J. S. Wong, M. A. Pleiss and S. Finkbeiner (2010). "A small-molecule scaffold induces autophagy in primary neurons and protects against toxicity in a Huntington disease model." Proc Natl Acad Sci U S A **107**(39): 16982-16987.

Vabulas, R. M. and F. U. Hartl (2005). "Protein synthesis upon acute nutrient restriction relies on proteasome function." Science **310**(5756): 1960-1963.

Van Damme, P., M. Dewil, W. Robberecht and L. Van Den Bosch (2005). "Excitotoxicity and amyotrophic lateral sclerosis." Neurodegener Dis **2**(3-4): 147-159.

van Eersel, J., Y. D. Ke, A. Gladbach, M. Bi, J. Götz, J. J. Kril and L. M. Ittner (2011). "Cytoplasmic accumulation and aggregation of TDP-43 upon proteasome inhibition in cultured neurons." PLoS One **6**(7): e22850.

van Es, M. A., O. Hardiman, A. Chio, A. Al-Chalabi, R. J. Pasterkamp, J. H. Veldink and L. H. van den Berg (2017). "Amyotrophic lateral sclerosis." Lancet **390**(10107): 2084-2098.

Van Langenhove, T., J. van der Zee and C. Van Broeckhoven (2012). "The molecular basis of the frontotemporal lobar degeneration-amyotrophic lateral sclerosis spectrum." Ann Med **44**(8): 817-828.

Vance, C., A. Al-Chalabi, D. Ruddy, B. N. Smith, X. Hu, J. Sreedharan, T. Siddique, H. J. Schelhaas, B. Kusters, D. Troost, F. Baas, V. de Jong and C. E. Shaw (2006). "Familial amyotrophic lateral sclerosis with frontotemporal dementia is linked to a locus on chromosome 9p13.2-21.3." Brain **129**(Pt 4): 868-876.

Vance, C., B. Rogelj, T. Hortobágyi, K. J. De Vos, A. L. Nishimura, J. Sreedharan, X. Hu, B. Smith, D. Ruddy, P. Wright, J. Ganesalingam, K. L. Williams, V. Tripathi, S. Al-Saraj, A. Al-Chalabi, P. N. Leigh, I. P. Blair, G. Nicholson, J. de Belleroche, J. M. Gallo, C. C. Miller and C. E. Shaw (2009). "Mutations in FUS, an RNA processing protein, cause familial amyotrophic lateral sclerosis type 6." Science **323**(5918): 1208-1211.

Voges, D., P. Zwickl and W. Baumeister (1999). "The 26S proteasome: a molecular machine designed for controlled proteolysis." Annu Rev Biochem **68**: 1015-1068.

Walker, A. K., K. J. Spiller, G. Ge, A. Zheng, Y. Xu, M. Zhou, K. Tripathy, L. K. Kwong, J. Q. Trojanowski and V. M. Lee (2015). "Functional recovery in new mouse models of ALS/FTLD after clearance of pathological cytoplasmic TDP-43." Acta Neuropathol **130**(5): 643-660.

Wang, I. F., B. S. Guo, Y. C. Liu, C. C. Wu, C. H. Yang, K. J. Tsai and C. K. Shen (2012). "Autophagy activators rescue and alleviate pathogenesis of a mouse model with proteinopathies of the TAR DNA-binding protein 43." Proc Natl Acad Sci U S A **109**(37): 15024-15029.

Wang, J., G. Xu and D. R. Borchelt (2002). "High molecular weight complexes of mutant superoxide dismutase 1: age-dependent and tissue-specific accumulation." Neurobiol Dis **9**(2): 139-148.

Wang, Q. J., Y. Ding, D. S. Kohtz, S. Kohtz, N. Mizushima, I. M. Cristea, M. P. Rout, B. T. Chait, Y. Zhong, N. Heintz and Z. Yue (2006). "Induction of autophagy in axonal dystrophy and degeneration." J Neurosci **26**(31): 8057-8068.

Webster, C. P., E. F. Smith, P. J. Shaw and K. J. De Vos (2017). "Protein Homeostasis in Amyotrophic Lateral Sclerosis: Therapeutic Opportunities?" Front Mol Neurosci **10**: 123.

Wegorzewska, I., S. Bell, N. J. Cairns, T. M. Miller and R. H. Baloh (2009). "TDP-43 mutant transgenic mice develop features of ALS and frontotemporal lobar degeneration." Proc Natl Acad Sci U S A **106**(44): 18809-18814.

Weissman, A. M. (2001). "Themes and variations on ubiquitylation." Nat Rev Mol Cell Biol **2**(3): 169-178.

Williams, A., L. Jahreiss, S. Sarkar, S. Saiki, F. M. Menzies, B. Ravikumar and D. C. Rubinsztein (2006). "Aggregate-prone proteins are cleared from the cytosol by autophagy: therapeutic implications." Curr Top Dev Biol **76**: 89-101.

Wils, H., G. Kleinberger, J. Janssens, S. Pereson, G. Joris, I. Cuijt, V. Smits, C. Ceuterick-de Groote, C. Van Broeckhoven and S. Kumar-Singh (2010). "TDP-43 transgenic mice develop spastic paralysis and neuronal inclusions characteristic of ALS and frontotemporal lobar degeneration." Proc Natl Acad Sci U S A **107**(8): 3858-3863.

Winton, M. J., L. M. Igaz, M. M. Wong, L. K. Kwong, J. Q. Trojanowski and V. M. Lee (2008). "Disturbance of nuclear and cytoplasmic TAR DNA-binding protein (TDP-43) induces disease-like redistribution, sequestration, and aggregate formation." J Biol Chem **283**(19): 13302-13309.

Winton, M. J., V. M. Van Deerlin, L. K. Kwong, W. Yuan, E. M. Wood, C. E. Yu, G. D. Schellenberg, R. Rademakers, R. Caselli, A. Karydas, J. Q. Trojanowski, B. L. Miller and V. M. Lee (2008). "A90V TDP-43 variant results in the aberrant localization of TDP-43 in vitro." FEBS Lett **582**(15): 2252-2256.

Wong, P. C., C. A. Pardo, D. R. Borchelt, M. K. Lee, N. G. Copeland, N. A. Jenkins, S. S. Sisodia, D. W. Cleveland and D. L. Price (1995). "An adverse property of a familial ALS-linked SOD1 mutation causes motor neuron disease characterized by vacuolar degeneration of mitochondria." Neuron **14**(6): 1105-1116.

Wu, L. S., W. C. Cheng, S. C. Hou, Y. T. Yan, S. T. Jiang and C. K. Shen (2010). "TDP-43, a neuro-pathosignature factor, is essential for early mouse embryogenesis." Genesis **48**(1): 56-62.

Xi, Z., I. Rainero, E. Rubino, L. Pinessi, A. C. Bruni, R. G. Maletta, B. Nacmias, S. Sorbi, D. Galimberti, E. I. Surace, Y. Zheng, D. Moreno, C. Sato, Y. Liang, Y. Zhou, J. Robertson, L. Zinman, M. C. Tartaglia, P. St George-Hyslop and E. Rogaeva (2014). "Hypermethylation of the CpG-island near the C9orf72 G4C2-repeat expansion in FTLD patients." Hum Mol Genet.

Xia, Q., H. Wang, Z. Hao, C. Fu, Q. Hu, F. Gao, H. Ren, D. Chen, J. Han, Z. Ying and G. Wang (2016). "TDP-43 loss of function increases TFEB activity and blocks autophagosome-lysosome fusion." EMBO J **35**(2): 121-142.

Xiao, S., T. Sanelli, H. Chiang, Y. Sun, A. Chakrabartty, J. Keith, E. Rogaeva, L. Zinman and J. Robertson (2015). "Low molecular weight species of TDP-43 generated by abnormal splicing form inclusions in amyotrophic lateral sclerosis and result in motor neuron death." Acta Neuropathol **130**(1): 49-61.

Xu, Y. F., T. F. Gendron, Y. J. Zhang, W. L. Lin, S. D'Alton, H. Sheng, M. C. Casey, J. Tong, J. Knight, X. Yu, R. Rademakers, K. Boylan, M. Hutton, E. McGowan, D. W. Dickson, J. Lewis and L. Petrucelli (2010). "Wild-type human TDP-43 expression causes TDP-43 phosphorylation, mitochondrial aggregation, motor deficits, and early mortality in transgenic mice." J Neurosci **30**(32): 10851-10859.

Xu, Y. F., Y. J. Zhang, W. L. Lin, X. Cao, C. Stetler, D. W. Dickson, J. Lewis and L. Petrucelli (2011). "Expression of mutant TDP-43 induces neuronal dysfunction in transgenic mice." Mol Neurodegener **6**: 73.

Yamashita, T., T. Hideyama, K. Hachiga, S. Teramoto, J. Takano, N. Iwata, T. C. Saido and S. Kwak (2012). "A role for calpain-dependent cleavage of TDP-43 in amyotrophic lateral sclerosis pathology." Nat Commun **3**: 1307.

Yang, C., H. Wang, T. Qiao, B. Yang, L. Aliaga, L. Qiu, W. Tan, J. Salameh, D. M. McKenna-Yasek, T. Smith, L. Peng, M. J. Moore, R. H. Brown, H. Cai and Z. Xu (2014). "Partial loss of TDP-43 function causes phenotypes of amyotrophic lateral sclerosis." Proc Natl Acad Sci U S A **111**(12): E1121-1129.

Zhang, Y. J., T. F. Gendron, Y. F. Xu, L. W. Ko, S. H. Yen and L. Petrucelli (2010). "Phosphorylation regulates proteasomal-mediated degradation and solubility of TAR DNA binding protein-43 C-terminal fragments." Mol Neurodegener **5**: 33.

Zhang, Y. J., Y. F. Xu, C. Cook, T. F. Gendron, P. Roettges, C. D. Link, W. L. Lin, J. Tong, M. Castanedes-Casey, P. Ash, J. Gass, V. Rangachari, E. Buratti, F. Baralle, T. E. Golde, D. W. Dickson and L. Petrucelli (2009). "Aberrant cleavage of TDP-43 enhances aggregation and cellular toxicity." Proc Natl Acad Sci U S A **106**(18): 7607-7612.

Zu, T., B. Gibbens, N. S. Doty, M. Gomes-Pereira, A. Huguet, M. D. Stone, J. Margolis, M. Peterson, T. W. Markowski, M. A. Ingram, Z. Nan, C. Forster, W. C. Low, B. Schoser, N. V. Somia, H. B. Clark, S. Schmechel, P. B. Bitterman, G. Gourdon, M. S. Swanson, M. Moseley and L. P. Ranum (2011). "Non-ATG-initiated translation directed by microsatellite expansions." Proc Natl Acad Sci U S A **108**(1): 260-265.

Zu, T., Y. Liu, M. Bañez-Coronel, T. Reid, O. Pletnikova, J. Lewis, T. M. Miller, M. B. Harms, A. E. Falchook, S. H. Subramony, L. W. Ostrow, J. D. Rothstein, J. C. Troncoso and L. P. Ranum (2013). "RAN proteins and RNA foci from antisense transcripts in C9ORF72 ALS and frontotemporal dementia." Proc Natl Acad Sci U S A **110**(51): E4968-4977.